# VLÁKNA A TEXTIL

## FIBRES AND TEXTILES

5

Volume 30
December
2023

TECHNICAL UNIVERSITY OF LIBEREC

STU FCHPT

Trenčianska univerzita Alexandra Dubčeka v Trenčíne
Fakulta priemyselných technológií v Púchove

VUTCH
RESEARCH INSTITUTE OF TEXTILE CHEMISTRY
VÝSKUMNÝ ÚSTAV TEXTILNEJ CHÉMIE

CHEMOSVIT FIBROCHEM

VÚCHV

ZSVTS

Indexed in:
SCOPUS
Chemical Abstract
World Textile Abstracts
EBSCO Essentials

ISSN 1335-0617
print version

ISSN 2585-8890
online version

# VLÁKNA A TEXTIL
http://www.vat.ft.tul.cz

PUBLISHED BY
Technical University of Liberec, Faculty of Textile Engineering
Slovak University of Technology in Bratislava, Faculty of Chemical and Food Technology
Alexander Dubček University of Trenčín, Faculty of Industrial Technologies
Slovak Society of Industrial Chemistry, Bratislava
Research Institute of Man-Made Fibres, JSC, Svit
Research Institute of Textile Chemistry (VUTCH) Ltd., Žilina
Chemosvit Fibrochem, JSC, Svit



PUBLISHER
Technical University of Liberec
Studentska 1402/2, 461 17 Liberec 1, CZ
Tel: +420 485 353615
e-mail: vat@tul.cz
IČO: 46747885

ORDER AND ADVERTISEMENT OF THE JOURNAL
Technical University of Liberec
Faculty of Textile Engineering
Studentska 1402/2, 461 17 Liberec 1, CZ
Tel: +420 485 353615
e-mail: vat@tul.cz

TYPESET AND PRINT
Vysokoškolský podnik, s.r.o., Voroněžská 1329/13, 460 01 Liberec 1, CZ

DATE OF ISSUE
January 2024

APPROVED BY
Rector's Office of Technical University of Liberec
Ref. no. RE 2/24, 12th January 2024

EDITION
First

PUBLICATION NUMBER
55-002-24

PUBLICATION
Quarterly

SUBSCRIPTION
60 EUR

REG. NO. MK ČR E 24338

# VLÁKNA A TEXTIL

Volume 30, Issue 5, December 2023

## CONTENT

*Fibres and Textiles* **30**(5), 2023, 3-10 DOI: 10.15240/tul/008/2023-5-001

# PREDICTION OF THE INCREASE IN YARN UNEVENNESS AFTER WINDING PROCESS USING STATISTICAL AND ARTIFICIAL NEURAL NETWORK MODELS

**TRUNG, TRAN DUC; TUAN, DAO ANH* AND HUONG, CHU DIEU***

Hanoi University of Science and Technology, Hanoi, Vietnam

## ABSTRACT

This paper investigated the prediction of the increase in unevenness of two types of yarn: Ne 30/1 CVCM (combed yarn Ne 30/1, 60% Cotton 40% Polyester) and Ne 30/1 COCM (combed yarn Ne 30/1 100% Cotton) after winding by artificial neural network (ANN) and by statistical models. Four technological winding parameters: the winding speed (Z1), the load on the friction discs of the yarn tensioner (Z2), the distance between the bobbin and the yarn guide (Z3) and the pressure of the package on the grooved drum (Z4) were used as the input parameters to investigate yarn unevenness after winding. The research results showed that by using statistical models, within the selected research range, four investigated technological parameters influenced the increase in unevenness of the two mentioned yarns. The regression coefficients represented the influence of each technological parameter on the increase in yarn unevenness: the winding speed parameter has the most influence on the increase in yarn unevenness with the biggest value coefficients b1 which was 1.2339 for the Ne 30/1 CVCM yarn and this value was 0.6996 for the Ne 30/1 COCM yarn. Moreover, the increase in yarn unevenness predicted by ANNs obtained a higher coefficient of determination (R2), while the mean square error (MSE) and the mean absolute error (MAE) were lower than the ones predicted by statistical models.

## KEYWORDS

Unevenness; Artificial neural network; Regression function; Predicting yarn unevenness; Winding.

## INTRODUCTION

Currently, Artificial Neural Network (ANN) is being widely applied in many fields, including textile and garment. Uster (Switzerland) has developed a fabric inspection system named Fabricscan. In this system, CCD (Change Coupled Device) cameras were used to scan the fabric surface. The scan signals were transmitted to ANN for analysis and evaluation [1, 2]. Samader AI. Malik et al. [3] have predicted yarn unevenness and tensile strength which were produced by ring spinning frame based on four different input parameters: the PES/CO blend ratio, twist multiplier, back roller cot hardness and break draft ratio by using ANN and Multiple Linear Regression (MLR). The built ANN has the following parameters: 4 - (3 - 3)2 - 1 (1 input layer with 4 neurons, 2 hidden layers (3 neurons each) and an output layer with 1 neuron). The number of learning samples in the research was 40 samples and the number of test samples was 8. The results showed that using ANN to predict yarn unevenness and tensile strength achieved higher accuracy than that predicted by MLR. Rocco Furfiri and Maurizio Gelli [4] predicted the tensile strength of yarn by ANN and MLR based on roving yarn. Input parameters included yarn count, yarn twist, mean length, average fineness and average strength of fibers in the roving yarn. The ANN was built with 3 layers: an input layer of 5 neurons (corresponding to 5 input parameters), a hidden layer of 10 neurons and an output layer of 1 neuron (corresponding to the strength of the yarn). The results showed that the yarn strength predicted by ANN was only 3% less different than this value measured by the real experimental strength while the prediction by MLR was 10% more different than in comparison to the experimental one. Ezzatollah Haghighat et al. [5] predicted the hairiness of PES/Viscose blended yarns by ANN and MLR based on the input parameters: the total draft, roving twist, yarn count, yarn twist, spindle speed, traveled weight, back zone setting, break draft, balloon control ring, front roller covering hardness and draft system angle. By comparing the parameters of coefficient of determination (R2), mean square error (MSE), and mean absolute error (MAE), the results showed that the prediction by ANN gave more accurate results

* **Corresponding author:** Huong Ch.D., e-mail: huong.chudieu@hust.edu.vn; Tuan, D.A., email: tuan.daoanh@hust.edu.vn

*Received June 9, 2023; accepted October 2, 2023*

**Table 1.** Central value and variation range of winding parameters.

| Parameters | Actual values | | | | Coded values | | | |
|---|---|---|---|---|---|---|---|---|
| | $Z_1$ [m/min] | $Z_2$ [cN] | $Z_3$ [cm] | $Z_4$ [N] | $x_1$ | $x_2$ | $x_3$ | $x_4$ |
| Top level | 1200 | 30 | 18 | 21 | +1 | +1 | +1 | +1 |
| Base level $Z_j^0$ | 900 | 20 | 14 | 14 | 0 | 0 | 0 | 0 |
| Bottom level | 600 | 10 | 10 | 7 | -1 | -1 | -1 | -1 |
| Variation range $\Delta Z_j$ | 300 | 10 | 4 | 7 | - | - | - | - |

than that predicted by MLR. Similar results have been obtained by the other researchers [6, 7].

ANN has been applied to predict yarn quality mainly at the spinning stage (before winding) and achieved high accuracy while using traditional techniques (MLR models) for prediction had many errors or predicted results with low accuracy. Up to now, the application of ANN to predict the yarn quality after winding based on technological parameters has not been mentioned.

Due to the influence of winding technology, the quality of yarn including the yarn unevenness after winding has changed in comparison to before winding [8]. For woven fabrics, the yarn's unevenness will make the fabric look bad. Particularly for knitted fabrics, in addition to bad fabric appearance, the yarn unevenness also causes a lot of yarn breakages, even broken needles. The reasons for the yarn unevenness are very complicated: due to the raw materials, the spinning technology and the equipment, including the winding. Though it is impossible to eliminate yarn unevenness, reducing and limiting this phenomenon is important. To reduce the production cost, to yarn usage orientation, the increase in unevenness of the yarn after winding needs to be predicted. This paper presents the research results of predicting the increase in the unevenness of two types of yarn: the Ne 30/1 CVCM yarn and the Ne 30/1 COCM yarn based on four typical winding parameters that can be tested, controlled and often need to be adjusted during the winding process, which were the winding speed (*Z1*), the load on the friction discs of the yarn tensioner (*Z2*), the distance between the bobbin and the yarn guide (*Z3*) and the pressure of package on the grooved drum (*Z4*). The research results will contribute to reducing yarn production costs and orient the efficient use of yarn after winding.

# MATERIALS AND METHODS

## Materials

Yarn materials: The research used two types of ring combed yarns produced by Vinatex NamDinh (Vietnam) spinning mill: Ne 30/1 CVCM yarn (60% Cotton, 40% PES) and Ne 30/1 COCM yarn (100% Cotton).

## Methods

The winding process was performed on the winding model developed at Hanoi University of Science and Technology [9]. The Uster Tester 5 (Switzerland) was used to measure the yarn unevenness before and after winding by standard ASTM D1425M/1425M-14 [10]. Before testing, the yarns were conditioned for 24 hours in standard atmospheric conditions (65 ± 2% relative humidity and 20 ± 2°C temperature). The acquired results were obtained by using the built ANN and statistical models.

The orthogonal experimental planning level II [11] was applied to set up an experimental matrix with 4 technological winding parameters *Z1, Z2, Z3, Z4*. The range of values of the winding parameters was selected based on the actual survey of winding conventional yarns in the spinning mills and the allowable capacity of the winding model (Table 1).

Statistical models of the increase in yarn unevenness after winding in comparison to before winding have the general form:

$\Delta U\ [\%] = b_0 + b_1x_1 + b_2x_2 + b_3x_3 + b_4x_4 + b_{12}x_1x_2 + b_{13}x_1x_3 + b_{14}x_1x_4 + b_{23}x_2x_3 + b_{24}x_2x_4 + b_{34}x_3x_4 + b_{11}x_1^2 + b_{22}x_2^2 + b_{33}x_3^2 + b_{44}x_4^2$,

where: $b_0$, $b_1$, $b_2$, $b_3$, $b_4$, $b_{12}$, $b_{13}$, $b_{14}$, $b_{23}$, $b_{24}$, $b_{34}$, $b_{11}$, $b_{22}$, $b_{33}$, $b_{44}$ - the coefficients of the model, $x_1$, $x_2$, $x_3$, $x_4$ - coding variables of winding parameters.

The real variables $Z_j$ and the encoding variable $x_j$ were related by the formula:

$$Z_j = x_j \Delta Z_j + Z_j^0. \quad (1)$$

The increase in yarn unevenness ΔU% was calculated by the formula:

$$\Delta U = \frac{U_s - U_t}{U_t} 100\ [\%], \quad (2)$$

where: $U_t$ - unevenness of yarn before winding ($U_t$ = 9.44 % and 8.94 % for CVCM yarn and COCM yarn respectively), $U_s$ - unevenness of the yarn after winding determined according to each experiment.

The number of experiments *N* with the number of variables $k = 4$ was determined by the formula $N = 2^k + n_0 + 2k$, where, $n_0$ is the number of experiments in the center ($n_0 = 1$). Thus, $N = 25$. Coefficient $\alpha = \sqrt{\sqrt{N.2^{k-2}} - 2^{k-1}} = \sqrt{\sqrt{25.2^2} - 2^3} = 1.414$ to set up the experimental matrix and conduct the experiment.

**Application of artificial neural network (ANN)**

By building an ANN with arbitrary concatenation or testing the learning process with many different networks and by examining the resulting errors, we can choose the network with the smallest error [12,13]. There are many types of neural networks, the most classic neural network application is the Multilayer Perceptron (MLP) network which is used commonly in many research fields.

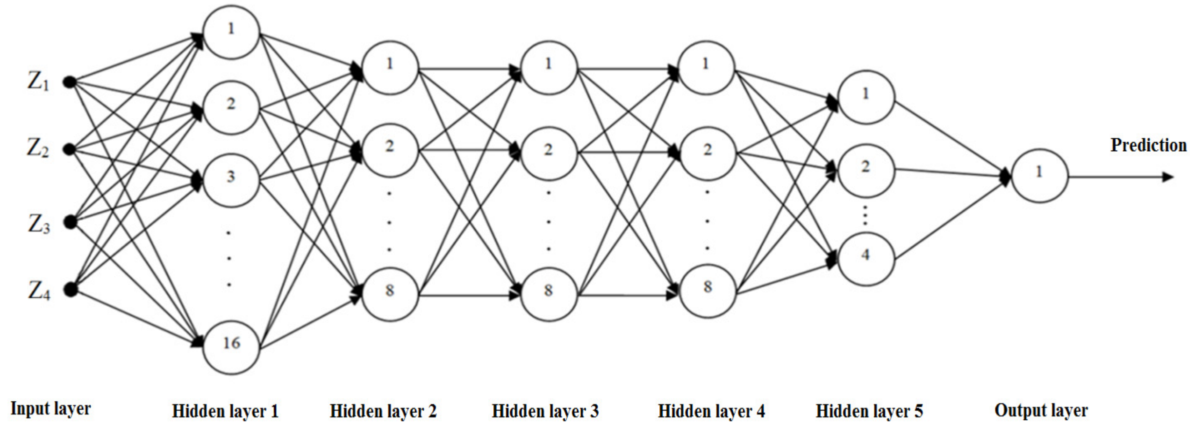


**Figure 1.** Structure of ANN model for predicting increase in unevenness of yarn.

In addition to the basic units, the ANN also has some general requirements on the network structure such as the neurons are arranged into layers, including a layer of input signal channels, a layer of output signal channels and may include several intermediate layers known as hidden layers. There are no connections between neurons on the same layer, only connections between neurons of two consecutive layers. The connections are oriented from the input to the output (linear network). Neurons on the same layer will have the same activation function.

The ANN networks (Figure 1) predict the increase in unevenness of yarn after winding based on 4 winding parameters (winding speed $Z_1$, the load on the friction discs of the yarn tensioner $Z_2$, the distance between the bobbin and the yarn guide $Z_3$ and the pressure of package on the grooved drum $Z_4$) which was a form of MLP network. For the feedforward network, learning by the error backpropagation algorithm using the Sigmoid activation function is suitable because of its continuity and its values do not suddenly decrease. Furthermore, the derivative of a Sigmoid function can be easily calculated and expressed as terms of a function of the form Sigmoid. Since there is no certain rule to select the number of layers and neurons in each layer, the network structure is selected by the trial-and-error method for several networks with different numbers of layers and different number units in layer(s). The training algorithm, training parameters and activation function have been trained with the objective of minimizing the training error and better generalization on unseen data. For example, the number of hidden neurons in every layer is selected with the trial-and-error method. A network with only 1 hidden neuron and one layer was started, and then the number of neurons and layer increased progressively and generated randomly in different networks. All the networks were trained with the data sets, and the network with the lowest error was selected. If the best error is still high, the number of hidden neurons is increased by 1. To avoid the overfitting effect, we chose the network with the lowest possible number of hidden neurons and acceptable error (i.e., the simplest possible network), which can still approximate the data. The ANN network structure in this study was selected by testing with 3 different networks (3, 4, 5 hidden layers) and evaluated by 3 performance parameters of the models: $R^2$ (Determining the number of systems), MSE (mean squared error), MAE (means absolute error).

The network has 3 hidden layers:

$4 - (8 - 4 - 4)_3 - 1$

$R_3^2 = 0.9681$, $MSE_3 = 0.0415$, $MAE_3 = 0.1210$

The network has 4 hidden layers:

$4 - (8 - 6 - 4 - 4)_4 - 1$

$R_4^2 = 0.9125$, $MSE_4 = 0.1137$, $MAE_4 = 0.1342$

The network has 5 hidden layers:

$4 - (16 - 8 - 8 - 8 - 4)_5 - 1$

$R_5^2 = 0.9997$, $MSE_5 = 0.0009$, $MAE_5 = 0.0187$

In comparison: $R_5^2 > R_3^2 > R_4^2$; $MSE_5 < MSE_3 < MSE_4$; $MAE_5 < MAE_3 < MAE_4$

So the network with 1 input layer of four neurons (4 winding parameters), 5 hidden layers (the number of neurons of the hidden layers is 16, 8, 8, 8, 4, respectively) and 1 output layer with the number of neurons is 1 (increase in yarn unevenness) has the highest $R_5^2$, and the smallest $MSE_5$, $MAE_5$ among the 3 tested networks and this network was chosen to predict the increase in the unevenness of yarn in our research.

Network training

To train the network, the supervised learning rule was used. Error backpropagation is a learning algorithm applied to adjust synaptic weight, which is a form of supervised learning. Currently, there is no general rule for selecting learning data sets, a simple way is to choose the learning data set which covers the entire possible input space. Here, the input of the algorithm is a set of learning data {($Z_s$, $D_s$)} where, $Z_s = [Z_1, Z_2, Z_3... Z_N]$ is the input vector (technological parameters) and $D_s = [d_1, d_2, d_3... d_N]$ is the desired output vector (increase in unevenness) of the yarn determined according to each experiment. The learning process includes the following steps:

1. Calculate output:

When a sample $Z_s$ = *[$Z_1$, $Z_2$, $Z_3$....$Z_N$]* is put on the network, it propagates from the input Z through the hidden layers Y to the output layer M. In the case of an ANN with one hidden layer:

a. Sum of input connections of the hidden neuron *j* was calculated by formula 3 [3; 15]:

$$a_j = \sum\nolimits_{i=1} u_{ji} Z_i + b_j, \quad (3)$$

where: $Z_i$ - input signal *i*, $u_{ji}$ - synaptic weight, $b_j$ - bias term connected to the *j* unit.

Calculate the output of the j hidden neuron:

$$Y_j = f(a_j). \quad (4)$$

In case the network is designed with many hidden layers, the calculation method is similar, the output of one hidden layer will be the input of the next hidden layer.

b. Output layer *M*

Input of the k output neuron:

$$b_k = \sum_{j=1} Y_j W_{kj}, \quad (5)$$

in where: $W_{kj}$ is the corresponding weight.

The output value of neuron k in the output layer M is:

$$M_k = f(b_k). \quad (6)$$

2. Evaluate output error:

Calculate the error of the network *E* according to the formula:

$$E = \frac{1}{2}\sum_k (d_k - M_k)^2, \quad (7)$$

in where: $d_k$ - the increase in unevenness determined by experiment, $M_k$ - the increase in unevenness predicted by ANN at the k neuron in the output layer for the sample $Z_s$.

The ANN was trained by feeding the output layer with samples and gradually adjusting the weight coefficients so that the output class response would match the desired values. In fact, after each learning cycle, if $E \le E_{max}$, the learning process is ended, and the result weights are given. If $E > E_{max}$, a new learning epoch is restarted by returning to the first step in adjusting the weights $W_{kj}$ and $u_{ji}$ based on the principle of backpropagation error. The values of the synaptic weight are gradually adjusted. In our research, the learning process using the error backpropagation algorithm can be ended with two specified conditions: the chosen value $E_{max}$ = 0.01 or the number of learning epochs is 300. The network will stop according to the first coming condition.

**Evaluation of the predictive performance of the models**

The prediction results of the ANN were compared to those predicted by statistical models by 3 performance parameters [3]:

The coefficient of determination represents the relationship between the predicted value and the experimental value ($R^2$).

Mean square error (MSE):

$$MSE = \frac{1}{N}\sum_{k=1}^{N}(M_k - d_k)^2 = \frac{1}{N}\sum_{i=1}^{N}(\Delta)^2, \quad (8)$$

Mean absolute error (MAE):

$$MAE = \frac{1}{N}\sum_{k=1}^{N}|M_k - d_k| = \frac{1}{N}\sum_{i=1}^{N}|\Delta|, \quad (9)$$

In where: $M_k$ - the increase in yarn unevenness predicted by ANN or statistical models, $d_k$ - the increase in yarn unevenness determined by experiment (desired value), *N* - number of experiments.

## RESULTS AND DISCUSSION

### Predicting increase in yarn unevenness by statistical model

To determine the mathematical relationship between the increase in yarn unevenness after winding and four selected technological parameters, it was necessary to establish an experimental matrix and conduct experiments to determine yarn unevenness. The experimental matrix and the determined results of the increase in yarn unevenness ΔU % (according to formula 2) were presented in Table 2.

Using the Design Expert software, we have calculated the regression coefficients, checked the coefficients according to Student's standards and checked the conformity of the regression equations according to Fisher's standards. The statistical models on the increase in yarn unevenness with the coding variables have the following forms:

For the Ne 30/1 CVCM yarn:

$\Delta U_1$ =3.9952 + 1.2339$x_1$ + 0.7221$x_2$ + 0.5688$x_3$ + 0.6318$x_4$ + 0.2994$x_2$ $x_4$ + 1.4831$x_3$ $x_4$

$R^2$ = 0.8733

For the Ne 30/1COCM yarn:

$\Delta U_2$ = 2.2396 + 0.6996$x_1$ + 0.3927$x_2$ + 0.31$x_3$ + 0.2966$x_4$ - 0.1394$x_2$ $x_3$ + 0.2869$x_2 x_4$ + 0.7994$x_3$ $x_4$

$R^2$ = 0.8986

Within the selected research range, four technological parameters (winding speed ($x_1$), the load on the friction discs of the yarn tensioner ($x_2$), the distance between the bobbin and the yarn guide ($x_3$) and the pressure of the package on the grooved drum ($x_4$) influence the increase in the unevenness of the two mentioned yarns. The regression coefficients represented the influence of the technological parameters on the increase in yarn unevenness. The winding speed parameter has the most influence on the increase in yarn unevenness (the coefficients $b_1$ = 1.2339 (in the $\Delta U_1$ model), $b_1$ = 0.6996 (in the $U_2$ model) mean the biggest values), followed by the influence of load $x_2$ (coefficient $b_2 < b_1$ in models $\Delta U_1$, $\Delta U_2$).

**Table 2.** Experimental matrix and the results of determining the increase in yarn unevenness ΔU %.

| $N^0$ | $x_0$ | $x_1$ | $x_2$ | $x_3$ | $x_4$ | $Z_1$ | $Z_2$ | $Z_3$ | $Z_4$ | Ne 30/1 CVCM | Ne 30/1 COCM |
|---|---|---|---|---|---|---|---|---|---|---|---|
| | | | | | | | | | | $\Delta U_1$ [%] | $\Delta U_2$ [%] |
| 1 | + | - | - | - | - | 600 | 10 | 10 | 7 | 1.8 | 1.23 |
| 2 | + | + | - | - | - | 1200 | 10 | 10 | 7 | 5.72 | 3.58 |
| 3 | + | - | + | - | - | 600 | 30 | 10 | 7 | 3.6 | 2.01 |
| 4 | + | + | + | - | - | 1200 | 30 | 10 | 7 | 6.07 | 3.42 |
| 5 | + | - | - | + | - | 600 | 10 | 18 | 7 | 1.17 | 0.78 |
| 6 | + | + | - | + | - | 1200 | 10 | 18 | 7 | 2.85 | 2.07 |
| 7 | + | - | + | + | - | 600 | 30 | 18 | 7 | 2.75 | 1.28 |
| 8 | + | + | + | + | - | 1200 | 30 | 18 | 7 | 2.97 | 1.79 |
| 9 | + | - | - | - | + | 600 | 10 | 10 | 21 | 1.06 | 0.11 |
| 10 | + | + | - | - | + | 1200 | 10 | 10 | 21 | 2.54 | 0.89 |
| 11 | + | - | + | - | + | 600 | 30 | 10 | 21 | 3.71 | 2.28 |
| 12 | + | + | + | - | + | 1200 | 30 | 10 | 21 | 3.81 | 2.35 |
| 13 | + | - | - | + | + | 600 | 10 | 18 | 21 | 4.03 | 2.46 |
| 14 | + | + | - | + | + | 1200 | 10 | 18 | 21 | 7.31 | 3.69 |
| 15 | + | - | + | + | + | 600 | 30 | 18 | 21 | 5.03 | 2.8 |
| 16 | + | + | + | + | + | 1200 | 30 | 18 | 21 | 11.03 | 5.15 |
| 17 | + | 0 | 0 | 0 | 0 | 900 | 20 | 14 | 14 | 3.92 | 2.27 |
| 18 | + | α | 0 | 0 | 0 | 1324 | 20 | 14 | 14 | 5.08 | 3.28 |
| 19 | + | -α | 0 | 0 | 0 | 475 | 20 | 14 | 14 | 1.17 | 0.45 |
| 20 | + | 0 | α | 0 | 0 | 900 | 34.14 | 14 | 14 | 4.77 | 3.02 |
| 21 | + | 0 | -α | 0 | 0 | 900 | 5.86 | 14 | 14 | 3.39 | 1.9 |
| 22 | + | 0 | 0 | α | 0 | 900 | 20 | 19.65 | 14 | 4.87 | 3.24 |
| 23 | + | 0 | 0 | -α | 0 | 900 | 20 | 8.34 | 14 | 3.07 | 1.79 |
| 24 | + | 0 | 0 | 0 | α | 900 | 20 | 14 | 23.9 | 4.45 | 2.91 |
| 25 | + | 0 | 0 | 0 | -α | 900 | 20 | 14 | 4.1 | 3.71 | 1.24 |

**Table 3.** The actual and predicted results of the increase in unevenness of Ne 30/1 CVCM yarn by ANN.

| $N_0$ | $\Delta U_1$ [%] | |
|---|---|---|
| | Experiments | ANN |
| 1 | 1.8 | 1.8027 |
| 2 | 5.72 | 5.7445 |
| 3 | 3.6 | 3.5868 |
| 4 | 6.07 | 6.0761 |
| 5 | 1.17 | 1.1325 |
| 6 | 2.85 | 2.8493 |
| 7 | 2.75 | 2.7335 |
| 8 | 2.97 | 2.9695 |
| 9 | 1.06 | 1.0510 |
| 10 | 2.54 | 2.5266 |
| 11 | 3.71 | 3.6915 |
| 12 | 3.81 | 3.8355 |
| 13 | 4.03 | 4.0110 |
| 14 | 7.31 | 7.325 |
| 15 | 5.03 | 5.0354 |
| 16 | 11.03 | 10.904 |
| 17 | 3.92 | 3.9111 |
| 18 | 5.08 | 5.0986 |
| 19 | 1.17 | 1.1458 |
| 20 | 4.77 | 4.7583 |
| 21 | 3.39 | 3.4130 |
| 22 | 4.87 | 4.8942 |
| 23 | 3.07 | 3.0788 |
| 24 | 4.45 | 4.438 |
| 25 | 3.71 | 3.7061 |

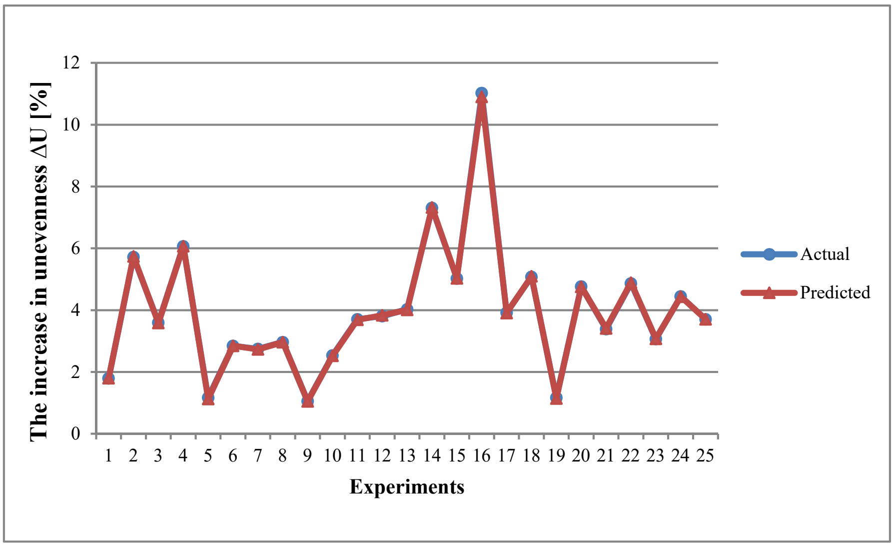


**Figure 2**. Performance of ANN model for the increase in yarn unevenness of Ne 30/1 CVCM yarn.

## Predicting increase in yarn unevenness by ANN

The software "Prediction of yarn product quality after winding" was established. The software was written in Python language. Its capacity was 656 MB and it runs on a Windows environment. The prediction results of the increase in yarn unevenness provided by this software based on the set of learning data (ΔU1, ΔU2 with 25 experiments which were used in the above statistical models) were presented in Table 3 and Table 4 and the graphs on Figures 2 and 3.

It can be seen in Figure 2 and Figure 3 above, that MLP models could approximate accurately the increase in yarn unevenness with very small differences between the actual values (the blue line) and the estimated values (the red line). Thus, the outputs of the network have almost coincided with the experimental values.

The performance was further assessed with the following measures: coefficient of determination ($R^2$), MSE (Mean Square Error), MAE (Mean Absolute Error). The numerical errors were collected in Table 5.

**Table 4.** The actual and predicted results of the increase in unevenness of Ne 30/1 COCM yarn by ANN.

| $N_0$ | $\Delta U_2$ [%] | |
|---|---|---|
| | **Experiments** | **ANN** |
| 1 | 1.23 | 1.3648 |
| 2 | 3.58 | 3.6340 |
| 3 | 2.01 | 2.2282 |
| 4 | 3.42 | 3.4864 |
| 5 | 0.78 | 0.7809 |
| 6 | 2.07 | 2.1865 |
| 7 | 1.28 | 1.3162 |
| 8 | 1.79 | 1.8497 |
| 9 | 0.11 | 0.1645 |
| 10 | 0.89 | 0.8961 |
| 11 | 2.28 | 2.5374 |
| 12 | 2.35 | 2.4137 |
| 13 | 2.46 | 2.6677 |
| 14 | 3.69 | 3.7911 |
| 15 | 2.8 | 2.8797 |
| 16 | 5.15 | 5.0074 |
| 17 | 2.27 | 2.3645 |
| 18 | 3.28 | 3.3000 |
| 19 | 0.45 | 0.5441 |
| 20 | 3.02 | 3.1038 |
| 21 | 1.9 | 2.0280 |
| 22 | 3.24 | 3.2621 |
| 23 | 1.79 | 2.0198 |
| 24 | 2.91 | 2.9480 |
| 25 | 1.24 | 1.3032 |

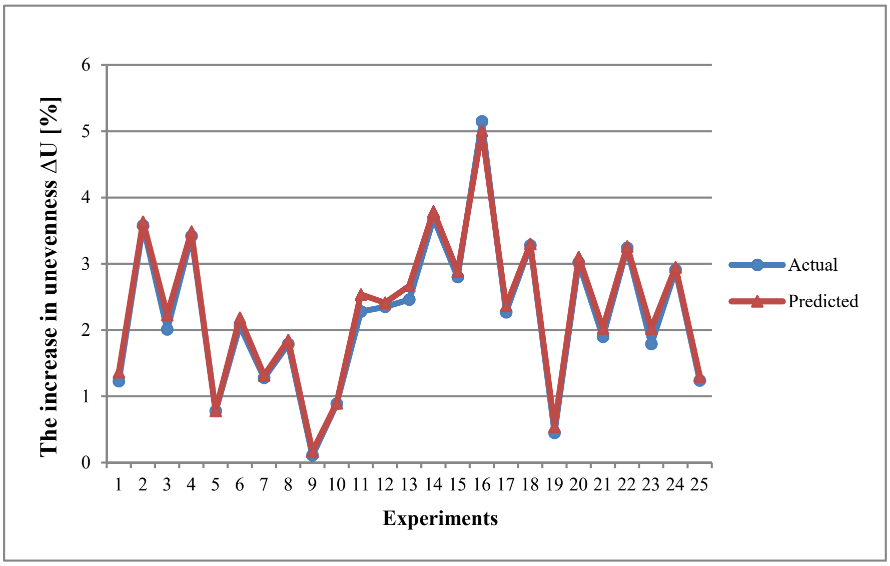


**Figure 3.** Performance of ANN model for the increase in unevenness of Ne 30/1 COCM yarn.

**Table 5.** The performance of predicting the increase in yarn unevenness of the models compared to the statistical model.

| Parameters | Ne 30/1 CVCM | | Ne 30/1 COCM | |
|---|---|---|---|---|
| | **Statistical Model** | **ANN** | **Statistical Model** | **ANN** |
| **$R^2$** | 0.8733 | 0.9997 | 0.8986 | 0.9893 |
| **MSE** | 0.6649 | 0.0009 | 0.3134 | 0.0138 |
| **MAE** | 0.6469 | 0.0187 | 0.1643 | 0.095 |

**Table 6.** Experimental results and prediction of ANN with testing dataset.

| Experiments | $Z_1$ [m/min] | $Z_2$ [cN] | $Z_3$ [cm] | $Z_4$ [N] | The increase in yarn unevenness | | | | | |
|---|---|---|---|---|---|---|---|---|---|---|
| | | | | | **Ne 30/1 CVCM yarn** | | | **Ne 30/1 COCM yarn** | | |
| | | | | | **Experiments** | **Statistics Model** | **ANN** | **Experiments** | **Statistics Model** | **ANN** |
| 1 | 700 | 20 | 12 | 7 | 3.18 | 2.99 | 3.02 | 1.68 | 1.72 | 1.56 |
| 2 | 900 | 10 | 10 | 7 | 4.13 | 3.86 | 4.10 | 3.36 | 2.19 | 3.17 |
| 3 | 600 | 30 | 10 | 4,1 | 3.81 | 3.69 | 3.92 | 2.13 | 2.08 | 1.97 |
| 4 | 1200 | 10 | 15 | 7 | 4.03 | 3.95 | 4.19 | 2.80 | 2.45 | 3.04 |
| 5 | 1000 | 10 | 15 | 14 | 4.24 | 3.83 | 4.31 | 2.46 | 2.19 | 2.57 |
| 6 | 800 | 15 | 14 | 14 | 3.07 | 3.22 | 2.95 | 1.23 | 1.81 | 1.23 |
| 7 | 800 | 14 | 10 | 14 | 2.65 | 2.58 | 2.60 | 1.12 | 1.38 | 1.31 |
| 8 | 900 | 10 | 12 | 4,1 | 4.13 | 3.57 | 3.84 | 2.91 | 2.17 | 2.64 |
| 9 | 700 | 12 | 14 | 7 | 2.12 | 2.20 | 2.10 | 1.34 | 1.39 | 1.10 |
| 10 | 1000 | 10 | 12 | 4,1 | 4.13 | 3.98 | 4.20 | 3.02 | 2.41 | 2.91 |
| 11 | 1000 | 12 | 10 | 7 | 4.77 | 4.35 | 4.92 | 3.36 | 2.47 | 3.39 |
| 12 | 800 | 20 | 10 | 14 | 2.86 | 3.02 | 3.12 | 1.45 | 1.70 | 1.34 |
| **MAE** | | | | | | **0.222** | **0.124** | | **0.439** | **0.148** |
| **MSE** | | | | | | **0.073** | **0.022** | | **0.313** | **0.028** |

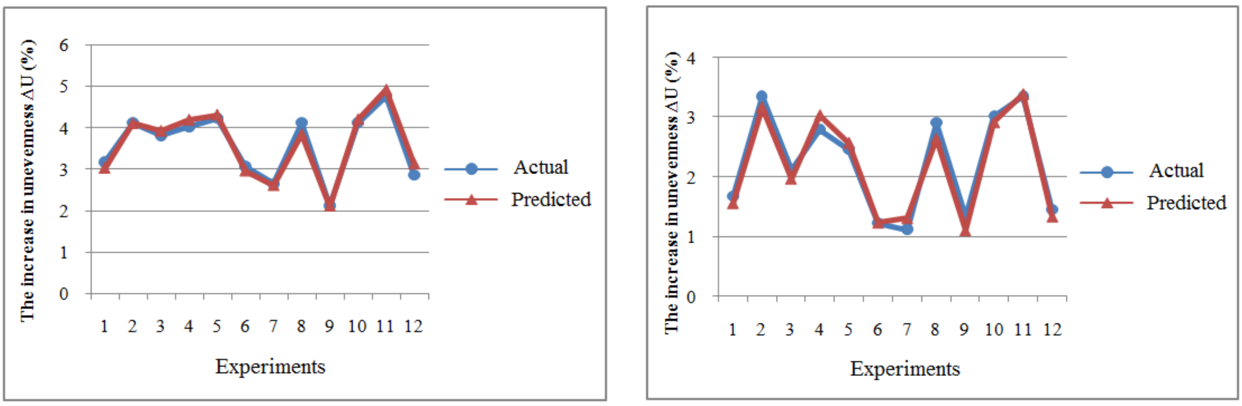


(a) (b)

**Figure 4.** Testing graph of ANN model for $\Delta U$ [%] of: (a) Ne 30/1 CVCM yarn, (b) Ne 30/1 COCM yarn.

Table 4 shows that predicted results by ANN have an $R^2$ value higher than that one given by the statistical model: 0.9997 > 0.8733 for Ne 30/1 CVCM yarn and 0.9893 > 0.8986 for the Ne 30/1 COCM yarn. Moreover, the MAE and MSE values determined by ANN were lower than those predicted by statistical models, with MAE values 0.0187 < 0.6469 for Ne 30/1 CVCM yarn and 0.095 < 0.1643 for Ne 30/1 COCM yarn and with MSE values: 0.0009 < 0.6649 for Ne 30/1 CVCM yarn and 0.0138 < 0.3134 for Ne 30/1 COCM yarn. The results show that the increase in yarn unevenness predicted by ANNs was more accurate than that predicted by statistical models. However, predictions by ANNs do not point out the influence of the factors on the results.

The performance of the built ANN model was further assessed by testing a data set of 12 experiments which were used for model testing and did not match with the learning data set, in which the technological parameters were selected in the defined research range. The test results are presented in Table 6. The graphs show the test results and the predicted values by the built ANN model are shown in Figure 4.

The test results of the ANN were accepted as good because the MAE and MSE errors were small which were 0.124; 0.022 for Ne 30/1 CVCM yarn and 0.148; 0.028 for Ne 30/1 COCM yarn. These results demonstrated that the built ANN model including 1 input layer, 5 hidden layers and 1 output layer obtained a good performance, and it was appropriate for determination of the increase in yarn unevenness. With the test set, the results confirmed that the predicting by using ANN has smaller MAE, and MSE values (achieving higher accuracy) than these of statistical models.

## CONCLUSIONS

1. In this study, the increase in unevenness of two types of yarn (Ne 30/1 CVCM, Ne 30/1 COCM) after winding was successfully predicted by statistical models and by artificial neural network (ANN) based on four winding technological parameters: Winding speed, the load on the friction discs of the yarn tensioner, the distance between the bobbin and the yarn guide and the pressure of package on the grooved drum. The ANN structure to predict the increase in yarn unevenness after winding has been built with 1 input layer, 5 hidden layers and 1 output layer. Among them, there were 4 neurons in the input layer which corresponded to 4 technological winding parameters, the number of neurons in the five hidden layers was 16, 8, 8, 8, and 4 respectively and the number neurons of in the output layer were 1, which was the increase in yarn unevenness value.

2. The coefficient of determination ($R^2$) of ANN models reached 0.9893; 0.9997 for Ne 30/1 CVCM yarn and Ne 30/1 COCM yarn, respectively which were higher than this parameter predicted by statistical models which were only 0.8733; 0.8986 for Ne 30/1 CVCM yarn and Ne 30/1 COCM yarn, respectively. Meanwhile, the parameters MAE and MSE predicted by ANN were smaller than those predicted by statistical models. That proves, predicting by ANN achieved higher accuracy than predicting by statistical models. However, predicting by statistical models can see the degree of influence of each factor on the predicted results.

3. In actual production, if it is found difficult to apply statistical models to predict the increase in yarn unevenness after winding, because the accuracy is low, and the results may be influenced by many factors, we should use ANN. However, predicted by ANN will not provide the influential degree of each factor on the results.

***Acknowledgement:*** *This research is funded by Hanoi University of Science and Technology (HUST) under project number T2022-PC-094.*

## REFERENCES


1. Nguyen, C.H., Tran, L.H., Ho, K.N.: Application of neural network to predict the workability parameters of self-compacting concrete. In: CIGOS 2019, Innovation for Sustainable Infrastructure. Lecture Notes in Civil Engineering, 54, 2020. https://doi.org/10.1007/978-981-15-0802-8_186
2. Doke S. and Shanmugam N.: Artificial Intelligence and its applications in textile, *Asian Textile Journal*, 49, 2002.
3. Malik, S., Farooq, A., Gereke, T. et al.: Prediction of blended yarn evenness and tensile properties by using artificial neural network and multiple linear regression, Autex Research Journal, 16(2), 2016, pp. 43-50. https://doi.org/10.1515/aut-2015-0018
4. Furferi R. and Gelli M.: Yarn strength prediction.: A practical model based on artificial neural networks, Advances in Mechanical Engineering, 2010, 640103. https://doi.org/10.1155/2010/640103
5. Haghighat E., Johari M.S., Etrati S.M., et al.: Study of the hairiness of polyester - viscose blended yarn: Part III - predicting yarn hairiness using an artificial neural networks, Fibres & Textiles in Eastern Europe, 20(1), 2012, pp. 33-38.
6. El-Geiheini A., Elkateb S., Abd-Elhamied M.R.: Yarn tensile properties modeling using Artificial Intelligence, Alexandria Engineering Journal, 59, 2020, pp. 4435-4440. https://doi.org/10.1016/j.aej.2020.07.049
7. Majumdar P.K., Majumdar A.: Predicting the breaking elongation of ring spun cotton yarns using mathematical, statistical, and artificial neural network models, Textile Research Journal, 74(7), 2004, pp. 652-655. https://doi.org/10.1177/004051750407400717
8. Islan MD. Z..: Effect of winding speed on yarn properties, Journal of Engineering Research and Application, 9(3), 2019, pp. 28 - 34.
9. Trung T.D., Huong Ch.D., Tuan D.A.: Research on new modeling of winding process for controlling yarn package pressure on grooved drum, In: Proceeding Aun/Seed-net joint regional conferences in transportation, energy and mechanical manufacturing engineering - RCTEMME 2021 pp. 162-168.
10. ASTM A1425/D1425M-14: Standard Test Method for Evenness of Textile Strands Using Capacitance Testing Equipment.
11. Trun T.D., Huong Ch.D., Tuan A.T.: Influence of some winding parameters on hairiness of yarn after winding process, Vlakna a textil, 29(4), 2022, pp. 29-37. https://doi.org/10.15240/tul/008/2022-4-004
12. Stjepanovič Z., Anton J..: Optimisation of cotton fibre blends using AI machine learning techniques, Department of

Textiles, Faculty of Mechanical Engineering, University of Maribor, 2001.

13. Shanbeh M., Hasani H., and Tabatabaei S.A.: Modelling and predicting the breaking strength and mass irregularity of cotton rotor-spun yarns containing cotton fiber recovered from ginning process by using artificial neural network algorithm, Modelling and Simulation in Engineering, 2011, 591905. https://doi.org/10.1155/2011/591905
14. Ünal P.G., Özdil N., Taşkın C.: The effect of fiber properties on the characteristics of spliced yarns Part I: Prediction of spliced yarns tensile properties, Textile Research Journal, 80, 2010, pp. 429-438. https://doi.org/10.1177/0040517509342318
15. Beltran R., Wang L., Wang X.: Predicting worsted spinning performance with an artificial neural network model, Textile Research Journal, 74(9), 2004, pp. 757-763. https://doi.org/10.1177/004051750407400902

*Fibres and Textiles* **30**(5), 2023, 11-23 DOI: 10.15240/tul/008/2023-5-002

# BUILDING DATABASE IN BALANCING KNITTED GARMENT LINES SOFTWARE IN INDUSTRY

**THAO, PHAN THANH* AND PHAN, DUY-NAM**

Hanoi University of Science and Technology, Hanoi 10000, Viet Nam

## ABSTRACT

The garment industry is one of the key industries contributing to the economic growth of Vietnam. Industry 4.0 has significantly altered the operational procedures of conventional enterprises. The implementation of technological, digital, and artificial intelligence applications has increased the global efficacy of corporate governance. To successfully assimilate into the regional and global economies, Vietnamese businesses must enhance their management capabilities and maximize both the quantity and quality of their products. In order to achieve this objective, the authors have conducted research to develop a database of sewing line balancing implemented in Assembly Line Balancing software for two common knitted products, namely Polo-Shirts, and T-Shirts. School of Textile-Leather and Fashion, Hanoi University of Science and Technology (HUST) methods compared and evaluated this result of sewing line balancing of 2 Polo-Shirt and T-Shirt products according to the manual, software, and actual calculation method at 3 enterprises: Star Fashion Company Ltd., Regent Garment Factory Ltd., and Hanoi General Textile Garment Joint Stock Company (Hanosimex). Since then, we have completed the sewing line balancing database for Polo-Shirt and T-Shirt products to row sewing lines for cases in which the path of semi-finished products is both straight and zigzag. The findings of this study can be applied to group conjugation lines and suspended lines transporting semi-finished goods. The database has been constructed meticulously and standardized to ensure the diversity, richness, and universality of all product technology structure options applicable to garment companies. The database is utilized in the Assembly Line Balancing software developed by the research team; this is an application-oriented research product that will transfer technology to garment enterprises producing knitwear, assisting them in overcoming current challenges. Reasonable production line layout contributes to optimizing existing production conditions, increasing labor productivity and the efficiency of production organization, and laying the groundwork for the application of digital technology.

## KEYWORDS

Sewing line; Assembly line balancing; Polo-Shirt; T-Shirt; Assembly line balancing software; Assembly line balancing methods.

## INTRODUCTION

Line balancing is a technique to arrange the ratio between several workers and machinery equipment at each stage in which output is equal and achieves the highest based on the actual conditions of the line, optimizing the actual situation on the line in the line balancing time. Line balancing is one of the most important issues for garment companies. It determines the capacity and output of the sewing line and simultaneously helps reduce workers' wasted time, optimize the number of machines, determine the shortest path of semi-finished products, and follow the turmeric work journey. It shows that line balancing significantly affects the profit and reputation of enterprises. Hence, businesses always want to find the most reasonable method of balancing line with the company and their garment products. In Vietnamese garment enterprises, line balancing is mainly done by traditional manual methods, is time-consuming, and the balancing performance is not high, not solving the problem of maximum efficiency in the production line and affecting the productivity of sewing line and the whole enterprise. Contributing to solving these bad problems, the authors have built a database of the sewing line balancing applied in the line balancing software by production practices.

Currently, there have been several research works on this issue. Santosh et al. applied the Rank Position Weight method (RPW) with a given number of workers to optimize cycle time [1]. Author Vrittika applies three methods including: Rank Position Weight (RPW); larger candidate rule and kill bridge and wester methods to optimize the cycle time when given several workers. The author points out that the

* **Corresponding author:** Thao P.T., e-mail: *thao.phanthanh@hust.edu.vn*

*Received March 23, 2023; accepted October 5, 2023*

results are the same [2]. Jayakumar et al. use RPW to enhance line efficiency [3]. The authors Dinh Mai Huong, Truong Van Long, Do Phan Thuan, Phan Thanh Thao, Nguyen Duc Nghia apply an exhaustive search for optimization assembly line balancing in garment industry [4]. Phan Thanh Thao and Dinh Mai Huong research various line-balancing methods for Polo-shirt products in Vietnam [5].

In this paper, the authors compare, evaluate the design results, and balance the sewing line of T-Shirt and Polo-Shirt products based on the Hanoi University of Science and Technology method by hand calculation and using BSL-HUST software with the results of actual production. Since then, we have proceeded to complete the design and balance database of the T-Shirt and Polo-Shirt products sewing line for the layout in which the path of the semi-finished products is straight and zigzag applied in industrial production. Compare and evaluate the design results and balance the sewing line of the T-Shirt and Polo-Shirt products based on the Hanoi University of Science and Technology method by hand calculation and using BSL-HUST software with the results of actual production. Complete the design and balance database of the T-Shirt and Polo-Shirt products sewing line for the layout in which the path of the semi-finished products is straight and zigzag applied in industrial production.

# EXPERIMENTAL

## Research subjects

T-Shirt products have a collar (neck) rib or collar facing, or neck tape (neckline), short-sleeved, slits or not. In the study, we chose a typical structure manufactured by three companies with the styles shown in Table 1. The product has a straight shape, rib roll collar, neckline from collar to shoulder, no split, bottom and sleeve-hem sewing dividing seams with two parallel lines. The product has a picture, as shown in Figure 1 (a).

Polo-shirt products have bottom down collar, neckline or not. Collar is by main fabric or rib. The shirt is made from single layer knit fabric. It is slip over dress, with collar and neck band placket (collar panel),short- or long-sleeve, slit or not, sleeve cuff or sleeve-hem sewing diving seams with two parallel lines.

**Table 1.** T-Shirt product codes, with each styled by three companies.

| No. | Code | Style | Company |
|---|---|---|---|
| 1 | T01 | DM21-008 | Hanosimex |
| 2 | T02 | PE19-025 | Hanosimex |
| 3 | T03 | PCN21-003 | Hanosimex |
| 4 | T04 | PE20-015 | Hanosimex |
| 5 | T05 | 5V2202128 | Star Fashion Co., Ltd |
| 6 | T06 | SV22-009 | Hanosimex |
| 7 | T07 | 142N212 | Tinh Loi Garment Co., Ltd |
| 8 | T08 | 242N276 | Tinh Loi Garment Co., Ltd |

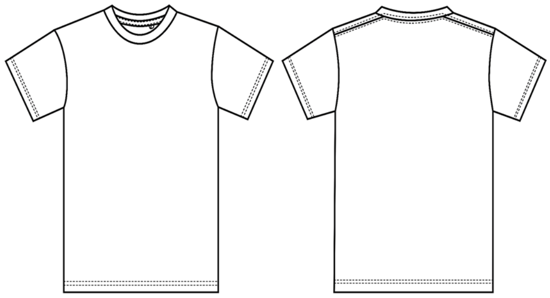
(a)

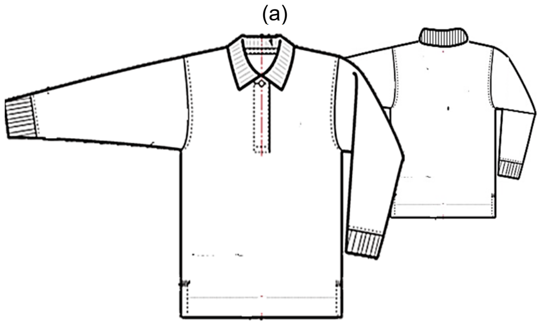
(b)

**Figure 1.** Representative images of (a) T-Shirt product - straight shape, rib roll collar, neckline from collar to shoulder, no split, bottom, and sleeve-hem sewing dividing seams with two parallel lines and (b) Polo-Shirt product - Bottom down collar by rib, not neckline; collar panel deviates; long sleeves by rib-knit cuff; split, bottom sewing one diving seam.

**Table 2.** Polo-Shirt product codes, with each style by two companies.

| No. | Code | Style | Company |
|---|---|---|---|
| 1 | PL01 | SNJ20-017 | Hanosimex |
| 2 | PL02 | PE18-019 | Hanosimex |
| 3 | PL03 | PE19-026 | Hanosimex |
| 4 | PL04 | 342F107 | Tinh Loi Garment Co., Ltd |
| 5 | PL05 | 06DHA22- 019 | Hanosimex |
| 6 | PL06 | DC1963 | Tinh Loi Garment Co., Ltd |

In the study, we choose a typical structure with the image described in Figure 1 (b), manufactured at two companies with the styles shown in Table 2. The product has bottom down collar by rib, not neckline; collar panel deviates; long sleeves by rib-knit cuff; split, bottom sewing one diving seam.

## Research methods

Methods of database construction

To build a database on line balancing, the first step is to analyze and classify detailed clusters of knitted products, make a technological process for each product, and after that, design and balance the line and arrange the line layout for two inputs: the capacity of line P (the number of products produced in a shift) and the number of workers on line N (People).

Methods of building sewing technology process

Based on the theory of the method of building a sewing technology process, the authors build a diagram to analyze the technological process of sewing T-Shirt and Polo-Shirt products.

Methods of designing and balancing the sewing line

Designing and balancing the sewing lines in two ways: manually and using BSL-HUST software built by the design project, based on the Hanoi University of Science and Technology method.

a, The order of designing and balancing the sewing line according to Hanoi University of Science and Technology method.

- Preliminary determination of the parameters of the line
- Build a production technology diagram and balance the line
- Precisely define the parameters of the line
- Layout of the workplace and sewing line
- Calculate the economic-technical indicators of the line

b, Principles of organizing and coordinating tasks.

- The workstations must be made up of successive tasks on the technological journey or from tasks of different processing groups that do not affect product processing.
- The sequence of the combined operations must be consistent with the sequence of the product processing technology.
- The workstation time must be equal to or an integer times the cycle.
- The level of workers must be equal or differ by one unit.
- The tasks of the workstation must be performed on the same type of equipment; the processing mode, method, and type of processing material must be relatively uniform; the complexity of the work must be relatively uniform.
- In addition, it is necessary to coordinate the tasks so that the workstation can only be performed on the same object.

Check the optimal condition of capacity by the graph method. Draw the load graph of the line, in which the horizontal axis is the workstations, and the vertical axis is the individual cycle of workstations. On the graph, simultaneously show the values: the cycle (R), and the allowable tolerance limit of cycle ΔR ($R_{max}$÷ $R_{min}$). Determine the ratio of the number of workstations with separate cycles within the allowable tolerance limit of the cycle to the total number of workstations in line *K* [%]. If K% ≥ 60%, the line balances in terms of load and calculated capacity to reach the optimal value.

c, Line designing and balancing process using BSL-HUST software

Implementation steps:

- Step 1: Start the program and double-click the software interface as shown below.
- Step 2: After the software interface appears, select "Create new code".
- Step 3: Input the information, including "Code details", "Technological process", "Process binding".
- Step 4: After inputting all the information, click "Optimize".
- Step 5: Enter the input data for the problem and continue to click "Optimize", you will get the results, including the workstation table, load chart, and line layout diagram.

## Methods of collecting actual data

The research team collected documents on production orders of T-shirt products at three companies: Hanosimex, Star Fashion Co., Ltd and Tinh Loi Garment Co., Ltd; for Polo-Shirt products from two companies: Hanosimex and Tinh Loi Garment Co., Ltd.

## Methods of analysis, evaluation and comparison

After obtaining the calculation results, analyze and compare to evaluate the efficiency of the production line's balance by the manual method, using BSL-HUST software and compare the actual production.

The codes T01, T02, T03, T04, T05, T06, PL01, PL02, PL03, and PL05 will compare the results of sewing line balancing design between the manual calculation method of HUST and BSL-HUST software. The criteria for comparison and evaluation include line balancing coefficient K%, balancing efficiency H%, capacity P, number of workers N, and cycle time R.

The codes T07, T08, PL04, and PL06 will compare the results of the sewing line balance design with the results of the actual production line at Tinh Loi Company, the manual calculation method of HUST, and BSL-HUST software. The criteria for comparison and evaluation include line balancing coefficient K%, balancing efficiency *H* %, capacity *P*, number of workers *N*, and cycle time *R*.

# RESULTS AND DISSCUTION

## Results of technical process analysis of sewing knitted products

During the research process, we calculated, compared, analyzed, and completed the sewing line balanced and design database, including eight T-Shirt codes and six Polo-Shirt codes. In the scope of this article, we represent a T-Shirt and a Polo-Shirt code.

We have developed a process analysis diagram for T-Shirt and Polo-Shirt sewing technology, and the results are presented in Figure 2 .

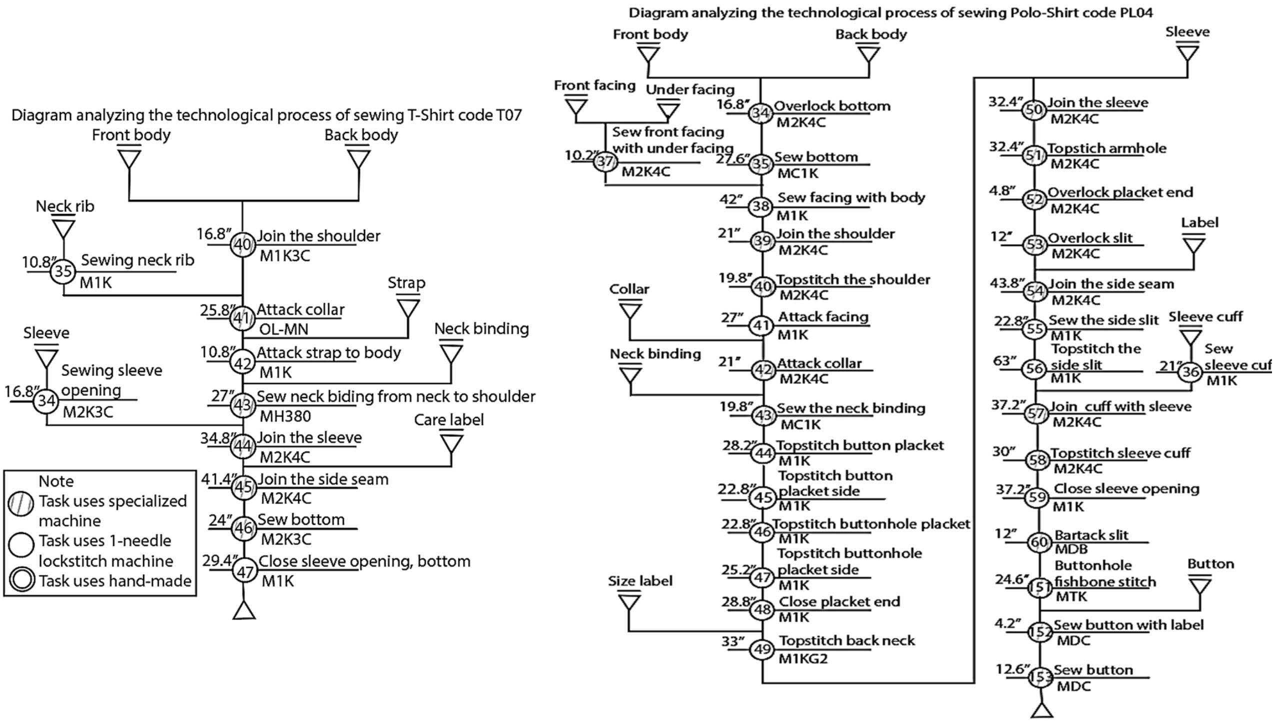


(a) (b)

**Figure 2.** T-Shirt sewing technology analysis chart: (a) code T07, code PL04.

**Table 3.** Table of organization and coordination of tasks into workstations result, T-shirt coded T07 with the given capacity *P*.

| Workstation | Task | Machine | Type | $T_i$ [s] | Line balancing by hand | | Line balancing by BSL-HUST software | | Line balancing by Tinh Loi Garment Co., Ltd plan | |
|---|---|---|---|---|---|---|---|---|---|---|
| | | | | | $T_j$ [s] | $N_j$ [people] | $T_j$ [s] | $N_j$ [people] | $T_j$ [s] | $N_j$ [people] |
| 1 | 34 | M2K3C | 4 | 16.8 | 8.4 | 2 | 8.4 | 2 | 16.8 | 1 |
| 2 | 35 | M1K | 3 | 10.8 | 10.8 | 1 | 10.8 | 1 | 10.8 | 1 |
| 3 | 40 | M1K3C | 3 | 16.8 | 16.8 | 1 | 8.4 | 2 | 16.8 | 1 |
| 4 | 41 | OL-MN | 4 | 25.8 | 12.9 | 2 | 12.9 | 2 | 8.6 | 3 |
| 5 | 42 | M1K | 3 | 10.8 | 10.8 | 1 | 10.8 | 1 | 10.8 | 1 |
| 6 | 43 | MH380 | 4 | 27 | 13.5 | 2 | 13.5 | 2 | 13.5 | 2 |
| 7 | 44 | M2K4C | 4 | 34.8 | 11.6 | 3 | 11.6 | 3 | 11.6 | 3 |
| 8 | 45 | M2K4C | 4 | 41.4 | 13.8 | 3 | 13.8 | 3 | 10.35 | 4 |
| 9 | 46 | M2K3C | 4 | 24 | 12 | 2 | 12 | 2 | 12 | 2 |
| 10 | 47 | M1K | 3 | 29.4 | 9.8 | 3 | 9.8 | 3 | 14.7 | 2 |
| Sum | | | | 237.6 | | 20 | | 21 | | 20 |

**Table 4.** Comparison of full line load chart for product T-shirt coded T07 with the given capacity *P*.

| | Line balancing by hand of HUST method | Line balancing by BSL-HUST software | Line balancing by Tinh Loi Garment Co., Ltd plan |
|---|---|---|---|
| Image | 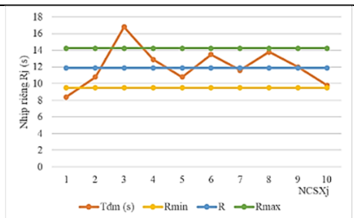  | 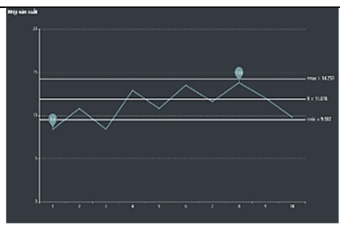 | 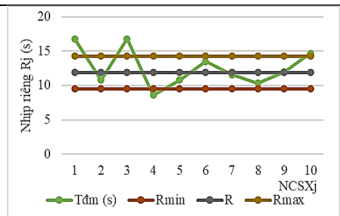  |
| Comment | One workstation is overloaded, one workstation is underloaded. | Two workstations are underloaded | Three workstations are overloaded, one workstation is underloaded |

**Table 5.** Comparison of the sewing line layout diagram for T-shirt coded T07 product with the given capacity *P*.

| | The sewing line layout diagram for T-shirt product coded T07 | Layout |
|---|---|---|
| By hand method of HUST | 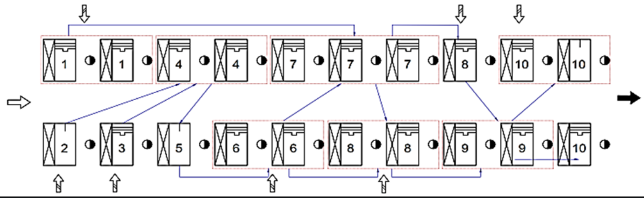 | Class-form, semi-finished products are shipped by zigzag, with boxes |
| By BSL-HUST software |  | Class-form, semi-finished products are shipped by zigzag, with boxes |
| By design plan of Tinh Loi Garment Co., Ltd | 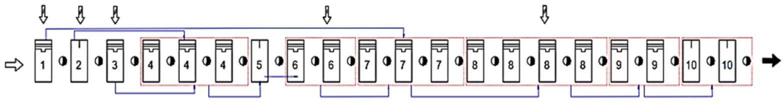 | Class-form, semi-finished products are shipped by zigzag, with semi-automatic hanging line |

**Table 6.** Table comparing line parameters - line balancing coefficient *K*%, balancing efficiency *H*%, capacity *P*, number of workers *N*, and cycle time *R* of T-shirt coded T07 with the given capacity *P*.

| *P*=2652 products/day | *K* [%] | *H* [%] | *N* [people] | *R* [s] |
|---|---|---|---|---|
| By Tinh Loi Garment Co., Ltd | 60 | 100 | 20 | 11.88 |
| By hand method of HUST | 80 | 100 | 20 | 11.88 |
| By BSL-HUST software | 80 | 95.26 | 21 | 11.88 |

## Comparing and evaluating the design and balance results T-Shirt sewing line according to HUST method by hand calculation, using BSL-HUST software and the actual results at IE room of Tinh Loi Garment Co., Ltd

Comparing and evaluating the design and balance result sewing line when given the capacity of line P (products/shift)

- The cycle time: $R$
- Cycle time limit: $\Delta R$=20%
- Line capacity: $P$ = 2652 products/shift
- Working time: $T_w$ = 8.75 (h)
- The time of task number $i$: $T_i$ (s)
- The average production time at each working station number $j$: $T_j$ (s)
- The number of workers for each task $i$: $N_i$ (people)

Comparison of the organization and coordination of tasks results is shown in Table 3. Comparison of the full-line load charts is shown in Table 4. Comparison of the sewing line layout diagrams is shown in Table 5. Comparison of the exact results of line parameters is shown in Table 6.

Two ways of line balancing according to the method of HUST (manual calculation and BSL-HUST software) gave $K$ = 80% > 60%, and line capacity $P$ = 2652 products/day, which is optimal and higher than the results of Tinh Loi Garment Co., Ltd.

The number of workers N in the line calculated by BSL-HUST software is more significant than one worker, and the load factor H is smaller than the other two ways of balancing.

The results of the sewing line layout with the given capacity P from BSL-HUST software have an area larger than the remaining two methods due to the increase in the number of employees to 1 worker. However, the software gives more optimal passing results on the path of the semi-finished product.

It is class - form, semi-finished products shipped straight and zigzag, but Tinh Loi Garment Co., Ltd. will combine the two lines running the same T-Shirt product code, using hanging lines to replace boxes, help save area, and improve labour productivity. Therefore, the research team realized that it was necessary to improve the software to diversify layout options.

Cause: It can be seen in the load chart of the whole line from the software that there are no overloaded locations but mainly under-loaded operations, thus leading to an increase in the number of workers, and H% lower than the other two methods. But this is a perfectly reasonable result for avoiding overloading and congestion on the line.

**Table 7.** Table of organization and coordination of tasks into workstations result, T-shirt product coded T07 with given the number of workers *N*.

| Workstation | Task | Machine | Type | $T_i$ [s] | Line balancing by hand | | Line balancing by BSL-HUST software | | Line balancing by Tinh Loi Garment Co., Ltd plan | |
|---|---|---|---|---|---|---|---|---|---|---|
| | | | | | $T_j$ [s] | $N_j$ [people] | $T_j$ [s] | $N_j$ [people] | $T_j$ [s] | $N_j$ [people] |
| 1 | 34 | M2K3C | 4 | 16.8 | 8.4 | 2 | 8.4 | 2 | 16.8 | 1 |
| 2 | 35 | M1K | 3 | 10.8 | 10.8 | 1 | 10.8 | 1 | 10.8 | 1 |
| 3 | 40 | M1K3C | 3 | 16.8 | 16.8 | 1 | 8.4 | 2 | 16.8 | 1 |
| 4 | 41 | OL-MN | 4 | 25.8 | 12.9 | 2 | 12.9 | 2 | 8.6 | 3 |
| 5 | 42 | M1K | 3 | 10.8 | 10.8 | 1 | 10.8 | 1 | 10.8 | 1 |
| 6 | 43 | MH380 | 4 | 27 | 13.5 | 2 | 13.5 | 2 | 13.5 | 2 |
| 7 | 44 | M2K4C | 4 | 34.8 | 11.6 | 3 | 11.6 | 3 | 11.6 | 3 |
| 8 | 45 | M2K4C | 4 | 41.4 | 13.8 | 3 | 13.8 | 3 | 10.35 | 4 |
| 9 | 46 | M2K3C | 4 | 24 | 12 | 2 | 12 | 2 | 12 | 2 |
| 10 | 47 | M1K | 3 | 29.4 | 9.8 | 3 | 14.7 | 2 | 14.7 | 2 |
| Sum | | | | 237.6 | | 20 | | 20 | | 20 |

**Table 8.** Comparison of the full line load chart for T-shirt product coded T07 with given the number of workers *N*.

| | Line balancing by hand of HUST method | Line balancing by BSL-HUST software | Line balancing by Tinh Loi Garment Co., Ltd plan |
|---|---|---|---|
| Image | 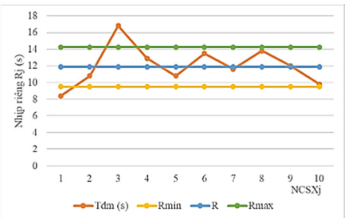  | 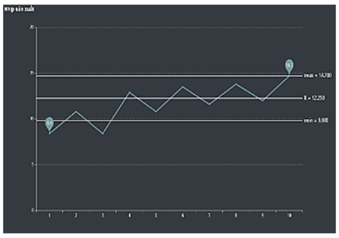 | 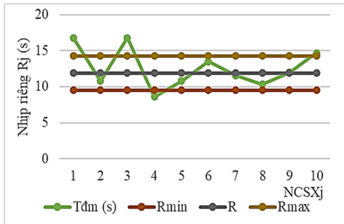  |
| Comment | One workstation is overloaded, one workstation is underloaded | Two workstations are underloaded | Three workstations are overloaded, one workstation is underloaded |

**Table 9.** Comparison of the sewing line layout diagram for T-shirt product coded T07 when given the number of workers *N*.

| | The sewing line layout diagram for T-shirt product coded T07 | Layout |
|---|---|---|
| By hand method of HUST | 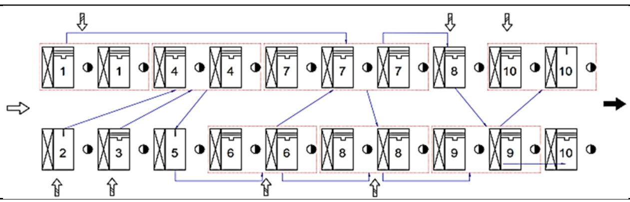 | Class-form, semi-finished products are shipped by zigzag, with boxes |
| By BSL-HUST software | 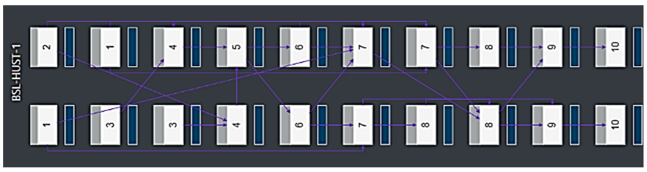  | Class-form, semi-finished products are shipped by zigzag, with boxes |
| By design plan of Tinh Loi Garment Co., Ltd | 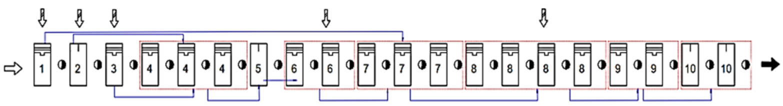 | Class-form, semi-finished products are shipped by straight, with semi-automatic hanging line |

**Table 10.** Table of comparing line parameters - line balancing coefficient *K*%, balancing efficiency *H*%, capacity *P*, number of workers *N* and cycle time *R* of code T07 when given *N*.

| ***N* = 20 people** | ***K* [%]** | ***H* [%]** | ***N* [people]** | ***R* [s]** |
|---|---|---|---|---|
| By Tinh Loi Garment | 60 | 100 | 20 | 11.88 |
| By hand method of HUST | 80 | 100 | 20 | 11.88 |
| By BSL-HUST software | 80 | 96.98 | 20 | 12.25 |

**Table 11.** Table of organization and coordination of tasks into workstations result of Polo-shirt coded PL04 when given the capacity *P*.

| Line balancing by hand of HUST method | | | | | Line balancing by BSL-HUST software | | | | | Line balancing by Tinh Loi Garment Co., Ltd plan | | | | |
|---|---|---|---|---|---|---|---|---|---|---|---|---|---|---|
| Workstation | Task | $T_i$ | $N_i$ | $T_j$ | Workstation | Task | $T_i$ | $N_i$ | $T_j$ | Workstation | Task | $T_i$ | $N_i$ | $T_j$ |
| 1 | 34 | 16.8 | 1 | 16.8 | 1 | 34 | 16.8 | 1 | 16.8 | 1 | 34 | 16.8 | 1 | 16.8 |
| 2 | 35 | 27.6 | 2 | 13.8 | 2 | 35 | 27.6 | 2 | 13.8 | 2 | 35 | 27.6 | 2 | 13.8 |
| 3 | 36 | 21 | 1 | 21 | 3 | 36 | 21 | 3 | 16 | 3 | 36 | 21 | 1 | 21 |
| 4 | 37 | 10.2 | 1 | 10.2 | | 41 | 27 | | | 4 | 37 | 10.2 | 1 | 10.2 |
| 5 | 38 | 39 | 2 | 19.5 | 4 | 37 | 10.2 | 1 | 10.2 | 5 | 38 | 39 | 2 | 19.5 |
| 6 | 39 | 21 | 1 | 21 | 5 | 38 | 39 | 2 | 19.5 | 6 | 39 | 21 | 1 | 21 |
| 7 | 40 | 19.8 | 1 | 19.8 | 6 | 39 | 21 | 1 | 21 | 7 | 40 | 19.8 | 1 | 19.8 |
| 8 | 41 | 27 | 2 | 13.5 | 7 | 40 | 19.8 | 1 | 19.8 | 8 | 41 | 27 | 2 | 13.5 |
| 9 | 42 | 21 | 1 | 21 | 8 | 42 | 21 | 1 | 21 | 9 | 42 | 21 | 1 | 21 |
| 10 | 43 | 19.8 | 1 | 19.8 | 9 | 43 | 19.8 | 1 | 19.8 | 10 | 43 | 19.8 | 1 | 19.8 |
| 11 | 44 | 27 | 2 | 13.5 | 10 | 44 | 27 | 2 | 13.5 | 11 | 44 | 27 | 1 | 27 |
| 12 | 45 | 21 | 1 | 21 | 11 | 45 | 21 | 1 | 21 | 12 | 45 | 21 | 3 | 22 |
| 13 | 46 | 21 | 1 | 21 | 12 | 46 | 21 | 1 | 21 | | 46 | 21 | | |
| 14 | 47 | 24 | 3 | 16.8 | 13 | 47 | 24 | 3 | 16.8 | | 47 | 24 | | |
| | 48 | 26.4 | | | | 48 | 26.4 | | | 13 | 48 | 26.4 | 2 | 13.2 |
| 15 | 49 | 33 | 2 | 16.5 | 14 | 49 | 33 | 2 | 16.5 | 14 | 49 | 33 | 1 | 33 |
| 16 | 50 | 32.4 | 2 | 16.2 | 15 | 50 | 32.4 | 2 | 16.2 | 15 | 50 | 32.4 | 2 | 16.2 |
| 17 | 51 | 32.4 | 2 | 16.2 | 16 | 51 | 32.4 | 2 | 16.2 | 16 | 51 | 32.4 | 2 | 16.2 |
| 18 | 52 | 4.8 | 1 | 16.8 | 17 | 52 | 4.8 | 1 | 16.8 | 17 | 52 | 4.8 | 1 | 4.8 |
| | 53 | 12 | | | | 53 | 12 | | | 18 | 53 | 12 | 3 | 18.6 |
| 19 | 54 | 43.8 | 2 | 21.9 | 18 | 54 | 43.8 | 2 | 21.9 | | 54 | 43.8 | | |
| 20 | 55 | 22.8 | 1 | 22.8 | 19 | 55 | 22.8 | 2 | 11.4 | 19 | 55 | 22.8 | 1 | 22.8 |
| 21 | 56 | 60 | 3 | 20 | 20 | 56 | 60 | 3 | 20 | 20 | 56 | 60 | 3 | 20 |
| 22 | 57 | 36 | 2 | 18 | 21 | 57 | 36 | 2 | 18 | 21 | 57 | 36 | 1 | 36 |
| 23 | 58 | 24 | 2 | 12 | 22 | 58 | 24 | 2 | 12 | 22 | 58 | 24 | 1 | 24 |
| 24 | 59 | 37.2 | 2 | 18.6 | 23 | 59 | 37.2 | 2 | 18.6 | 23 | 59 | 37.2 | 2 | 18.6 |
| 25 | 60 | 12 | 1 | 12 | 24 | 60 | 12 | 1 | 12 | 24 | 60 | 12 | 1 | 12 |
| 26 | 151 | 24.6 | 1 | 24.6 | 25 | 151 | 24.6 | 2 | 12.3 | 25 | 151 | 24.6 | 1.5 | 16.4 |
| 27 | 152 | 4.2 | 1 | 16.8 | 26 | 152 | 4.2 | 1 | 16.8 | 26 | 152 | 4.2 | 1 | 16.8 |
| | 153 | 12.6 | | | | 153 | 12.6 | | | 27 | 153 | 12.6 | | |

Comparing and evaluate the design and balance result sewing line when given the number of workers N (people)

- Cycle time limit: $\Delta R$ = 20%
- Number of workers: *N* = 20 people
- Working time: $T_w$ = 8.75 (h)
- The time of task number *i*: $T_i$ (s)
- The average production time at each working station number *j*: $T_j$ (s)
- The number of workers for each task *i*: $N_i$ (people)

Comparison of the organization and coordination of tasks results is shown in Table 7. Comparison of the full-line load charts is shown in Table 8. Comparison of the sewing line layout diagrams is shown in Table 9. Comparison of the exact results of line parameters is shown in Table 10.

Two ways of line balancing according to the method of HUST gave K = 80% > 60%, which was higher than the company's result. The R value calculated from software is significantly larger than the other two methods, resulting in a smaller P value.

The results of sewing line layouts are similar: Class-form, semi-finished products shipped zigzag; but Tinh Loi Garment Co., Ltd. will combine the two lines running the same T-Shirt product code, using hanging lines to replace boxes, help save area, and improve labour productivity. Therefore, the research team realized that it was necessary to improve the software to diversify layout options. Cause: To ensure that the number of workers on the line is 20 people, the software has increased the cycle time to ensure efficiency, thereby affecting the load factor of the whole line.

## Comparing and evaluating the design and balance results Polo-Shirt sewing line according to HUST method by hand calculation, using BSL-HUST software and the actual results at IE room of Tinh Loi Garment Co., Ltd

Comparing and evaluating the design and balance result sewing line when given the capacity of line *P* (products/shift)

- Cycle time limit: $\Delta R$ = 20%
- Line capacity: *P* = 1667 products/shift
- Working time: $T_w$=8.75 (h)
- The time of task number *i*: $T_i$ (s)
- The average production time at each working station number *j*: $T_j$ (s)
- The number of workers for each task *i*: $N_i$ (people)

Comparison of the organization and coordination of tasks results is shown in Table 11. Comparison the full-line load charts is shown in Table 12. Comparison the sewing line layout diagrams is shown in Table 13. Comparison the exact results of line parameters is shown in Table 14.

With the given P, BSL-HUST software gave *K*% > 60%, much higher than the manual calculation of the HUST or IE department of Tinh Loi Garment Co., Ltd. However, the number of workers and the load factor have not been optimized.

The results of sewing line layouts are similar: Class-form, semi-finished products shipped zigzag; but Tinh Loi Garment Co., Ltd. will combine the two lines running the same T-Shirt product code, using hanging lines to replace boxes, help save area, and improve labour productivity. Therefore, the research team realized that it was necessary to improve the software to diversify layout options. Cause: It can be seen that the software gave no overloaded positions but mainly underloaded workstations, thus leading to an increase in the number of workers and the load factor is not optimal. But this is a perfectly reasonable result that can be applied to high performance.

**Table 12.** Table of comparison of full line load chart for product Polo-shirt coded PL04 when given the capacity *P*.

| | Line balancing by hand of HUST method | Line balancing by BSL-HUST software | Line balancing by Tinh Loi Garment Co., Ltd plan |
|---|---|---|---|
| Image | 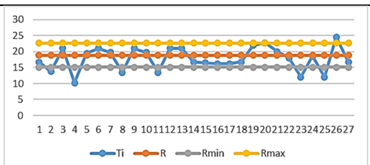 | 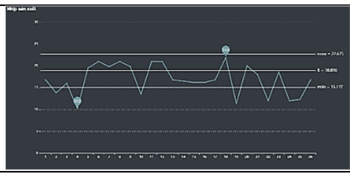 | 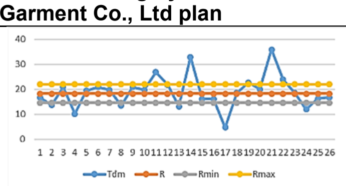 |
| Comment | One workstation is overloaded, six workstations are underloaded | Seven workstations are underloaded | Five workstations are overloaded, six workstations are underloaded |

**Table 13.** Table of comparison of sewing line layout diagram for PL04 product when given the capacity *P* of Polo-shirt coded PL04.

| | The sewing line layout diagram for Polo-shirt product coded PL04 | Layout |
|---|---|---|
| By hand method of HUST | 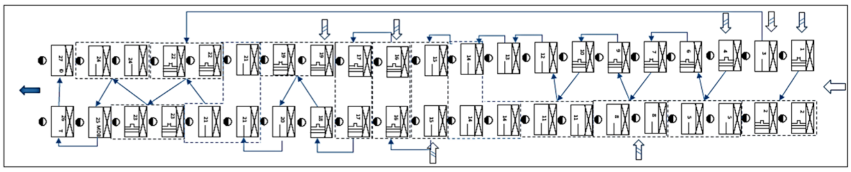 | Class-form, semi-finished products are shipped by zigzag, with boxes |
| By BSL-HUST software | 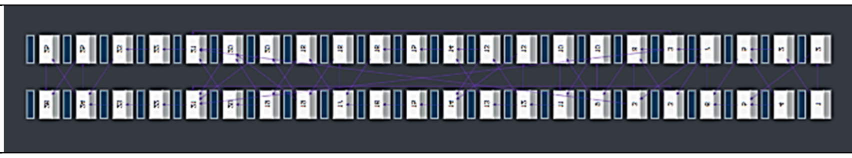 | Class-form, semi-finished products are shipped by zigzag, with boxes |
| By design plan of Tinh Loi Garment Co., Ltd | 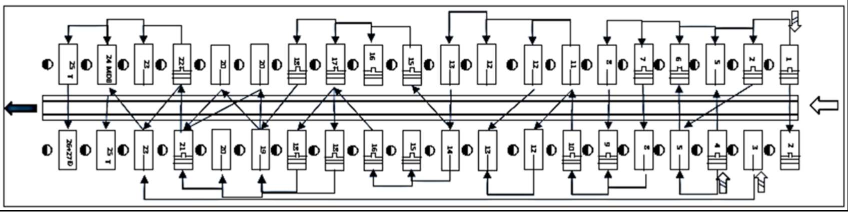 | Class-form, semi-finished products are shipped by zigzag, with semi-automatic hanging line |

**Table 14.** Table of comparing line parameters of Polo-shirt coded PL04 when given the capacity *P*.

| *P*=1667 products/day | *K* [%] | *H* [%] | *N* [people] | *R* [s] |
|---|---|---|---|---|
| By Tinh Loi Garment Co., Ltd | 59 | 100 | 40 | 18.36 |
| By hand method of HUST | 70.4 | 93 | 42 | 18.9 |
| By BSL-HUST software | 73.1 | 88.3 | 44 | 18.9 |

Comparing and evaluating the design and balance result sewing line when given N (people)

- Cycle time limit: $\Delta R$ = 20%
- Number of workers: $N$ = 40 people
- Working time: $T_w$ = 8.75 (h)
- The time of task number $i$: $T_i$ (s)
- The average production time at each working station number $j$: $T_j$ (s)
- The number of workers for each task $i$: $N_i$ (people)

Comparison the organization and coordination of tasks results is shown in Table 15. Comparison the full-line load charts is shown in Table 16. Comparison the sewing line layout diagrams is shown in Table 17. Comparison of the exact results of line parameters is shown in Table 18.

With the given the number of workers $N$, the BSL-HUST software gave an efficiency result of $K$% > 60%, much higher than the manual calculation method of the HUST or IE department of Tinh Loi Garment Co., Ltd. The power according to the balance software is lower, but the difference is not much. The load factor is not optimized by manual calculation of HUST or IE room; however, the software results only for five under-loaded workstations, with no overload.

The results of sewing line layouts are similar: Class-form, semi-finished products shipped zigzag; but Tinh Loi Garment Co., Ltd. will combine the two lines running the same T-Shirt product code, using hanging lines to replace boxes, help save area, and improve labour productivity. Therefore, the research team realized that it was necessary to improve the software to diversify layout options. Cause: With the number of 40 workers, the software has increased the cycle time to ensure efficiency, thereby affecting the load factor and capacity results.

**Table 15.** Table of organization and coordination of tasks into workstations result of Polo-shirt coded PL04 when given the number of workers $N$.

| Line balancing by hand of HUST method | | | | | Line balancing by BSL-HUST software | | | | | Line balancing by Tinh Loi Garment Co., Ltd plan | | | | |
|---|---|---|---|---|---|---|---|---|---|---|---|---|---|---|
| Workstation | Task | $T_i$ | $N_i$ | $T_j$ | Workstation | Task | $T_i$ | $N_i$ | $T_j$ | Workstation | Task | $T_i$ | $N_i$ | $T_j$ |
| 1 | 34 | 16.8 | 1 | 16.8 | 1 | 34 | 16.8 | 1 | 16.8 | 1 | 34 | 16.8 | 1 | 16.8 |
| 2 | 35 | 27.6 | 2 | 13.8 | 2 | 35 | 27.6 | 2 | 13.8 | 2 | 35 | 27.6 | 2 | 13.8 |
| 3 | 36 | 21 | 1 | 21 | 3 | 36 | 21 | 2 | 24 | 3 | 36 | 21 | 1 | 21 |
| 4 | 37 | 10.2 | 1 | 10.2 | | 41 | 27 | | | 4 | 37 | 10.2 | 1 | 10.2 |
| 5 | 38 | 39 | 2 | 19.5 | 4 | 37 | 10.2 | 1 | 10.2 | 5 | 38 | 39 | 2 | 19.5 |
| 6 | 39 | 21 | 1 | 21 | 5 | 38 | 39 | 2 | 19.5 | 6 | 39 | 21 | 1 | 21 |
| 7 | 40 | 19.8 | 1 | 19.8 | 6 | 39 | 21 | 1 | 21 | 7 | 40 | 19.8 | 1 | 19.8 |
| 8 | 41 | 27 | 1 | 27 | 7 | 40 | 19.8 | 1 | 19.8 | 8 | 41 | 27 | 2 | 13.5 |
| 9 | 42 | 21 | 1 | 21 | 8 | 42 | 21 | 1 | 21 | 9 | 42 | 21 | 1 | 21 |
| 10 | 43 | 19.8 | 1 | 19.8 | 9 | 43 | 19.8 | 1 | 19.8 | 10 | 43 | 19.8 | 1 | 19.8 |
| 11 | 44 | 27 | 1 | 27 | 10 | 44 | 27 | 2 | 13.5 | 11 | 44 | 27 | 1 | 27 |
| 12 | 45 | 21 | 1 | 21 | 11 | 45 | 21 | 1 | 21 | 12 | 45 | 21 | 3 | 22 |
| 13 | 46 | 21 | 1 | 21 | 12 | 46 | 21 | 3 | 23.8 | | 46 | 21 | | |
| 14 | 47 | 24 | 3 | 16.8 | | 47 | 24 | | | | 47 | 24 | | |
| | 48 | 26.4 | | | | 48 | 26.4 | | | 13 | 48 | 26.4 | 2 | 13.2 |
| 15 | 49 | 33 | 2 | 16.5 | 13 | 49 | 33 | 2 | 16.5 | 14 | 49 | 33 | 1 | 33 |
| 16 | 50 | 32.4 | 2 | 16.2 | 14 | 50 | 32.4 | 2 | 16.2 | 15 | 50 | 32.4 | 2 | 16.2 |
| 17 | 51 | 32.4 | 2 | 16.2 | 15 | 51 | 32.4 | 2 | 16.2 | 16 | 51 | 32.4 | 2 | 16.2 |
| 18 | 52 | 4.8 | 1 | 16.8 | 16 | 52 | 4.8 | 1 | 16.8 | 17 | 52 | 4.8 | 1 | 4.8 |
| | 53 | 12 | | | | 53 | 12 | | | 18 | 53 | 12 | 3 | 18.6 |
| 19 | 54 | 43.8 | 2 | 21.9 | 17 | 54 | 43.8 | 2 | 21.9 | | 54 | 43.8 | | |
| 20 | 55 | 22.8 | 1 | 22.8 | 18 | 55 | 22.8 | 1 | 22.8 | 19 | 55 | 22.8 | 1 | 22.8 |
| 21 | 56 | 60 | 3 | 20 | 19 | 56 | 60 | 3 | 20 | 20 | 56 | 60 | 3 | 20 |
| 22 | 57 | 36 | 2 | 18 | 20 | 57 | 36 | 2 | 18 | 21 | 57 | 36 | 1 | 36 |
| 23 | 58 | 24 | 2 | 24 | 21 | 58 | 24 | 1 | 24 | 22 | 58 | 24 | 1 | 24 |
| 24 | 59 | 37.2 | 2 | 18.6 | 22 | 59 | 37.2 | 2 | 18.6 | 23 | 59 | 37.2 | 2 | 18.6 |
| 25 | 60 | 12 | 1 | 12 | 23 | 60 | 12 | 1 | 12 | 24 | 60 | 12 | 1 | 12 |
| 26 | 151 | 24.6 | 1 | 24.6 | 24 | 151 | 24.6 | 2 | 12.3 | 25 | 151 | 24.6 | 1.5 | 16.4 |
| 27 | 152 | 4.2 | 1 | 16.8 | 25 | 152 | 4.2 | 1 | 16.8 | 26 | 152 | 4.2 | 1 | 16.8 |
| | 153 | 12.6 | | | | 153 | 12.6 | | | 27 | 153 | 12.6 | | |

**Table 16.** Comparison of full line load chart for Polo-shirt product coded PL04 when given the number of workers $N$.

| | Line balancing by hand of HUST method | Line balancing by BSL-HUST software | Line balancing by Tinh Loi Garment Co., Ltd plan |
|---|---|---|---|
| Image | 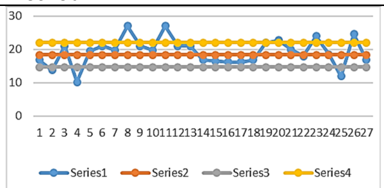 | 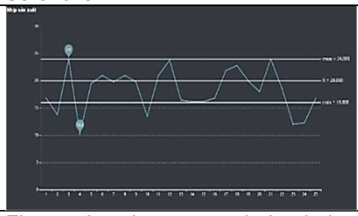 | 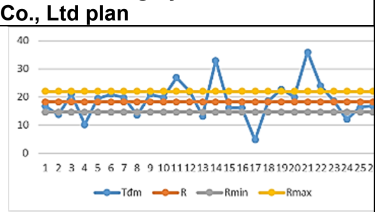 |
| Comment | Five workstations are overloaded, three workstations are underloaded | Five workstations are underloaded | Five workstations are overloaded, six workstations are underloaded |

**Table 17.** Comparison of sewing line layout diagram for Polo-shirt coded PL04 product when given the number of workers *N*.

| | The sewing line layout diagram for Polo- shirt product coded PL04 | Layout |
|---|---|---|
| By hand method of HUST | 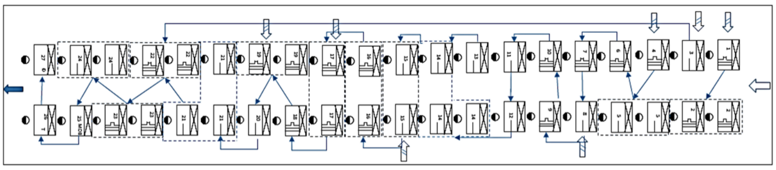 | Class-form, semi-finished products are shipped by zigzag, with boxes |
| By BSL-HUST software | 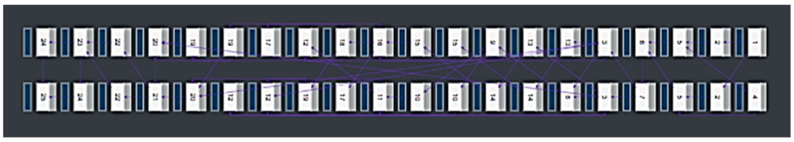 | Class-form, semi-finished products are shipped by zigzag, with boxes |
| By design plan of Tinh Loi Garment Co., Ltd | 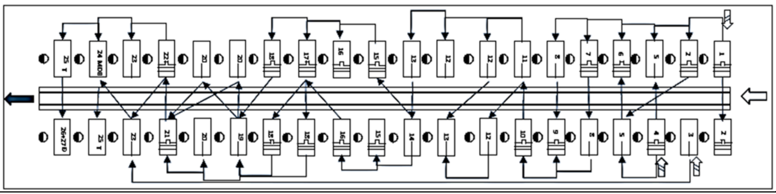 | Class-form, semi-finished products are shipped by zigzag with a semi-automatic hanging line. |

**Table 18.** Table comparing line parameters - line balancing coefficient *K*%, balancing efficiency *H*%, capacity *P*, number of workers *N* and cycle time *R* of Polo-shirt coded PL04 when given the number of workers *N*.

| *N* = 40 people | *K* [%] | *H* [%] | *P* [products/day] | *R* [s] |
|---|---|---|---|---|
| By Tinh Loi Garment Co., Ltd | 59 | 100 | 1667 | 18.36 |
| By hand method of HUST | 70.4 | 100 | 1667 | 18.9 |
| By BSL-HUST software | 80 | 91.8 | 1575 | 20.0 |

## Completing the design and balance database the sewing line two products T-Shirt and Polo-Shirt

Completing the design and balance database of T-Shirt product

a. Given the capacity *P*

The authors found that the design and line balancing results according to the method of Hanoi University of Science and Technology are the most optimal, so this result will be used as the standard database without the need to correct the algorithm and software design techniques (Table 19).

b. Given the number of workers *N*

The authors found that the design and line balancing results according to BSL-HUST software are the most optimal, so this result will be used as the standard database without the need to correct the algorithm and software design techniques (Table 20).

Completing the design and balance database of Polo-Shirt product

a. Given the capacity *P*

The authors found that the design and line balancing results according to BSL-HUST software are quite optimal because *K*% > 60%. However, the number of workers and the load factor are not optimal. Because the software accepts increasing the number of workers so that the transmission is always smooth and not overloaded, the result is acceptable (Table 21).

b. Given the number of workers *N*

The authors found that the design and line balancing results according to BSL-HUST software are the most optimal, so this result will be used as the standard database without the need to correct the algorithm and software design techniques (Table 22).

## CONCLUSION

After conducting the research, the authors have completed the database on the design and line balancing of two typical products made from knitted fabrics, namely Polo-Shirt and T-Shirt. The authors compared and evaluated the design and balance results T-shirt sewing line according to HUST method by hand calculation, using BSL-HUST software and the actual results at IE room of Tinh Loi Garment Co., Ltd. With the given the capacity of line P (products/shift) and the given the number of workers *N* (people), the team compared and evaluated the design and balanced result sewing line by comparing the organization and coordination of tasks results, the full-line load charts, the sewing line layout diagrams and the exact results of line paraments. Then the authors compared and evaluated the

**Table 19.** Table of organization and coordination of tasks into workstations result according to the manual calculation method of HUST, T-shirt coded T07 when given the capacity *P*.

| Workstation | Task | Machine | $T_i$ [s] | $T_j$ [s] | $N_i$ [people] |
|---|---|---|---|---|---|
| 1 | 34 | M2K3C | 16.8 | 8.4 | 2 |
| 2 | 35 | M1K | 10.8 | 10.8 | 1 |
| 3 | 40 | M1K3C | 16.8 | 16.8 | 1 |
| 4 | 41 | OL-MN | 25.8 | 12.9 | 2 |
| 5 | 42 | M1K | 10.8 | 10.8 | 1 |
| 6 | 43 | MH380 | 27 | 13.5 | 2 |
| 7 | 44 | M2K4C | 34.8 | 11.6 | 3 |
| 8 | 45 | M2K4C | 41.4 | 13.8 | 3 |
| 9 | 46 | M2K3C | 24 | 12 | 2 |
| 10 | 47 | M1K | 29.4 | 9.8 | 3 |
| **Sum** | | | 237.6 | | 20 |

**Table 20.** Table of organization and coordination of tasks into workstations result according to BSL-HUST software, T-shirt coded T07 when given the number of workers *N*.

| Workstation | Task | Machine | $T_i$ [s] | $T_j$ [s] | $N_i$ [people] |
|---|---|---|---|---|---|
| 1 | 34 | M2K3C | 16.8 | 8.4 | 2 |
| 2 | 35 | M1K | 10.8 | 10.8 | 1 |
| 3 | 40 | M1K3C | 16.8 | 8.4 | 2 |
| 4 | 41 | OL-MN | 25.8 | 12.9 | 2 |
| 5 | 42 | M1K | 10.8 | 10.8 | 1 |
| 6 | 43 | MH380 | 27 | 13.5 | 2 |
| 7 | 44 | M2K4C | 34.8 | 11.6 | 3 |
| 8 | 45 | M2K4C | 41.4 | 13.8 | 3 |
| 9 | 46 | M2K3C | 24 | 12 | 2 |
| 10 | 47 | M1K | 29.4 | 14.7 | 2 |
| **Sum** | | | 237.6 | | 20 |

**Table 21.** Table of organization and coordination of tasks into workstations result according to BSL-HUST software. Polo-shirt coded PL04 when given the capacity *P*.

| Workstation | Task | Machine | $T_j$ [s] | Type | $N_i$ [people] | $T_j$ [s] |
|---|---|---|---|---|---|---|
| 1 | 34 | M2K4C | 16.8 | 3 | 1 | 16.8 |
| 2 | 35 | MC1K | 27.6 | 4 | 2 | 13.8 |
| 3 | 36 | M1K | 21 | 3 | 3 | 16 |
| | 41 | M1K | 27 | | | |
| 4 | 37 | M2K4CG1 | 10.2 | 3 | 1 | 10.2 |
| 5 | 38 | M1KG1 | 39 | 4 | 2 | 19.5 |
| 6 | 39 | M2K4C | 21 | 3 | 1 | 21 |
| 7 | 40 | MC1KG1 | 19.8 | 3 | 1 | 19.8 |
| 8 | 42 | M2K4C | 21 | 4 | 1 | 21 |
| 9 | 43 | MC1KV | 19.8 | 4 | 1 | 19.8 |
| 10 | 44 | M1KG2 | 27 | 3 | 2 | 13.5 |
| 11 | 45 | M1K | 21 | 3 | 1 | 21 |
| 12 | 46 | M1K | 21 | 3 | 1 | 21 |
| 13 | 47 | M1K | 24 | 3 | 3 | 16.8 |
| | 48 | M1K | 26.4 | | | |
| 14 | 49 | M1KG3 | 33 | 4 | 2 | 16.5 |
| 15 | 50 | M2K4C | 32.4 | 4 | 2 | 16.2 |
| 16 | 51 | MC1KG1 | 32.4 | 4 | 2 | 16.2 |
| 17 | 52 | M2K4C | 4.8 | 3 | 1 | 16.8 |
| | 53 | M2K4C | 12 | | | |
| 18 | 54 | M2K4C | 43.8 | 4 | 2 | 21.9 |
| 19 | 55 | M1KG4 | 22.8 | 3 | 2 | 11.4 |
| 20 | 56 | M1KG3 | 60 | 4 | 3 | 20 |
| 21 | 57 | M2K4C | 36 | 4 | 2 | 18 |
| 22 | 58 | MC1K | 24 | 4 | 2 | 12 |
| 23 | 59 | M1K | 37.2 | 3 | 2 | 18.6 |
| 24 | 60 | MDB | 12 | 3 | 1 | 12 |
| 25 | 151 | MTK | 24.6 | 3 | 2 | 12.3 |
| 26 | 152 | MDC | 4.2 | 3 | 1 | 16.8 |
| | 153 | MDC | 12.6 | | | |

**Table 22.** Table of organization and coordination of tasks into workstations result according to BSL-HUST software, Polo-shirt coded PL04 code when given the number of workers *N*.

| Workstation | Task | Machine | $T_j$ [s] | Type | $N_i$ [people] | $T_i$ [s] |
|---|---|---|---|---|---|---|
| 1 | 34 | M2K4C | 16.8 | 3 | 1 | 16.8 |
| 2 | 35 | MC1K | 27.6 | 4 | 2 | 13.8 |
| 3 | 36 | M1K | 21 | 3 | 2 | 24 |
| | 41 | M1K | 27 | | | |
| 4 | 37 | M2K4CG1 | 10.2 | 3 | 1 | 10.2 |
| 5 | 38 | M1KG1 | 39 | 4 | 2 | 19.5 |
| 6 | 39 | M2K4C | 21 | 3 | 1 | 21 |
| 7 | 40 | MC1KG1 | 19.8 | 3 | 1 | 19.8 |
| 8 | 42 | M2K4C | 21 | 4 | 1 | 21 |
| 9 | 43 | MC1KV | 19.8 | 4 | 1 | 19.8 |
| 10 | 44 | M1KG2 | 27 | 3 | 2 | 13.5 |
| 11 | 45 | M1K | 21 | 3 | 1 | 21 |
| 12 | 46 | M1K | 21 | 3 | 3 | 23.8 |
| | 47 | M1K | 24 | | | |
| | 48 | M1K | 26.4 | | | |
| 13 | 49 | M1KG3 | 33 | 4 | 2 | 16.5 |
| 14 | 50 | M2K4C | 32.4 | 4 | 2 | 16.2 |
| 15 | 51 | MC1KG1 | 32.4 | 4 | 2 | 16.2 |
| 16 | 52 | M2K4C | 4.8 | 3 | 1 | 16.8 |
| | 53 | M2K4C | 12 | | | |
| 17 | 54 | M2K4C | 43.8 | 4 | 2 | 21.9 |
| 18 | 55 | M1KG4 | 22.8 | 3 | 1 | 22.8 |
| 19 | 56 | M1KG3 | 60 | 4 | 3 | 20 |
| 20 | 57 | M2K4C | 36 | 4 | 2 | 18 |
| 21 | 58 | MC1K | 24 | 4 | 1 | 24 |
| 22 | 59 | M1K | 37.2 | 3 | 2 | 18.6 |
| 23 | 60 | MDB | 12 | 3 | 1 | 12 |
| 24 | 151 | MTK | 24.6 | 3 | 2 | 12.3 |
| 25 | 152 | MDC | 4.2 | 3 | 1 | 16.8 |
| | 153 | MDC | 12.6 | | | |

design and balanced results Polo-Shirt sewing line according to HUST method by hand calculation, using BSL-HUST software and the actual results at IE room of Tinh Loi Garment Co., Ltd. Similar to the process of T-shirt product, the author compared the organizaion and coordination of tasks results, the full-line load chart, the sewing line layout diagrams, the exact results of line parameters with given the capacity *P* (products/shift) and the number of workers *N* (people). Finnally the researcher completed the design and balanced database sewing line two products T-shirt and Polo-shirt with given the capacity *P* and the number of workers *N*. The design and line balance results according to BSL – HUST software are the most optimal compared to line balancing by hand of HUST method and Line balancing by Tinh Loi Garment Co., Ltd plan. The authors found that the result will be used as the standard database without the need to correct the algorithm and software design techniques. In the future, the author team will continue to research and expand with other items to diversify the database of designs and balance sewing lines.

**Acknowledgement:** *This study was carried out within the framework of the Science and Technology 01C – 02/04-2019-3. We would like to thank the Hanoi Department of Science and Technology, Hanoi University of Science and Technology, Star Fashion Co., Ltd., Tinh Loi Garment Company and Hanosimex factory for supporting us to in completing this study.*

## REFERENCES

1. Ghutukade S. T., Sawant S. M.: Use of ranked position weighted method for assembly line balancing, International Journal of Advanced Engineering Research and Studies, 2013, pp. 5–7
2. Pachghare V., Dalu R. S.: Assembly line balancing methods–A case study, International Journal of Science and Research, 3(5), 2012, pp. 2319–7064.
3. Jayakumar A., Krishnaraj A. K.: Productivity improvement in stitching section of a garment manufacturing company. International Journal of Innovative Research in Advanced Engineering, vol. 4, no. 12, 2017, pp. 8–11.
4. Huong D. M., Long T. V., Thuan D. P., et al.: Application of exhaustive search for Int. J. Sci. Res. Eng. DevOptimization assembly line balancing in garment industry. Journal of Science & Technology Technical Universities 141, 2020, pp. 34-41.
5. Thao P. T., Huong D. M.: Research on apply of Polo-shirt assembly line balancing methods in Vietnam garment industry. In: Proceedings the 2nd National Scientific Conference on Textile, Apparel and Leather Engineering. Agricultural Academy Publisher, 2021, pp. 307-318.
6. Thao P.T., Anh L.T.M., Phan D.N., et al.: Researching the optimal method of balancing the sewing line with T-shirt product in the garment industry in Vietnam. ECS Transactions, 107(1), 2022, pp. 7869-7887. https://doi.org/10.1149/10701.7869ecst
7. Rahman H., Roy P.K., Karim R. et al.: Effective way to estimate the standard minute value (SMV) of a t-shirt by work study. European Scientific Journal, 10(30), 2014, pp. 196-203.
8. Jung W.K., Kim H., Park Y.C., et al.: Smart sewing work measurement system using IoT-based power monitoring device and approximation algorithm. International Journal of Production Research, 58(20), 2020, pp. 6202-6216. https://doi.org/10.1080/00207543.2019.1671629

9. Alam F.B., Hasan M.M.: Analysis on SMV to increase productivity in sewing section: a case study on T-shirt manufacturing in Bangladesh. International Journal of Research in Engineering and Science, 6(8), 2018, pp. 18-24.
10. Mulani S. J., Awasare A. D., Shetenawar R. M., et al.: Line Balancing by Using Time Study. International Journal of Scientific Research and Engineering Development, 2(4), 2019, pp. 302–304.
11. Alzoubi K., Hijazi H., Alkhateeb A.: Facility planning and assembly line balancing in garment industry. 2019 6th International Conference on Frontiers of Industrial Engineering, 2019, pp. 11-15.
12. Andreu-Casas E., García-Villoria A., Pastor R.: Multi-manned assembly line balancing problem with dependent task times: a heuristic based on solving a partition problem with constraints. European Journal of Operational Research, 302(1), 2022, pp.96-116. https://doi.org/10.1016/j.ejor.2021.12.002

# IMPROVEMENT OF FLAME RETARDANT AND ANTIBACTERIAL PROPERTIES OF COTTON-POLYESTER BLEND FABRICS

**HOROKHOV, IHOR; KULISH, IRINA*; ASAULYUK, TATYANA; SARIBYEKOVA, YULIA; SEMESHKO, OLGA AND MYASNYKOV, SERGEY**

Kherson National Technical University, 11 Instytutska st., 29016 Khmelnytskyi, Ukraine

## ABSTRACT

The fire retardant and antibacterial characteristics of cotton-polyester blend fabric have been improved. A composition has been developed for complex finishing of fabric using a phosphorus-containing substance on a biological basis, which, due to its high phosphorus content, can provide a fire-retardant function to textile material, as well as increase its antimicrobial properties. The thermal characteristics of treated textile materials have been studied and it has been established that the presence of phytic acid at the initial stage of destruction shifts the temperature towards lower values due to the activation of phytic acid degradation before the decomposition of the main substrate. The maximum temperature at which the final destruction of the cotton-polyester fabric occurs shifts to higher temperatures from 507°C for the untreated fabric to 565°C for the treated fabric, and the presence of dry residue increases by more than 2.5 times, which proves an increase in the heat resistance of the textile material. The length of the damaged area in the vertical combustion test was 6.5 cm, and the absence of drop formation of the polyester component was also noted, which eliminates the potential destructive effect due to the possible formation of additional fire areas. An increase in fabric antimicrobial activity is confirmed by a zone of inhibition of 2 – 4 mm around the sample using the diffusion method with gram-positive bacteria Staphylococcus pyogenes, as well as a pronounced growth inhibition of microorganisms around fabric samples examined by the method of inoculation of microflora from the environment. Treatment with the studied composition improves washing resistance and does not impair the mechanical properties of the textile material by increasing the degree of crosslinking of the polymer components used in the finishing composition.

## KEYWORDS

Phytic acid; Polyhexamethylene guanidine phosphate; Thermal analysis; Antimicrobial finishing compositions; Fire-retardant finishing compositions; Cotton-polyester fabrics.

## INTRODUCTION

The living conditions of a modern person dictate more and more new requirements for clothing, which should not only be comfortable and beautiful, but in the current difficult epidemiological situation, including the coronavirus pandemic, provide protection from the pathogenic effects of viruses and microorganisms. First of all, this concerns medical textiles, but the functionalization of home textiles, as well as fabrics for transport, military use, etc., is now acquiring no less importance. The search for effective sterilizing preparations against common pathogenic microorganisms, but at the same time non-toxic, is an important requirement of our time for the development of innovative technologies for imparting antimicrobial properties to textile materials.

No less popular in modern textile materials is resistance to fire. This requirement is caused by numerous fires provoked by global climate change, man-made disasters, hostilities, etc. Despite the rather high degree of fire protection of textiles with halogen- and formaldehyde-containing preparations, they must be abandoned due to the negative impact on the human body and the environment due to the release of hazardous halides, dioxins, benzofurans, and formaldehyde during combustion.

Due to the negative state of the environment in the world, there is a tendency to abandon the use of organic synthesis products. Substances originating from natural sources – biological or mineral – are increasingly used, in particular in textile finishing. Along with this, it is promising to search for and introduce into production multifunctional substances of natural origin, which, together with flame retardant properties, will impart antibacterial activity in order to ensure the functionality of finished products and the economic efficiency of their production.

* **Corresponding author:** Kulish I., e-mail: *kulish.in.411@gmail.com*

*Received September 14, 2023; accepted 20 October, 2023*

Currently, the attention of researchers is attracted by biologically based antimicrobial agents and fire retardants, which is the result of the society's desire to use environmentally friendly products and substances that are not generated from oil [1-3]. Scientists are developing and improving such preparations taking into account the fundamentals of "green technologies", namely, biologically active additives are being studied that can increase protection against fire and pathogenic microflora that threatens human life and health. Among natural plant products, extracts of neem, pomegranate, aloe vera, turmeric, cloves, etc. have antibacterial properties [4].

Biologically active substances can be added to synthetic fibres during the formation process [5], thus polyacrylonitrile, acetate and polypropylene fibres are functionalized and already on the market. However, this method of modification is fundamentally impossible for the processing of natural fibres. A more universal method of fibre modification is the formation of a polymer coating on the textile material, which makes it possible to immobilize various functional substances depending on the purpose of the textile and consumers [6]. For example, a composition with chitosan, a substance obtained from crustacean shells, has been developed to impart antimicrobial properties to nylon, cotton, and wool [7-9]. The disadvantages of chitosan are the need to use it in high concentrations, which worsens the hygienic properties of textile materials, increases their rigidity, as well as insufficient resistance of treatment to washing.

Recently, the interest of inventors is directed to bioorganic phytic acid, known as inositol hexakisphosphate or phytate in the form of a salt, which is considered as a "green" molecule, contained in sufficient quantities in plant tissues [10]. As a biocompatible, environmentally friendly, nontoxic, and easily obtained organic acid, it is widely used in antioxidant, biosensor, cation exchange, nanomaterial, and other fields due to its special structure of inositol hexakisphosphate [11].

Phytic acid contains 28 wt.% phosphorus in terms of molecular weight and is a promising biomacromolecule for use as a fire retardant. In [12], phytic acid was used as a doping acid to significantly improve the flame-retardant characteristics of composite paper deposited with polyaniline. The compositions phytic acid /chitosan and phytic acid /nitrogen-modified silane hybrids were used by layer-by-layer assembly to produce thin fire-resistant films on cotton fabric [13]. The potential fire protection effect of various metal phytates was evaluated as a biosource of phosphorus additives for composites based on polylactic acid [14].

In general, the use of phytic acid allows it to be considered as one of the components of antimicrobial treatment. This is confirmed by the publication [15], which describes a method for treating cotton fabric coated with phytic acid with silicon and a nitrogen-containing compound, poly-[3-(5,5-cyanuric acid propyl-siloxane-tri-methylammoniumpropyl-siloxane-chloride)] by layer-by-layer assembly (Cotton-PEI/(PCQS/PA) 30-Cl). Treated cotton fabrics reduced the effects of E. coli and S. aureus by 100% within 1 minute of contact.

Cationic polymers such as quaternary ammonium compounds and guanidine-based polymers are known for their antimicrobial activity. They are widely used as active agents to fight cross-infections and contribute to the overall reduction of bacterial nosocomial infections. The effectiveness of antimicrobial treatment of cotton fabrics intended for use in everyday life and public buildings with coatings based on various types of polymers – guanidines or polymer nanocomposite materials with permanent antimicrobial properties without deterioration of their physicochemical and mechanical characteristics has been confirmed [16]. In addition, it is known [17] to use biodegradable polycarbonates functionalized with guanidine to provide in vivo antimicrobial activity against A. baumannii, E. coli, Klebsiella pneumoniae, S. aureus, and P. aeruginosa. In another study [18], polymer film coatings based on PVA/chitosan with the addition of polyhexamethylene guanidine were obtained, which are characterized by antibacterial properties.

An analysis of the results obtained by scientists indicates the relevance of the issue of simultaneously imparting flame retardant and antimicrobial properties to textile materials, as well as the existence of a whole range of unresolved issues, in particular, the search for environmentally friendly preparations and the development of resource-saving technologies for imparting appropriate special properties and characteristics to cotton textile materials.

The use of biomacromolecules in modern technologies as functional substances that can be used as fire retardants and as antimicrobials is a potential innovative environmentally friendly and non-toxic strategy that goes beyond the traditional chemical approach in creating "green" technologies.

The aim of this work is to develop a composition for the complex functional finishing of cotton-polyester textile material using a bio-based phosphorus-containing substance that can provide the flame-retardant function of the textile material due to phosphorus-nitrogen synergy, as well as increase its antimicrobial properties.

## MATERIALS AND METHODS

Phytic acid and polyhexamethylene guanidine phosphate (PHMG-p) have been investigated as functional substances capable of providing a complex finish to fabrics and imparting both antimicrobial and flame retardant properties. Finishing was subjected to bleached and plain dyed blended cotton-polyester fabrics (PJSC Cherkasy Silk Plant).

**Table 1.** Characteristics of textile materials.

| Fabric construction | Fabric composition | Surface weight [g/m$^2$] | Density [yarns per 10 cm] | |
|---|---|---|---|---|
| | | | warp | weft |
| 2/1 twill | 47% polyester, 53% cotton | 220±11 | 300±6 | 160±6 |

The characteristics of the textile materials under study are presented in Table 1. The choice of the presented textile material is not accidental and is due to the fact that blended fabrics are widely used in everyday life to one degree or another.

In the case of imparting to textile materials any new properties that were not previously characteristic of them (bactericidal, reduced flammability, hydro-, oleophobicity, etc.) the principle of "transfer" of a substance with predetermined and specified properties to a polymeric textile material is used.

The textile material was treated with an aqueous solution of phytic acid (PhA) with the addition of citric acid (CA), which improves the solubility of PhA in water and increases the carbon residue during the combustion of the fabric. The tricarboxylic acid addition also provides cross-linking with the –OH groups of the cellulose component of the fabric.

The composition of the impregnating bath contained as a binder acrylic polymer Neoprint NPO – 60 g/l; PhA – 300 g/l; CA – 200 g/l; PHMG-p (6% aqueous solution) up to 1000 g. The acrylic dispersion is introduced to increase the stabilization of functional components and is able to provide a set of necessary fabric properties. After impregnation with the finishing composition, the textile materials were pressed on a laboratory padder to a residual moisture content of 90%, dried to a constant weight in an oven at a temperature of 80 °C, followed by heat setting at a temperature of 120 °C for 5 minutes.

The behaviour of the studied textile material under the influence of high temperatures was evaluated by the method of thermogravimetric and differential thermal analysis after examining the samples on the Thermoscan-2 derivatograph. Studies were carried out with treated and untreated fabric samples in the temperature range up to 700 °C, using quartz crucibles. Aluminium oxide was used as a reference. The weight of the samples was 0.1 g. The samples were heated in air from 10°C to 700 °C at a constant heating rate of 10 °C/min.

## RESULTS AND DISCUSSION

The heat resistance results of the textile materials under study are compared with untreated textile samples in Table 2.

Mass loss at temperatures from $T_{0\%}$ to $T_{5\%}$ for the original cotton-polyester fabric occurs mainly due to the dehydration of cotton fibres and reaches 5%. According to the literature data, thermal degradation of polyester fabric occurs at 410°C. However, the presence of cotton fibres in the fabric affects the decomposition of the untreated sample. The main stage of destruction occurs at 314°C, which is actually close to the decomposition temperature of the cotton component of the fabric, since the thermal decomposition of cotton begins at a lower temperature than polyester. The final destruction temperature for the initial sample occurs at $T_f$ = 507°C. In the case of a cotton-polyester blend fabric, the cotton acts as the initial ignition source, and the mass loss is mainly due to the complete decomposition of the cotton and the partial decomposition of the polyester in the second temperature range.

**Table 2.** Heat resistance of textile materials.

| Treatment | Mass loss temperature | | | | | Mass fraction of residue, $\varepsilon_m$ [%] |
|---|---|---|---|---|---|---|
| | $T_{0\%}$ [°C] | $T_{5\%}$ [°C] | $T_{10\%}$ [°C] | $T_{20\%}$ [°C] | $T_f$ [°C] | |
| Untreated fabric | 122 | 232 | 292 | 314 | 507 | 1.7 |
| PhA+CA | 194 | 208 | 234 | 290 | 546 | 4.82 |
| PhA+CA+PHMG-p | 205 | 219 | 241 | 298 | 565 | 5.07 |

Note: $T_{5\%}$ (°C), $T_{10\%}$ (°C), $T_{20\%}$ (°C) – correspond to the temperatures at which fabric samples lose weight by 5%, 10%, 20%, respectively; $T_{0\%}$ – the beginning of destruction; $T_f$ – the final temperature of mass loss (end of destruction).

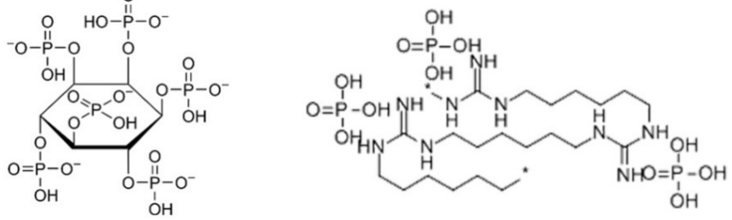

(a) (b)

**Figure 1.** Structural formulas of macromolecules: (a) phytic acid; (b) polyhexamethylene guanidine phosphate.

The initial stage of destruction of the cotton-polyester fabric sample treated with PhA occurs with the formation of a protective barrier at a temperature equal to 194°C – 208°C, which is due to the decomposition temperature of PhA. The value of the mass loss of the fabric sample treated with PhA is significantly shifted towards lower temperatures at the first stage. Thus, with a mass loss of 10%, the temperature decreased from $T_{10\%}$ = 292°C for untreated fabric to 234°C, which is explained by the catalytic effect of PhA, which contributes to the carbonization of cotton. The same trend persists with a loss of fabric mass of 20%. The decomposition temperature of $T_{20\%}$ is still 24°C lower than that of the untreated fabric. This property belongs to the phosphate groups of the PhA biomacromolecule, which, decomposing at a temperature of about 200°C and releasing phosphoric acid, promotes fabric dehydration, which leads to the formation of a residue that is thermally stable up to 500°C – 600°C [19,20]. The significant advantages of this biomacromolecule include not only the formation of acid, but also the fact that it is, by its nature, a carbon source that promotes the formation of a carbonized layer on the surface of textile materials [21]. The structural formula of PhA is shown in Fig. 1.

Phosphorus-containing compounds, which include the biomacromolecule of PhA, are thermally decomposed to $PO^{\bullet}$, which can block combustion, although $H^{\bullet}$ and $HO^{\bullet}$ are formed when the matrix combustion is extinguished. On the other hand, phosphorus-containing compounds can catalyse dehydration and carbonization reactions containing –OH groups [22].

The temperature of the end of destruction of the studied textile material treated with PhA $T_f$ = 546°C shifts relative to the untreated sample, the end temperature of which is 507°C and moves to a higher temperature region. This confirms the improvement in the fire resistance of the textile compared to the untreated fabric. At temperatures above 500°C, the process of thermal oxidation occurs, that is the formation of a carbonized residue, the value of which on the fabric depends mainly on the organic and inorganic substances deposited on the surface. The condensed phase mechanism based on the use of PhA is further enhanced by the inclusion of PHMG-p containing nitrogen.

When the system is functionalized with nitrogen-containing compounds, mechanisms of gas-phase and intumescent action are observed through the release of $NH_3$ during combustion. During the decomposition of the nitrogen-containing agent, a gas barrier of ammonia is formed above the surface of the substrate, which impedes the access of oxygen and inhibits the oxidation of carbon in the gas phase. Phosphorylation of cellulose is catalysed by nitrogen-containing molecules through the intermediates PN, $CO_2$, $NH_3$. It was shown in [23] that the formed carbon layer and the formed dense framework in this case may contain POP, POC, PNC bonds. As a result of the study, it was found that the mass fraction of residues of the treated textile material is 4.82% and 5.07% in the case of the addition of PHMG-p. The coke residue of the initial cotton-polyester fabric at a temperature of 700°C was 1.7%.

The results of thermal analysis were confirmed by fire resistance tests of the studied fabric samples in terms of afterburning time and charring height. The charring height after exposure to a flame for 15 seconds was 6.5 cm for the fabric sample treated with the composition containing PHMG-p (Fig. 2). At the same time, this sample is characterized by the intumescent nature of the fabric behaviour during combustion.

There was no residual burning of the fabric after removal from the fire. The absence of drop formation of the polyester component of the fabric was also noted.

The studied samples of cotton-polyester fabric showed the presence of a significant charred residue after burning compared to untreated ones, and the absence of drop formation of the synthetic component was also noted, in contrast to the untreated fabric. The formation of an isolated dense protective layer is important for improving the flame-retardant properties of textile materials, as it prevents its subsequent heating and blocks the free access of atmospheric oxygen, contributing to the further formation of a carbonized layer.

The versatility of polyhexamethylene guanidines is confirmed by the fact that they are also effective and environmentally friendly antimicrobial agents [24, 25]. Thus, the presence of PHMG-p in the finishing composition will not only enhance the fire retardant and antimicrobial properties of textile materials, but also additional film formation on the surface of textile

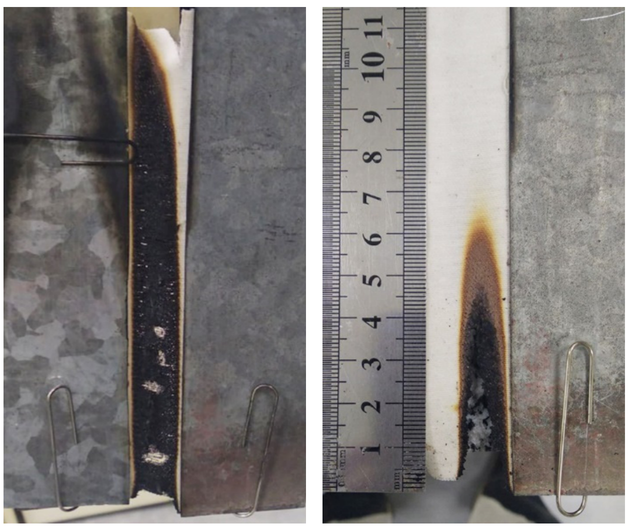

(a) (b)

**Figure 2.** The nature of carbonization of cotton-polyester fabric samples treated with the studied compositions: (a) PhA+CA; (b) PhA+CA+PHMG-p.

fibres, which will increase the resistance of the finishing to physical and chemical influences. Also, the macromolecular nature of PHMG-p due to film formation is able to provide a prolonged antimicrobial effect as a result of the formation of a biocidal film on the surface, which provides long-term (several months) protection of the treated surface from microorganisms.

Polyguanidines by their nature are polycationic amines capable of destroying bacterial cells due to electrostatic attraction [26, 27] and, according to the literature, they are classified as low-hazard substances when applied to the skin.

For example, [28, 18] presents studies of biodegradable polycarbonates functionalized with guanidine to provide in vivo antimicrobial activity against A. baumannii, E. coli, Klebsiella pneumoniae, S. aureus and P. aeruginosa. The mechanism of action is described as a significant electrostatic attraction between a cationic polymer and a negatively charged bacterial cell, facilitating its rapid destruction under the influence of guanidine biocides [29].

Identification of the effectiveness of antibacterial sensitivity of textile materials treated with finishing compositions was carried out on LB medium of the following composition (g/l): peptone – 10.0; yeast extract – 5.0; NaCl – 5.0; agar-agar – 14.0; at pH – 7.0±0.2. As a test culture, we used one of the representatives of the wound microflora – the gram-positive bacterium Staphylococcus pyogenes from the Ukrainian collection of microorganisms, which was cultivated at 37°C for 24 hours. After cultivation, part of the culture was added to physiological solution and aliquots from the resulting suspension were transferred to fresh LB medium, then fabric samples treated with the compositions were added. After keeping in a desiccator for 24 hours, the resistance of the treated fabric samples to the action of microorganisms was determined.

The results of the study showed that around samples of cotton-polyester blend fabric treated with phytic and citric acids, there is a zone of growth inhibition of Staphylococcus pyogenes microorganisms within 1 – 4 mm.

In the photos of Fig. 3 shows the zone of growth inhibition of treated fabric samples with and without heat setting. Analysis of the results shows that the growth inhibition zone of Staphylococcus pyogenes microorganisms is within 2 – 4 mm (Fig. 3). The inhibition of the growth of Staphylococcus pyogenes bacteria culture, confirming the antimicrobial properties of the textile samples treated with the studied composition, was evaluated by degree during their incubation.

Given that textile materials are used in everyday life, transport and other public places, determining the effectiveness of antimicrobial treatment to inhibit bacterial pollution of air microflora is of great importance. This method is one of the simplest and fastest methods for studying air microflora and is used for comparative analysis of bacterial environmental pollution. For inoculation of microorganisms from the microflora of the environment, Petri dishes with solidified agar were left in an open space in a room for 15 min. Fabric samples in the form of a round disk were placed in a Petri dish on the surface of air-inoculated agar, covered, placed in a thermostat for incubation for 72 hours at a temperature of 38°C. The antimicrobial properties of textile materials were determined by analysing the diffusion of a fabric disk. The results of the study are presented in Fig. 4.

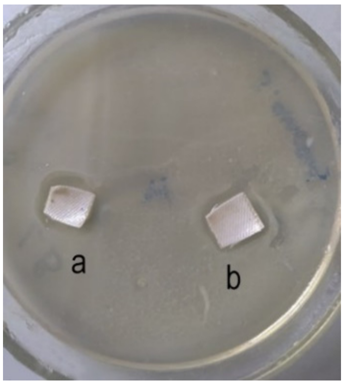


**Figure 3.** Staphylococcus pyogenes growth inhibition zone around the fabric samples treated with PhA+CA+PHMG-p: a) with heat setting; b) without heat setting.

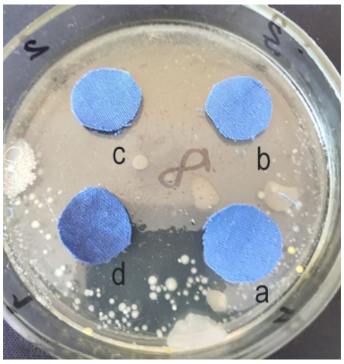


**Figure 4.** Inhibition of bacterial contamination of microflora inoculated from the air: a) untreated sample; b) sample treated with PhA+CA+PHMG-p+heat setting; c) treated sample after 1 washing cycle; d) treated sample after 5 washing cycles.

As can be seen from the photo in Fig. 4, the initial fabric (Fig. 4a) is characterized by high bacterial contamination, the absence of an inhibition zone around it, and the development of various microflora inoculated from the air. Composite treatment (Fig. 4b) shows a significant zone of growth inhibition of pathogenic microflora, that is observed even after the first washing (Fig. 4c). After the fifth washing (Fig. 4d), the quality of the antimicrobial treatment decreases, but still, at a distance of 1 – 2 mm around the sample, the maximum amount of microflora is suppressed.

**Table 3.** Structural characteristics of the formed polymer films.

| Composition of polymer film | Sol fraction, *S* [%] | Degree of polymer crosslinking, *j* [%] | Crosslinking coefficient | Fraction of active polymer chains, *Vc* [mol/cm$^3$] |
|---|---|---|---|---|
| Without additives | 3.20 | 4.74 | 9.48 | 0.75 |
| PhA+CA | 2.89 | 2.89 | 5.78 | 0.77 |
| PhA+CA+PHMG-p | 0.42 | 14.50 | 29.0 | 0.92 |
| PhA+CA+PHMG-p+ heat setting | 0.39 | 15.07 | 30.14 | 0.93 |

The zone of inhibition formed around textile samples treated with PHMG-p and biological PhA confirms the effectiveness of the antimicrobial treatment against a variety of airborne bacteria.

Taking into account that textile materials during operation are subjected to various physical and chemical influences, in particular washings, an acrylic polymer was additionally introduced into the finishing composition as a film former capable of immobilizing various substances on the surface of textile fibres. To confirm the effectiveness of the introduction of the film former, the structural characteristics of the films formed from the acrylic polymer Neoprint NPO, as well as films from Neoprint NPO with the addition of acids and PHMG-p, were studied. Studies were carried out using the limited swelling properties of cross-linked polymer systems in solvents. Structural characteristics were evaluated by the amount of the acetone-insoluble fraction of the studied polymer films during the extraction of samples in a solvent.

To determine the structural characteristics, polymer films were formed on a glass substrate from individual Neoprint NPO and the polymer filled with functional components to impart a flame retardant and antimicrobial finish. Extraction of polymer films was carried out with acetone for 18 hours and benzene for 16 hours in a Soxhlet apparatus according to the standard procedure. The mass of the swollen sample was determined, as well as the dry residue from it. The amount of benzene extract corresponds to the content of the sol fraction S (%) and is determined by the relation:

$$\boldsymbol{S} = \frac{\boldsymbol{m_a - m_b}}{\boldsymbol{m_a}} \cdot \mathbf{100\%}, \quad (1)$$

where $m_a$ is the mass of the sample after extraction with acetone, g; $m_b$ is the mass of the sample after extraction with benzene, g.

The presence of the sol fraction after extraction in the Soxhlet apparatus indicates the content of the macromolecules remaining outside the network in the crosslinked sample of the composite polymer film. The sol fraction is washed out of the polymer film by the solvent, since it is not bound into a three-dimensional network of the polymer formation.

The degree of polymer crosslinking (crosslinking coefficient), showing the number of monomer chains, along which the crosslink was formed, in terms of the average macromolecule, was determined by the relation:

$$\boldsymbol{j} = \frac{\mathbf{1}}{\boldsymbol{S} + \sqrt{\boldsymbol{S}}}, \quad (2)$$

The fraction of active polymer chains was found by formula:

$$\boldsymbol{V_c} = (\mathbf{1} - \boldsymbol{S})^2(\mathbf{1} - \mathbf{2}\boldsymbol{jS})(\mathbf{1} + \boldsymbol{jS}), \quad (3)$$

The calculation results are presented in Table 3.

When PhA and CA are added to the acrylic polymer, the cross-link density of the polymer compared to an unfilled film is reduced by 39%, while the fraction of active chains is 0.77 compared to an unfilled film, the fraction of active chains of which is 0.75. The addition of PHMG-p to the polymer composition makes it possible to increase the degree of film crosslinking by almost 3 times and reach 14.50%. An increase in the degree of crosslinking of the polymer film is associated with the ability of PHMG-p to film formation, which leads to an increase in the number of interlinkages of polymer macromolecules. After heat setting, the degree of crosslinking of the composite polymer film somewhat increases.

Tensile tests were performed to compare the mechanical properties of treated and untreated cotton-polyester textile materials. The research results are shown in Fig. 5. Qualitative indicators of functional finishes are included in the Table 4.

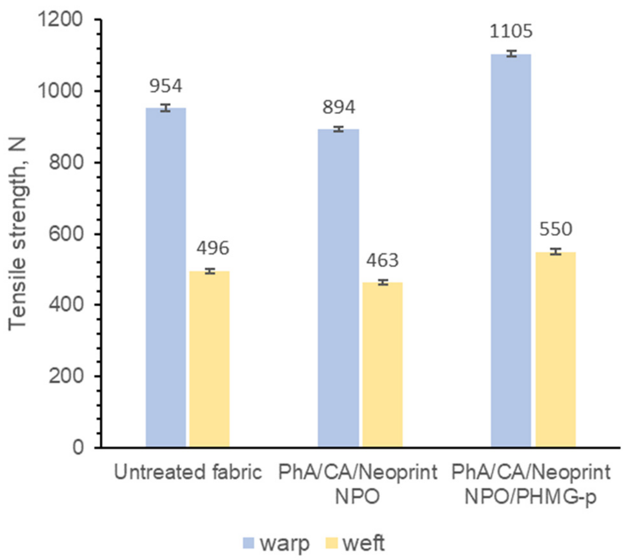


**Figure 5.** Tensile strength of untreated and treated cotton-polyester fabrics.

**Table 4.** Qualitative indicators of the functional finish of cotton-polyester fabric.

| Treatment | Height of the charred area [cm] | Afterflame time [s] | Afterglow time [s] | Height of charred area after washing [cm] | Washing fastness |
|---|---|---|---|---|---|
| Untreated fabric | – | – | – | – | – |
| PhA – 300 g/l; CA – 200 g/l; Neoprint NPO – 60 g/l | 12.5 | – | – | 15 | resistant to 1 washing cycle |
| PhA – 300 g/l; CA – 200 g/l; Neoprint NPO – 60 g/l; PHMG-p – up to 1000 g | 6.5 | 0 | 0 | 12.4 | resistant to 5 washing cycles |

Textile materials treated with a composition with PhA have a slightly reduced tensile strength, which can be explained by the acidic nature of the biomacromolecule used. The composition, which includes PHMG-p, restores tensile strength by increasing the degree of crosslinking of the polymers in the composition.

The decrease in resistance of the functional treatment to washing can be explained by the fact that the washing process takes place at high pH values (~10.5) arising from the presence of detergent, as well as by ion exchange with alkali metal cations, such as sodium, released from detergent agents and hard water. At the same time, given that PhA has six phosphoric acid groups, it can be used to obtain reactive fire retardants by interacting with amino groups and hydroxyl groups to improve washing fastness [30].

Table data confirm that the developed finishing composition makes it possible to obtain textile materials with enhanced antimicrobial and flame retardant properties. Thus, the result of the work is the developed composition for obtaining a complex antimicrobial and fire-retardant textile material that has barrier functions against pathogenic microorganisms and an open flame.

## CONCLUSIONS

The composition containing phytic acid and polyhexamethylene guanidine phosphate, due to the high content of phosphorus and nitrogen, gives the cotton-polyester fabric flame retardant and antimicrobial properties. The damaged length of the fabric decreased to 6.5 cm in the vertical burn test. TGA showed a shift in the temperature of the final destruction of the fabric to higher temperatures, which indicates an increase in the thermal stability of the fabric and contributes to the formation of charred parts that can prevent the transfer of heat and fuel in the condensed phase. An increase in the antimicrobial activity of the fabric is confirmed by a zone of inhibition of 2 – 4 mm around the sample according to the diffusion method using gram-positive bacteria Staphylococcus pyogenes, and is also characterized by a pronounced retardation of the growth of microorganisms around fabric samples studied by the method of inoculation microflora from the environment. Treatment with the studied composition improves the resistance to washing by increasing the degree of crosslinking of the polymer components used in the finishing composition, and also does not impair the mechanical properties of the textile material.

## REFERENCES


1. Kolb V. M.: Green Organic Chemistry and Its Interdisciplinary Applications (1st ed.), CRC Press, Boca Raton, FL, USA, 2016, 193 p., ISBN: 9781315371856. https://doi.org/10.1201/9781315371856
2. Kim H. J., Im S., Kim J. C., et al.: Phytic Acid Doped Polyaniline Nanofibers for Enhanced Aqueous Copper(II) Adsorption Capability, ACS Sustainable Chem. Eng. 5(8), 2017, pp. 6654-6664. https://doi.org/10.1021/acssuschemeng.7b00898
3. Malucelli G.: Textile finishing with biomacromolecules: A low environmental impact approach in flame retardancy, In: Shahid-ul-Islam, Butola B.S. (eds) The Textile Institute Book Series, The Impact and Prospects of Green Chemistry for Textile Technology, Woodhead Publishing, 2019, pp. 251-279, ISBN: 9780081024911. https://doi.org/10.1016/B978-0-08-102491-1.00009-5
4. Reshma A., Brindha Priyadarisini V., Amutha K.: Sustainable antimicrobial finishing of fabrics using natural bioactive agents – a review, Int. J. Life Sci. Pharma Res. 8(4), 2018, pp. 10-20. http://dx.doi.org/10.22376/ijpbs/lpr.2018.8.4.L10-20/
5. Perepelkin K. E.: Principles and Methods of Modification of Fibres and Fibre Materials. A Review, Fibre Chemistry 37, 2005, pp. 123-140. https://doi.org/10.1007/s10692-005-0069-6/
6. Billah S. M. R.: Textile Coatings, In: Jafar Mazumder M., Sheardown H., Al-Ahmed A. (eds) Functional Polymers, Polymers and Polymeric Composites: A Reference Series, Cham., Springer, 2019, 10, pp. 825-882. https://doi.org/10.1007/978-3-319-95987-0_30
7. Sadeghi-Kiakhani M., Safapour S.: Improvement of dyeing and antimicrobial properties of nylon fabrics modified using chitosan-poly(propylene imine) dendreimer hybrid, Journal of Industrial and Engineering Chemistry 33, 2016, pp. 170-177. https://doi.org/10.1016/j.jiec.2015.09.034
8. Arif D., Niazi M., Ul-Haq N., et al.: Preparation of Antibacterial Cotton Fabric Using Chitosan-silver Nanoparticles, Fibers and Polymers 16, 2015, pp. 1519-1526. https://doi.org/10.1007/s12221-015-5245-6
9. Xue Z.: Microwave-assisted antimicrobial finishing of wool fabric with chitosan derivative, Indian Journal of Fibre and Textile Research 40(1), 2015, pp. 51-56.
10. Moccelini S. K., Fernandes S. C., Vieira I. C.: Bean sprout peroxidase biosensor based on l-cysteine self-assembled monolayer for the determination of dopamine, Sensors and Actuators B: Chemical 133(2), 2008, pp. 364-369. https://doi.org/10.1016/j.snb.2008.02.039

11. Laufer G., Kirkland C., Morgan A. B., et al.: Intumescent Multilayer Nanocoating, Made with Renewable Polyelectrolytes, for Flame-Retardant Cotton, Biomacromolecules 13(9), 2012, pp. 2843-2848. https://doi.org/10.1021/bm300873b/
12. Zhou Y., Ding C., Qian X., et al.: Further improvement of flame retardancy of polyaniline-deposited paper composite through using phytic acid as dopant or co-dopant, Carbohydrate Polymers 115, 2015, pp. 670-676. https://doi.org/10.1016/j.carbpol.2014.09.025/
13. Wang X., Romero M. Q., Zhang X. Q., et al.: Intumescent multilayer hybrid coating for flame retardant cotton fabrics based on layer-by-layer assembly and sol–gel process, RSC Adv. 5, 2015, pp. 10647-10655. https://doi.org/10.1039/C4RA14943B
14. Costes L., Laoutid F., Dumazert L., et al.: Metallic phytates as efficient bio-based phosphorous flame retardant additives for poly(lactic acid), Polymer Degradation and Stability 119, 2015, pp. 217-227. https://doi.org/10.1016/j.polymdegradstab.2015.05.014
15. Li S., Lin X., Liu Y., et al.: Phosphorus-nitrogen-silicon-based assembly multilayer coating for the preparation of flame retardant and antimicrobial cotton fabric, Cellulose 26, 2019, pp. 4213-4223. https://doi.org/10.1007/s10570-019-02373-5
16. Chin W., Zhong G., Pu Q., et al.: A macromolecular approach to eradicate multidrug resistant bacterial infections while mitigating drug resistance onset, Nature Communications 9(1), 2018, pp. 917. https://doi.org/10.1038/s41467-018-03325-6
17. Cao Y., Gu J., Wang S., et al.: Guanidine-Functionalized Cotton Fabrics for Achieving Permanent Antibacterial Activity Without Compromising their Physicochemical Properties and Cytocompatibility, Cellulose 27(10), 2020, pp. 6027-6036. https://doi.org/10.1007/s10570-020-03137-2
18. Olewnik-Kruszkowska E., Gierszewska M., Jakubowska E., et al.: Antibacterial Films Based on PVA and PVA-Chitosan Modified with Poly-(Hexamethylene Guanidine), Polymers 11(12), 2019, pp. 2093. https://doi.org/10.3390/polym11122093
19. Alongi J., Carletto R. A., Blasio A. D., et al.: DNA: a novel, green, natural flame retardant and suppressant for cotton, J. Mater. Chem. A 1, 2013, pp. 4779-4785. https://doi.org/10.1039/C3TA00107E
20. Alongi J., Blasio A. D., Milnes J., et al.: Thermal degradation of DNA, an all-in-one natural intumescent flame retardant, Polymer Degradation and Stability 113, 2015, pp. 110-118. https://doi.org/10.1016/j.polymdegradstab.2014.11.001
21. Shang S., Yuan B., Sun Y., et al.: Facile preparation of layered melamine-phytate flame retardant via supramolecular self-assembly technology, Journal of Colloid and Interface Science 553, 2019, pp. 364-371. https://doi.org/10.1016/j.jcis.2019.06.015
22. Peng H., Wang D., Li M., et al.: N-P-Zn-containing 2D supermolecular networks grown on MoS2 nanosheets for mechanical and flame-retardant reinforcements of polyacrylonitrile fiber, Chemical Engineering Journal 372, 2019, pp. 873-885. https://doi.org/10.1016/j.cej.2019.04.209
23. Xu B., Wu X., Ma W., et al.: Synthesis and characterization of a novel organic-inorganic hybrid char-forming agent and its flame-retardant application in polypropylene composites, J. Anal. Appl. Pyrol. 134, 2018, pp. 231–242.
24. Sahraro M., Yeganeh H., Sorayya M.: Guanidine hydrochloride embedded polyurethanes as antimicrobial and absorptive wound dressing membranes with promising cytocompatibility, Mater. Sci. Eng. C 59, 2016, pp. 1025–1037.
25. Lazar S. T., Kolibaba T. J., Grunlan J. C.: Flame-retardant surface treatments, Nat. Rev, Mater. 5, 2020, pp. 259–275.
26. Zhao T., Chen Q.: Halogenated phenols and polybiguanides as antimicrobial textile finishes, Antimicrobial Textiles, 2016, pp. 141-153. https://doi.org/10.1016/B978-0-08-100576-7.00009-2
27. Li Z., Chen J., Cao W., et al.: Permanent antimicrobial cotton fabrics obtained by surface treatment with modified guanidine, Carbohydr Polym 180, 2018, pp. 192-199. https://doi.org/10.1016/j.carbpol.2017.09.080/
28. Cao Y., Gu J., Wang S., et al.: Guanidine-Functionalized Cotton Fabrics for Achieving Permanent Antibacterial Activity Without Compromising their Physicochemical Properties and Cytocompatibility, Cellulose 27(10), 2020, pp. 6027-603683.
29. Brocato R. L., Hammerbeck C. D., Bell T. M., et al.: A lethal disease model for hantavirus pulmonary syndrome in immunosuppressed syrian hamsters infected with sin nombre virus, Journal of Virology 88(2), 2014, pp. 811– 819.
30. Jin W. J., Cheng X. W., He W. L., et al.: A bio-based flame retardant coating for improving flame retardancy and anti-dripping performance of polyamide 6 fabric, Polymer Degradation and Stability 203, 2022, pp. 110087. https://doi.org/10.1016/j.polymdegradstab.2022.110087

# DESIGN A BRA SIZING SYSTEM FOR VIETNAMESE WOMEN BASED ON 3D SCAN DATA

**NGUYEN, THANH TUNG[1,2]; TRAN, THI MINH KIEU[1*]; PENG, LI-HSUN[3] AND HOANG, SY TUAN[4]**

[1] School of Material Science and Engineering, Hanoi University of Science and Technology, Vietnam
[2] Faculty of Garment and Fashion Design, Hanoi University of Industry, Vietnam
[3] Department of Creative Design, National Yunlin University of Science and Technology, Taiwan
[4] Faculty of Mechatronics, School of Mechanical Engineering, Hanoi University of Science and Technology, Vietnam

## ABSTRACT

This study focuses on the body shape of Vietnamese women, collected from large-scale measurement data, to establish a bra size system for mature Vietnamese women aged 18 to 55. Measurement data was collected from 1100 subjects using a 3D scanner. During the data collecting process, 18 measurements at the chest area were classified and used for the research and analysis. Data analysis is performed by the Principal Component Analysis (PCA) method and Numerical Analysis. Mean and median values are used to understand the central tendency of sizing charts. Standard deviation is leveraged to derive size categories, intervals and separate the outliers. Two size-matching solutions are implemented to find the optimal sizing system. The result found a 26 sizes bra system which is a combination of 5 band sizes and 6 cup sizes, with a response rate of 98.27% based on the primary dimensions of bust girth and underbust girth. The study's results were compared with the bra size systems of some countries in Asia and around the world, showing that differences in body shape have led to differences in the systems. the number of sizes. The ultimate goal of this research is to systematically establish a data database with local characteristics and significance that will contribute to sustainable development in academic research, industrial production, application, commercial activities, and service design in the future. The results of this study are meaningful for bra manufacturers in the Vietnamese market and for women in selecting suitable bras for their somatotype.

## KEYWORDS

Bra; Sizing system; Size categories; Size intervals; Vietnamese women; 3D scan data.

## INTRODUCTION

Vietnam has been and is a potential garment production and fashion market. Global brands through representative stores and online sales platforms are present in Vietnam, contributing to enriching and diversifying consumer choices. Therefore, domestic manufacturers are also increasingly investing in technology and design quality to compete for market share and strengthen their position with domestic consumers. Clothing is an integral part of everyday life. It protects not only the body but also the wearer, expresses their personality and aesthetic, helps individuals communicate confidently, and enhances their appearance, especially when it comes to bras.

Bras contribute a significant role in a woman's life. A correctly fitting bra is not only good for health [1, 2], as it can alleviate breast pain [2] and muscle fatigue or pain [3], but it also helps to shape and support the breasts [4]. It helps make the bust fuller and more attractive [5], and minimizes the effects of gravity, slowing down the sagging process of the breasts [6]. However, if the size is wrong, it will not provide practical support [7]. It can affect health, make the wearer lose confidence in communication, and inhibit women from participating in daily physical activities [8] due to a less attractive appearance or difficulty in movement. Therefore, choosing a bra that fits your body size is something every woman desires.

Currently, in Vietnam, there has not been a system of bra sizes for Vietnamese women. Each manufacturer uses its sizing methods, such as Triumph [9], Victoria's Secret [10], and Calvin Klein [11]. Domestic bra manufacturers such as Vera [12], and Relax [13] also use their own developed sizing systems. This greatly affects consumers when they find it difficult to choose a bra suitable for their body size. Therefore, the goal of this research is to systematically establish a data database with local characteristics and significance that will support industrial production, application, commercial activities, and service design in the future. At the same time, this research helps

* **Corresponding author:** Tran T.M.K., e-mail: kieu.tranthiminh@hust.edu.vn

*Received October 3, 2022; accepted December 4, 2023*

Vietnamese women easily choose a bra suitable for their body size.

## LITERATURE REVIEW

Bras not only have the function of protecting and shaping the women's bust but also make them more attractive, helping the wearer feel comfortable at work and confident in communication. Choosing a bra that matches the bust size is not easy for Vietnamese women, and this is because there is currently no specific bra size system for the Vietnamese body type. There has been no official research conducted on the bra sizing system for Vietnamese women.

Bra sizing systems are built around dividing users into groups with similar body measurements. Body size determines the key primary dimensions of grouping [14]. The bra size is composed of Band size and Cup size, denoted by two primary dimensions: Bust and Underbust [14, 15]. Therein, the underbust measurement determines the size of the bra band, which encircles the wearer's rib cage. Meanwhile, the difference between the bust girth and the underbust girth determines the bra cup size, representing the volume of the bust [14, 16]. Edward A.P. [17] developed a system of bra measurement for predicting post-augmentation breast size. In this research, the bras band size is still determined by underbust girth, while the cup size is determined by directly measuring the breast in proportion to the underbust circumference.

Research results from the paper ‘breast volume and bra size [18] demonstrate the range of breast volumes within each size and the variations amongst different bra sizes. The authors measured the breast volume of 104 women via water displacement and compared it to their professionally fitted bra sizes. The results showed that the large variation in breast volumes is associated with different band sizes. Therefore, the authors suggest that women should not consider themselves solely based on cup size but rather as a combination of band and cup size. Some research has proposed a method of classifying bra cup size based on breast arc length, as accurate measurements of breast arc length could be useful for bra cup sizing and design. Pechter [19] defined bra cup size A as a breast arc length of 7 inches and size B as a breast arc length of 8 inches. Each additional inch in breast arc length corresponded to the next larger bra cup size. In Bengtson's research [20], the author used the direct measurement method to collect and analyze breast arc length from more than five thousand volunteers. The author proposes that there is a 2 cm difference in the breast arc length among different bra sizes. This is also the basis for the author to propose a method for choosing the bra size in women undergoing breast augmentation surgery based on breast size.

Many bras are unsuitable because wearers often choose the wrong cup size, incorrect bra band size, or incorrectly determine their bust size. Previous international research has primarily focused on improving bust cup suitability. In a study on the bra sizing system for Chinese women, Zheng [21] presented a new approach to determine bra sizes based on the established sizing system. In this method, the underbust measurement determines the band size, while the bra cup size is determined by the ratio of bust depth and width. In the research of Seoyoung Oh [14], the author proposed a novel method to determine bra sizes. According to this research, the bra band size is determined by the underbust measurement, and the cup size is determined by three measurements: the bust's width, depth, and arc length. Yu Liu [22] suggested the inclusion of bust width when constructing a bra sizing system. While these studies hold theoretical significance, they lack practicality as wearers face challenges in accurately measuring their bust depth, width, and breast volume comfortably.

Therefore, this research utilizes basic 3D measurements of the human body and applies the principal component analysis method to identify the dominant dimensions. The main objectives of this study involve determining the optimal bra sizing system for Vietnamese women through discriminant analysis and crosstabulation, which are the two primary components of the sizing trials.

## METHODOLOGY

### Determine the research size sample

Formula (1) is used to determine the minimum sample size:

$$\boldsymbol{n} = \frac{S^2 * Z^2}{e^2} \tag{1}$$

Where n is size sample; $S$ is the standard deviation; $Z$ is features of the probability and e is standard error

The standard deviation of 5.75 cm was determined by experimentally measuring the bust size of 30 random samples. The probability features a value of 2.58, which is determined by a probability $P$ = 0.99, and a standard error of 0.5. Base on these values, the minimum sample size required is calculated to be 880.3. A Scanning study was conducted on 1145 adult female models working in Hanoi, aged 18-55 during the period from 2017 to 2022. Throughout the data collection process, the models wore thin bras without cup pads to minimize measurement errors.

### Determine body measurements

Based on previous research conducted by Oh Seolyoung [14], Zheng [21], Kristina Shin [23], and Avşar [24], a total of 18 body measurements in the bust region were determined. These measurements including four circumferences, five height measurements, six horizontal measurements, and three vertical measurements, all extracted from 3D data. The specific measuring positions are illustrated

**Table 1.** Abbreviations and reports of the research measurements.

| Ord | Measurements | ABBr | Descriptions |
|---|---|---|---|
| 1. | Side neck to waist | Cc-e | Distance from the side neck point to waist plane |
| 2. | Shoulder to waist | Cv-e | Distance from the shoulder point to the waist plane |
| 3. | Upper bust to waist | Cnt-e | Distance from upper bust plane to waist plane |
| 4. | Bust point to waist | Cdn-e | Distance from bust point to waist plane |
| 5. | Underbust to waist | Ccn-e | Distance from under-bust plane to waist plane |
| 6. | Side neck to bust point length | Dc-n | Length clings to the body from the side neck to the bust point. |
| 7. | Side neck to under bust-length | Dc-in | Length clings to the body from the side neck point over the bust to the underbust point. |
| 8. | Neck hollow point to bust pt | Dh-n | Length from Neck hollow point to bust point |
| 9. | Upper bust arc width | Rnt | Length clings to the body from the front right armpit crease point to the left. |
| 10. | Bust arc width | Rn | Length clings to the body over the bust line from the front right side to the left. |
| 11. | Underbust arc width | Rcn | Length clings to the body over the underbust line from the front right side to the left. |
| 12. | Waist arc width | Reo | Length clings to the body over the waistline from the front right side to the left. |
| 13. | Bust point to bust point | Rdn | Distance from the left bust point to the right |
| 14. | Bust cup length | Dcv | Length clings on the body over the bust line from the end side of the cup over the bust point to the center front. |
| 15. | Upper bust girth | Vnt | Measure clings on the body the upper bust girth |
| 16. | Full bust girth | Vn | Measure clings on the body the full girth through the two bust points |
| 17. | Underbust girth | Vcn | Measure clings on the body the underbust girth |
| 18. | Waist girth | Veo | Measure clings on the body, the waist girth through the smallest of the torso |

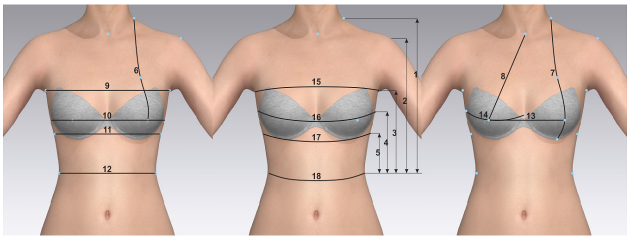

**Figure 1.** Research measurements positions.

in Figure 1. Abbreviations and descriptions for each measurement used in this study can be found in Table 1.

## Determine the bust's primary dimensions

The Principal Component Analysis (PCA) method is employed to identify the primary dimensions. In this process, the factors with the highest value in each column of the rotated factor matrix is selected as the primary dimension. The dimensions chosen as master sizes undergo testing for standard distribution, considering the conditions: the mean value approximates the median, the standard distribution chart is examined, the asymmetric coefficient (Sk) approaches zero, the Inspection Kolmogorov - Smirnov test is conducted for sample sizes exceeding 500 with Sig. value larger than 0.05, and the normal Q-Q Plot indicates a linear pattern in the average probability chart.

## Determine the bra size system's average size, size interval, and size number for the bra size system

The average size is determined by considering the frequency of occurrence for each size. The size interval for the primary dimension is established using standard deviation (SD) of the measurements and is then compared with previous research findings. The number of sizes is determined based on the response rate for each of individual sizes.

# RESULTS AND DISCUSSIONS

## Results 3D data statistics

To ensure the reliability of this research and the results, the study uses the *Z* coefficient to determine the unknown number [27]. If the z-value of some $X_i$ values < 3, those values are considered to fall within the acceptable range of distribution.

*Z*-value is determined by (2)

$$z = \frac{|X_i - \bar{X}|}{\sigma} \quad (2)$$

Where $X_i$ is any value of *X*; $\bar{X}$ is Mean; $\sigma$ is the standard deviation

With Z < 3, which mean

$$\frac{|X_i - \bar{X}|}{\sigma} < 3 \quad (3)$$

Equation (3) can be rewritten as

$$\bar{X} - 3\sigma < X_i < \bar{X} + 3\sigma \quad (4)$$

**Table 2.** Descriptive analysis results of chest measurements.

| Ord. | ABBr. | N | Mode | Min | Max | Median | SD | Mean | $\bar{X}-3\sigma$ | $\bar{X}+3\sigma$ |
|---|---|---|---|---|---|---|---|---|---|---|
| 1. | Cc-e | 1100 | 41.25 | 33.50 | 48.55 | 40.75 | 2.67 | 40.61 | 32.59 | 48.63 |
| 2. | Cv-e | 1100 | 35.50 | 27.00 | 42.59 | 35.00 | 2.69 | 34.72 | 26.65 | 42.79 |
| 3. | Cnt-e | 1100 | 22.50 | 15.00 | 32.75 | 24.50 | 3.22 | 24.36 | 14.69 | 34.03 |
| 4. | Cdn-e | 1100 | 21.00 | 12.00 | 28.00 | 20.00 | 2.79 | 19.96 | 11.58 | 28.33 |
| 5. | Ccn-e | 1100 | 14.00 | 6.50 | 19.50 | 13.00 | 2.50 | 12.82 | 5.32 | 20.31 |
| 6. | Dc-n | 1100 | 24.94 | 18.25 | 31.38 | 24.51 | 2.30 | 24.63 | 17.73 | 31.53 |
| 7. | Dc-cn | 1100 | 33.48 | 25.93 | 41.31 | 33.34 | 2.66 | 33.53 | 25.56 | 41.50 |
| 8. | Dh-n | 1100 | 20.09 | 14.86 | 25.27 | 19.59 | 1.89 | 19.71 | 14.03 | 25.38 |
| 9. | Rnt | 1100 | 42.45 | 31.38 | 53.09 | 40.85 | 3.55 | 40.92 | 30.28 | 51.56 |
| 10. | Rn | 1100 | 43.09 | 34.25 | 54.73 | 43.55 | 3.31 | 43.69 | 33.77 | 53.62 |
| 11. | Rcn | 1100 | 32.18 | 24.06 | 42.80 | 33.12 | 3.27 | 33.14 | 23.33 | 42.95 |
| 12. | Reo | 1100 | 39.19 | 29.18 | 46.04 | 36.94 | 3.07 | 37.01 | 27.81 | 46.21 |
| 13. | Rdn | 1100 | 17.20 | 12.89 | 21.21 | 16.70 | 1.51 | 16.73 | 12.19 | 21.26 |
| 14. | Dcv | 1100 | 19.20 | 13.10 | 26.90 | 19.80 | 2.39 | 19.69 | 12.53 | 26.84 |
| 15. | Vnt | 1100 | 84.82 | 70.12 | 100.24 | 84.61 | 5.31 | 84.64 | 68.71 | 100.57 |
| 16. | Vn | 1100 | 92.43 | 73.64 | 101.10 | 86.47 | 4.97 | 86.47 | 71.55 | 101.40 |
| 17. | Vcn | 1100 | 68.02 | 61.84 | 88.51 | 72.87 | 5.21 | 73.11 | 57.48 | 88.75 |
| 18. | Veo | 1100 | 76.63 | 58.95 | 92.66 | 74.47 | 5.14 | 74.57 | 56.15 | 93.00 |

**Table 3.** Bartlett's test results and KMO index.

**KMO and Bartlett's Test**

| | | |
|---|---|---|
| Kaiser-Meyer-Olkin Measure of Sampling Adequacy. | | .755 |
| Bartlett's Test of Sphericity | Approx. Chi-Square | 31906.403 |
| | df | 153 |
| | Sig. | .000 |

After removing the unknown numbers, 1100 sets of body size parameters with *Z*-coefficients of dimensions all smaller than 3 are used for the analysis, as shown in Table 2.

Table 2 shows measurements for adult women, indicating an average bust girth of 86.47 cm with standard deviation of 4.97 cm. The smallest bust girth (Vn) recorded is 73.64 cm, while the largest is 101.10 cm, resulting in a difference range is 27.46 cm. The average under-bust girth (Vnt) is 73.11 cm, with the standard deviation of 5.21 cm. The smallest measurement is 61.84 cm, and the largest is 88.51 cm, showing the difference range of 26.67 cm. Furthermore, the overbust girth (Vnt) measures at an average of 84.64 cm, with an standard deviation of 5.31, the smallest is 70.12 cm, the largest is 100.24 cm, and the difference range is 30.12 cm.

## Results of determining principal dimensions

PCA results in Table 3 show that the KMO index is 0.755, which is greater than 0.5. This proves that the data used for factor analysis is entirely appropriate [28].

Barlett's test result is 31906.403 with a significance level of <0.05, which means that the variable numbers are correlated and satisfy the conditions for factor analysis. Factor analysis performed 74.718% according to Total Variance Explained with Varimax rotation Sums of squared loadings. Table 4 showed the initially grouping of the 18 observed variables into three factors. Group 1 gathers ten similar characteristic variables related to girths and widths of the upper torso, accounting for 37.742%. The variables of bust girth (Vn) and underbust girth (Vcn) have the highest values in the first factor. Group 2 consists of five similar characteristic variables related to distance from the waist to extreme points of the upper torso, accounting for 21.861%. Group 3 comprises three similar characteristic variables and denotes the relationship between the bust and neck points, accounting for 15.115%. The variable with the highest value at factor 3 is the length from the side neck point to the bust point (Dcn). This result is similar to the current bra sizing systems. The ISO system of international standards (ISO 4416) [29] also the bra size system of other countries [16] use bust girth and underbust girth to determine the bra size system. Commercial lingerie brands such as Triumph [9], Calvin Klein [10], Amoena [30], and Eva's Intimates [31]... all use bust and underbust circumference to determine the size of bras.

Therefore, this research uses bust girth and underbust girth to determine the sizes for Vietnamese female bras. These two variables hold the highest value in the first factor, indicating their strong influence on the sizing system. Moreover, these measurements can be easily obtained by the wearers themselves, ensuring convenience and accuracy.

**Table 4.** Result of factor analysis with Varimax rotation.

| Factor name | Variables | ABBr | Component | | |
|---|---|---|---|---|---|
| | | | 1 | 2 | 3 |
| 1: Girths and widths of the upper torso | Full bust girth | Vn | .925 | -.012 | .221 |
| | Underbust girth | Vcn | .925 | .005 | .083 |
| | Upper bust girth | Vnt | .908 | .057 | .157 |
| | Underbust arc width | Rcn | .862 | -.176 | -.002 |
| | Upper bust arc width | Rnt | .841 | -.066 | .073 |
| | Bust arc width | Rn | .835 | -.177 | .232 |
| | Waist girth | Veo | .816 | .284 | .283 |
| | Waist arc width | Reo | .816 | .285 | .284 |
| | Bust cup length | Dcv | .560 | -.114 | .147 |
| | Bust point to bust point | Rdn | .454 | -.109 | .276 |
| 2: Distance from waist to extreme points of the upper torso | Side neck to waist | Cc-e | .046 | .900 | .343 |
| | Shoulder to waist | Cv-e | .057 | .888 | .237 |
| | Bust point to waist | Cdn-e | -.044 | .886 | -.327 |
| | Underbust to waist | Ccn-e | .043 | .861 | -.255 |
| | Upper bust to waist | Cnt-e | -.235 | .720 | -.065 |
| 3: Relationship between the bust point and neck points | Side neck to bust point length | Dc-n | .281 | -.054 | .869 |
| | Side neck to under bust-length | Dc-cn | .135 | .110 | .789 |
| | Neck hollow point to bust point | Dh-n | .313 | -.139 | .770 |
| Factor loading (%) | | | 37.742% | 21.861% | 15.115% |

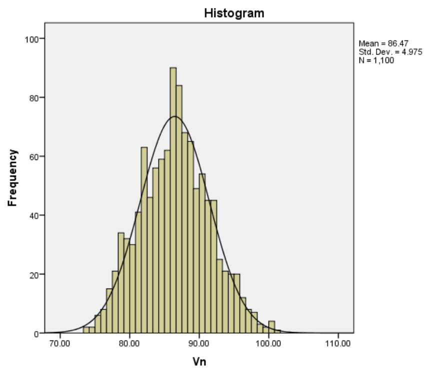


(a)

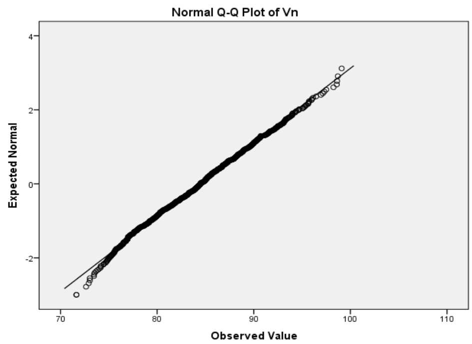


(b)

**Figure 2.** The standard distribution test of bust girth; (a) bell-shaped; (b) Q_Q plot.

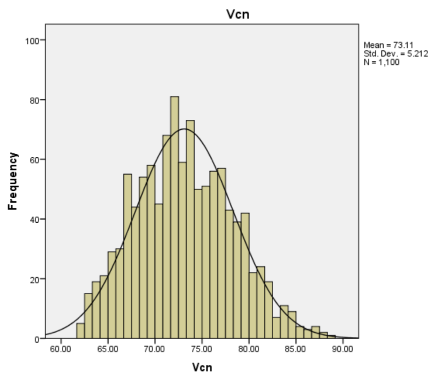


(a)

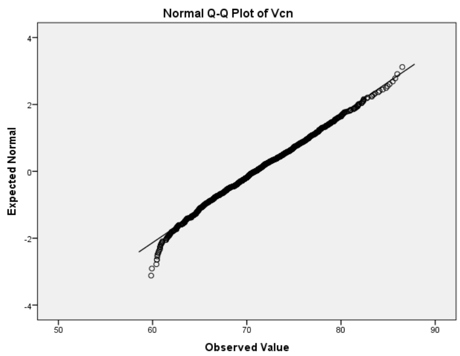


(b)

**Figure 3.** The standard distribution test of underbust girth; (a) bell-shaped; (b) Q_Q plot.

The standard distribution test shows that the Mean of bust girth, at 86.47, is approximately equal to its Median of 86.47. The Mean of underbust girth, at 73.11, is roughly equivalent to the Median of 72.87. The *Sk* value is close to zero for bust and underbust girth, with values of 0.001 and 0.14, respectively. The distribution charts of these two measurements, shown in Figures 2a and 3a, exhibit a is bell-shaped curve. The Kolmogorov-Smirnov test yields significant results for bust and underbust girth, with values of 0.2 and 0.68, respectively, exceeding the threshold of 0.05. The standard probability Q-Q plots, in Figures 2b and 3b, demonstrate a linear relationship, indicating that the measured values of the bust and underbust girth adhere to the standard distribution rule.

## Determine the average size, size interval, and size number of the bra size system

Bra size including two parts band size and cup size [15]. The first crucial step is determining the average band size, following by selecting the size intervals for the band and the cup for the adjacent sizes. In Vietnam, the Metric system in centimeters (cm) is widely used and familiar, making it the unit of choice for the band size measurements. Cup size, on the other hand, is determined by the difference between bust girth and underbust girth [15]. According to the statistical results, the average underbust girth is 73.11 cm. The frequency chart of underbust girth in Figure 3a illustrates that an underbust girth of 70 cm to 75 cm (Vcn) has the highest frequency. Moreover, round numbers are more advantageous for communication purposes, also 73.11 leaning toward 75. Therefore, the primary dimensions for underbust girth with a value of 75 cm, will serve as the foundation for developing a bra size system in this research.

In previous research on sizing system for Vietnamese women, various intervals have been proposed for the bust size. Some studies suggested a 5 cm interval (Tran, MK [32, 33],) or 4 cm (TCVN 5782 – 2009 [34]; 2010 [35]; 2015 [36]; 2019 [37]). Several famous bras sizing systems worldwide, including those from Japan [16], China [21], Korea [23], Britain [16], US [16], Calvin Klein [10], and Victoria's Secret [11] also use 5 cm interval for bust and underbust size. Besides, other bras sizing systems such as ISO 4416, Imperial, and metrics for bras use a 4 cm interval for bust and underbust size. In addition, Italian [16], France [16], Spain [16], Australian [16], Triumph [9], and Amoena [30] bra size charts use a 5 cm bust size interval and a 4 cm underbust size interval. Considering that the standard deviation of the underbust girth in this research is 5.21 cm, a 5 cm interval for the bra band size would align with be recognized as previous studies mentioned above and be appropriate.

The statistical results describing measurement Drop: Birth girth (Vn) – Underbust girth (Vcn) in Table 5 show that the smallest difference is 7.21 cm, and the largest is 21.88 cm. The average difference between these two circumferences is 13.36 cm, with the standard deviation of 2.37. In addition, previous researchers applied standard deviation as the size interval [32, 38, 39]. Since the difference between bust and underbust girth is a criterion related to breast size, further analysis is necessary to determine the value round standard deviation, 2 cm or 2.5 cm, which would be the size interval between adjacent bra cup sizes. As mentioned above, the underbust girth determines the bra band size; therefore, 5 cm sets the size interval for the bra band. Therefore, two sizing models will be conducted with different size intervals for the dominant measurement. The two trial sizing models are: 85(± 2.5 cm) and 75(± 5 cm); 85(± 2 cm) and 75(± 5 cm).

**Table 5.** Descriptive Statistics of measurement Drop: Birth girth – Underbust girth.

| | N | Range | Minimum | Maximum | Mean | Std. Deviation |
|---|---|---|---|---|---|---|
| Vn - Vcn | 1100 | 14.67 | 7.21 | 21.88 | 13.3607 | 2.37103 |
| Valid N (listwise) | 1100 | | | | | |

**Table 6.** The response ratio of the sizes for the two options.

| The minimum response rate for size [%] | System 1 85(2.5)&75(5) | | System 2 85(2)&75(5) | |
|---|---|---|---|---|
| | Total response [%] | Size quantity | Total response [%] | Size quantity |
| From 0.5% | 98.27 | 26 | 96.64 | 29 |
| From 1.0% | 94.00 | 20 | 92.65 | 23 |
| From 1.5% | 90.27 | 17 | 89.09 | 20 |
| From 2.0% | 86.91 | 15 | 82.73 | 16 |

**Table 7a.** Response ratio of size system 85 (±2.5) & 75 (±5).

| | Bust girth [cm] | | | | | | | | | | |
|---|---|---|---|---|---|---|---|---|---|---|---|
| **Underbust girth [cm]** | **72.5-75** | **75-77.5** | **77.5-80** | **80-82.5** | **82.5-85** | **85-87.5** | **87.5-90** | **90-92.5** | **92.5-95** | **95-97.5** | **97.5-100** |
| 65(61-65) | 0.36 | 1.82 | 3.64 | 1.55 | 0.73 | 0.09 | 0.00 | 0.00 | 0.00 | 0.00 | 0.00 |
| 70(66-70) | 0.00 | 0.82 | 4.09 | 9.27 | 7.91 | 4.27 | 0.55 | 0.00 | 0.00 | 0.00 | 0.00 |
| 75(71-75) | 0.00 | 0.00 | 0.18 | 1.36 | 5.45 | 14.73 | 9.91 | 2.73 | 0.82 | 0.09 | 0.00 |
| 80(76-80) | 0.00 | 0.00 | 0.00 | 0.00 | 0.55 | 2.36 | 6.09 | 9.36 | 2.73 | 1.36 | 0.18 |
| 85(81-85) | 0.00 | 0.00 | 0.00 | 0.00 | 0.00 | 0.00 | 0.09 | 1.00 | 2.27 | 2.09 | 0.82 |
| 90(86-90) | 0.00 | 0.00 | 0.00 | 0.00 | 0.00 | 0.00 | 0.00 | 0.00 | 0.18 | 0.09 | 0.45 |
| **Total (%)** | **0.36** | **2.64** | **7.91** | **12.18** | **14.64** | **21.45** | **16.65** | **13.09** | **6.00** | **3.64** | **1.45** |

**Table 7b.** Response ratio of size system 85 (±2) & 75 (±5).

| | Bust girth [cm] | | | | | | | | | | | | | |
|---|---|---|---|---|---|---|---|---|---|---|---|---|---|---|
| **Underbust girth [cm]** | **73-75** | **75-77** | **77-79** | **79-81** | **81-83** | **83-85** | **85-87** | **87-89** | **89-91** | **91-93** | **93-95** | **95-97** | **97-99** | **99-101** |
| 65(61-65) | 0.36 | 1.09 | 2.91 | 2.00 | 1.18 | 0.55 | 0.09 | 0.00 | 0.00 | 0.00 | 0.00 | 0.00 | 0.00 | 0.00 |
| 70(66-70) | 0.00 | 0.64 | 2.36 | 4.27 | 8.27 | 6.55 | 3.91 | 0.73 | 0.09 | 0.00 | 0.00 | 0.00 | 0.00 | 0.00 |
| 75(71-75) | 0.00 | 0.00 | 0.18 | 0.36 | 1.55 | 4.91 | 11.18 | 10.45 | 4.82 | 1.55 | 0.18 | 0.00 | 0.09 | 0.00 |
| 80(76-80) | 0.00 | 0.00 | 0.00 | 0.00 | 0.00 | 0.55 | 1.55 | 4.55 | 6.45 | 6.00 | 2.00 | 1.27 | 0.27 | 0.00 |
| 85(81-85) | 0.00 | 0.00 | 0.00 | 0.00 | 0.00 | 0.00 | 0.00 | 0.00 | 0.45 | 0.82 | 2.09 | 1.73 | 0.73 | 0.45 |
| 90(86-90) | 0.00 | 0.00 | 0.00 | 0.00 | 0.00 | 0.00 | 0.00 | 0.00 | 0.00 | 0.00 | 0.18 | 0.09 | 0.27 | 0.27 |
| **Total (%)** | **0.36** | **1.73** | **5.45** | **6.64** | **11.00** | **12.55** | **16.73** | **15.73** | **11.82** | **8.36** | **4.45** | **3.09** | **1.36** | **0.73** |

Previous studies have suggested that the optimal sizing system is the one that can satisfy the majority of wearers while having the smallest number of sizes, achieved by selecting the response ratio of the measurements in the system [40]. The minimum response ratio for each size was 1.53% in Gupta's study [41], 1.6% in Park's study [42], and 1% in Tran, MK's study [ 33]. The results of the trials, presented in Table 6, provide details on the response rates of sizes when considering minimum response levels from 0.5%, 1.0%, 1.5%, and 2.0%, respectively. The response rate indicates the percentage of people who fit into each bra size.

Table 7a illustrates the number of sizes for the Vn&Vcn size of 85(± 2.5) & 75(± 5) when taking the response level of 0.5% or higher. Although the other rates have significant total response rates (94.00 with 1.0%, 90.27 with 1.5%, 86.91 with 2.0%), they serve more than 80% of the subjects. However, choosing these rates will remove many sizes that have a high frequency of occurrence. For example, selecting the 1% response rate would eliminate five sizes, the 1.5% response rate would remove eight sizes, and the 2.0% response rate would discard ten sizes. Therefore, the study selected the 0.5% response rate to establish the numerical size system, which resulted in a total response rate of 98.27% and included 26 numerical measures. Table 7b illustrates the number of sizes for the Vn&Vcn size of 85 (± 2) & 75 (± 5) when taking the response level of 0.5% or higher. When comparing the data dispersion between Tables 7a and 7b, a difference in concentration of the highest response rate is evident. Table 7a shows that the average number for a 75 cm underbust girth and an 85-87.5cm bust girth reaches 14.73%, while table 7b only reaches 11.18%. A higher concentration of individual sizes is preferred for the size system.

From the results in Table 6, it can be seen that the combination 85 (2.5) & 75 (5) achieved better results for bra sizing systems. Among the two options tested with response rates of 0.5%, 1.0%, 1.5%, and 2.0%, the size factor 85 (2.5) & 75 (5) archived the highest total response rates and the smallest number of sizes. Therefore, the study selected the number 85 (5) & 75 (5) systems as the basis for developing a bra size numbering system for Vietnamese women. Table 7a describes the response rates for each size, taking response levels from 0.5% or higher to 1.0%, 1.5%, and 2.0%.

## Labelling the size for the Vietnamese bra size system

The cup sizes in the international bra numbering system are assigned alphabetically starting with AA, A, B, C, and D. These are numerical sizing systems; other bras are widely applied in the manner of names and shown as above [14]. The difference between bustline and underbust circumference for Cup A is 10cm [14, 16]. Cup sizes AA, B, C, D... there are differences with cup A with corresponding size intervals. This study has determined that the optimal size interval for the Vn-Vcn difference of adult Vietnamese women is 2.5 cm.

**Table 8.** Bra cup sizes classified by the range difference between bust girth and underbust girth.

| **Difference [cm] (Vn-Vcn)** | < 10.0 | 10.0-12.5 | 12.5-15.0 | 15.0 – 17.5 | 17.5-20.0 | > 20.0 |
|---|---|---|---|---|---|---|
| **Bra cup sizes** | AA | A | B | C | D | E |

**Table 9.** The range of difference between bust girth – underbust girth corresponding to the range of size.

| **Underbust girth** | **Difference bust girth – underbust girth [cm]** | | **Range of size** |
|---|---|---|---|
| | **Min** | **Max** | |
| 65(61-65) | 9.92 | 20.48 | **A – D** |
| 70(66-70) | 7.59 | 21.36 | **AA–E** |
| 75(71-75) | 7.21 | 21.88 | **AA–E** |
| 80(76-80) | 7.29 | 20.73 | **AA-E** |
| 85(81-85) | 7.36 | 16.73 | **AA-C** |

**Table 10.** Vietnamese bra size system.

| **BRA BAND SIZE** | **Underbust girth [cm]** | **BRA CUP SIZE** | | | | | |
|---|---|---|---|---|---|---|---|
| | | **AA** | **A** | **B** | **C** | **D** | **E** |
| | | **Bust girth [cm]** | | | | | |
| **65** | 61 - 65 | - | **75-77.5** | **77.5-80** | **80-82.5** | **82.5-85** | - |
| **70** | 66 - 70 | **75-77.5** | **77.5-80** | **80-82.5** | **82.5-85** | **85-87.5** | **87.5-90** |
| **75** | 71 - 75 | **80-82.5** | **82.5-85** | **85-87.5** | **87.5-90** | **90-92.5** | **92.5-95** |
| **80** | 76 - 80 | **82.5-85** | **85-87.5** | **87.5-90** | **90-92.5** | **92.5-95** | **95-97.5** |
| **85** | 81 - 85 | **90-92.5** | **92.5-95** | **95-97.5** | **97.5-100** | - | - |

**Table 11.** Conversion between Band size and Underbust girth[16].

| **UNDERBUST GIRTH [cm]** | | **60-65** | **65-70** | **70-75** | **75-80** | **80-85** |
|---|---|---|---|---|---|---|
| **BAND SIZE** | This research | 65 | 70 | 75 | 80 | 85 |
| | International | 60 | 65 | 70 | 75 | 80 |
| | Japan, Korea | 60 | 65 | 70 | 75 | 80 |
| | UK, USA | 28 | 30 | 32 | 34 | 36 |
| | France, Spain | 75 | 80 | 85 | 90 | 95 |

**Table 12.** Bra cup size comparison between several size systems.

| **DIFFERENCE BUST-UNDERBUST VN-VCN [cm]** | | **<10** | **10-12** | **12-14** | **14-16** | **16-18** | **18-20** | **20-22** |
|---|---|---|---|---|---|---|---|---|
| **CUP SIZE** | This research | AA | A | A/B | B/C | C/D | D | E |
| | International | | AA | A | B | C | D | E |
| | Japan, Korea | AA | A | B | B/C | C | D | E |
| | UK, USA | AA | A | B | B/C | C | D | E/DD |
| | France, Spain | | AA | A | B | C | D | E |

Moreover, the results in Table 5 show that the minor cup size corresponding to the Vn-Vcn difference is 7.21 cm, the giant cup size corresponding to the Vn-Vcn difference is 21.88 cm, and the average cup size corresponding to the mean Vn-Vcn difference is 13.36 cm. Considering, the 14.67 cm range difference between bust and underbust girth, it is possible to identify six cup sizes, namely AA, A, B, C, D, and E. These results are shown in Table 8.

Table 9 shows the difference between bust girth and underbust for each bra band size group. This table allows for the identification of smallest and largest cup size as well as the cup size range for each belt size group. Combining the results from Tables 7, 8, and 9, the bra sizing system proposed in this study is determined and presented in Table 10.

The results in Table 10 show the Vietnamese bra sizing system, which consists of a total of 26 numerical sizes, divided into five groups based on five bra band sizes: 65, 70, 75, 80, and 85. The smallest band size is 65 with 4 cup sizes, the most prominent band size is 85 with 4 cup sizes, while the other average band sizes have more cup sizes. These 26 sizes can meet 98.27% of Vietnamese women aged 18 to 55 years. From the bra sizing Table 10, the wearers can determine their bra size. Customers collate the underbust circumference in the first and second columns to select the band size; then collate the bust girth to fit their bust cup size.

Table 11 shows the similarities in bra band sizes between this study and other sizing systems, particularly in Asian countries such as Japan and Korea. This table also provides a comparison of band sizes between this study and sizing systems used in UK, USA, France, and Spain. Table 12 compares the cup bra sizes in this research to those used in several countries' bra sizing systems. The results indicate that the relationship between the cup size name and the difference between bust and underbust measurements in Japanese, Korean, British, and American sizing systems has no difference with the findings of this study. For instance, a difference range of 10-12 cm corresponds to a cup size of A, which aligns with the AA cup size in France and Spain. In the survey, bra size is closely resemble the dimensions used in Japan and Korea, both in terms of band size and cup size. The number size in the study is similar to that of Japan and Korea. This result also demonstrates the practical significance of the study.

## CONCLUSION

The breast area is a sensitive part of a women's body. Choosing a bra suitable for the bust size is one of the critical factors that help support and protect the bust area, creating confidence and comfort for women when using it. In this study, the bra size system for Vietnamese women builds on 3D measurements taken from 2017 to 2022, of 1100 adult Vietnamese women living in Hanoi, Vietnam, aged 18-55. Using principal component analysis and crosstabulation, the author has established a system of bra sizes for Vietnamese women, meeting 98.27% of the population in the study age group. The parameter set includes 26 different sizes, including the system of 5 band sizes and 6 cup sizes.

This research will be a valuable database in industrial garment manufacturing practices when designing patterns for mass-customization, applied in teaching-related subjects on women's bra design, and contributing to the section that proposes options for adjusting the fit of the bras to the Vietnamese body. The limitation of the topic is that the size of bras for bigsize women with bust size greater than 100 cm has not been determined yet.

**Acknowledgement**: *This research was supported by the Hanoi University of Science and Technology (HUST) under project number T2018-PC-048.*

## REFERENCES

1. White J., Scurr J.: Evaluation of professional bra fitting criteria for bra selection and fitting in the UK. Ergonomics, 55(6), 2012, pp. 704-711. https://doi.org/10.1080/00140139.2011.647096
2. Smith R.L., Sandhya P., Lorraine A.F.: Evaluation and management of breast pain. Mayo Clinic Proceedings, 79(3), 2004, pp. 353-372. https://doi.org/10.4065/79.3.353
3. Wood K., Cameron M., Fitzgerald K..: Breast size, bra fit and thoracic pain in young women: a correlational study. Chiropractic & osteopathy, 16(1), 2008, pp. 1-7. https://doi.org/10.1186/1746-1340-16-1
4. Hardaker C.H.M., Fozzard G.J.W.: The bra design process - a study of professional practice. International Journal of Clothing Science and Technology, 9(4), 1997. https://doi.org/10.1108/09556229710175795
5. Wang J. P., Wei Y. Z.: An approach to predicting bra cup dart quantity in the 3D virtual environment. International Journal of Clothing Science and Technology, 19(5), 2007. https://doi.org/10.1108/09556220710819546
6. Benefits of bras for women - 2014. Available online: https://vnexpress.net/4-loi-ich-cua-ao-nguc-doi-voi-phu-nu-2952486.html 2022/07/05
7. Page K.A., Julie R.S.: Breast motion and sports brassiere design. Sports Medicine, 27(4), 2012, pp. 205-211. https://doi.org/10.2165/00007256-199927040-00001
8. McGhee D.E., Julie R.S.: Optimising breast support in female patients through correct bra fit. A cross-sectional study. Journal of Science and Medicine in Sport, 13(6), 2010, pp. 568-572. https://doi.org/10.1016/j.jsams.2010.03.003
9. Triumph bra size charts- 2022. Available online: https://www.triumph.com/pages/size-charts/ 2022/07/10
10. Calvin Klein bra size chart – 2022. Available online: https://www.calvinklein.co.uk/bra-sizes-explained 2022/07/08
11. Victoriassecret bra size – 2022. Available online: https://www.victoriassecret.com/vn/vs/bras/how-to-measure-bras/ 2022/07/05
12. Vera bra size charts – 2022. Available online: https://vera.com.vn/pages/huong-dan-chon-size/ 2022/07/02
13. Relax bra size charts – 2022. Available online: https://relaxunderwear.com/pages/huong-dan-chon-size/ 2022/07/04
14. Oh S., Chun J.: New breast measurement technique and bra sizing system based on 3D body scan data. Journal of the Ergonomics Society of Korea, 33(4), 2014.
15. Yu W., et al.: Innovation and technology of women's intimate apparel. Sawston: Woodhead Publishing, 2006, pp. 20
16. Bra Size Charts and Conversions. Available online: https://www.evasintimates.com/blog/ 2022/07/03
17. Edward A. P.: Method for determining bra size and predicting post augmentation breast size. Chapter 11: Breast Augmentation. Berlin: Springer, 2009, pp. 77-83.
18. McGhee D.E., Julie R.S.: Breast volume and bra size. International Journal of Clothing Science and Technology, 23(5), 2011, pp. 351-360. https://doi.org/10.1108/09556221111166284
19. Pechter E.A.: A new method for determining bra size & predicting post augmentation breast size. Plastic and Reconstructive Surgery, 102(4), 1998, pp. 1259-1265.
20. Bengtson B.P., Caroline A.G.: The standardization of bra cup measurements: redefining bra sizing language. Clinics in plastic surgery, 42(4), 2015, pp. 405-411. https://doi.org/10.1016/j.cps.2015.06.002
21. Rong Z., Yu W., Fan J.: Development of a new Chinese bra sizing system based on breast anthropometric measurements. International Journal of Industrial Ergonomics, 37(8), 2007, pp. 697-705. https://doi.org/10.1016/j.ergon.2007.05.008
22. Liu Y., Wang J., Cynthia L. I.: Study of optimum parameters for Chinese female underwire bra size system by 3D virtual anthropometric measurement. The Journal of The Textile Institute, 108(6), 2017, pp. 877-882. https://doi.org/10.1080/00405000.2016.1195954
23. Shin K.: Patternmaking for underwear design. The Journal of the Textile Institute, 98(4), 2010. https://doi.org/10.1080/00405000701503006
24. Avşar D. K., et al.: Anthropometric breast measurement: a study of 385 Turkish female students. Aesthetic Surgery Journal, 30(1), 2010, pp. 44-50.

https://doi.org/10.1177/1090820X09358078
25. Hoang T., Chu N. M. N.: Analysis of research data with SPSS, published in Hong Duc, 2008.
26. Hair J.F., et al.: Multivariate Data Analysis: A Global Perspective. 7th ed. Upper Saddle River: Prentice Hall, 2009.
27. Quatest 3, Directorate for standards, metrology and quality, 2017. Available online: http://quatest3.com.vn/Content/UserImages/Files/TNTT/2.1.%20Gi%E1%BB%9Bi%20thi%E1%BB%87u%20v%E1%BB%81%20TNTT.pdf
28. Nikita E.: Osteoarchaeology: A guide to the macroscopic study of human skeletal remains. Cambridge: Academic Press, 2016.
29. International Standard (ISO 4416): Size designation of clothes – women's and girl's underwear, nightwear, foundation garments, and shirts. The International Organization for Standardization, 1981.
30. Amoena bra size charts. Available online: https://www.amoena.com/global/about-us/lingerie-and-swimwear-measuring-guide/, 2022/07/01
31. Eva's Intimates bra size charts. Available online: https://www.evasintimates.com/bras/ 2022/07/01
32. Tran M.K., Park, S.J.: Somatotype Analysis and development size charts for Vietnamese women using 3D body scanner data. Proceedings for 2011 Asian Textiles Conference ATC11. 1PS-107, pp. 141.
33. Tran M.K.: Somatotype analysis and torso pattern development for Vietnamese women in their 30s using 3D body scan data. Ph.D. Dissertation, Yeungnam University Korea, 2012.
34. TCVN 5782: 2009. Standard sizing systems for clothers.
35. Nga B. T.: Research on building a hierarchy of size tables for some women's garment products. Scientific research, Ministry of Industry and Trade, 2010.
36. Nguyen T. T. T.: Building a sizing system for the lower body of women in Ho Chi Minh City aged 25 to 35. Master thesis, Hanoi University of Science and Technology, 2015.
37. Pham T. H.: Building a body size system for female students at Hanoi University of Industry, applying clothing desig. Scientific research of Hanoi University of Industry, 2019.
38. Tiwari M., Noopur A.: Development of Bottom-Wear Size Chart for Indian Male Youth. Ergonomics for Improved Productivity. Singapore: Springer, 2021, pp. 43-56. https://doi.org/10.1007/978-981-15-9054-2_5
39. Yadav S., Chanana B.: Developing standard size chart for teenage girls of 17-19 years using anthropometry. International Research Journal on Advanced Science Hub 2, 2020, pp. 15-20. https://doi.org/10.47392/IRJASH.2020.254
40. Petrova A.: Creating sizing systems. Sizing in Clothing: Developing effective sizing systems for ready-to-wear clothing. 2007, pp. 57-87.
41. Gupta D., Gangadhar B. R.: A statistical model for developing body size charts for garments. International Journal of Clothing Science and Technology, 2004. https://doi.org/10.1108/09556220410555641
42. Park S.J.: Upper garment sizing system for obese school boys based on somatotype analysis. Journal of the Korean Home Economics Association, 46(9), 2008, pp. 99-112.

*Fibres and Textiles* **30**(5), 2023, 42-51 DOI: 10.15240/tul/008/2023-5-005

# USAGE OF BIOSURFACTANTS AS ENVIRONMENTAL FRIENDLY DETERGENTS FOR TEXTILE PRODUCTS CLEANING

**PARASKA, OLGA[1*]; SYNYUK, OLEH[1]; RADEK, NORBERT[2]; ZOLOTENKO, ELLA[1] AND MYKHAYLOVSKIY, YURIY[1]**

[1] Khmelnytskyi National University, Instytutska Street 11, Khmelnytskyi, Ukraine
[2] Kielce University of Technology, Millennium of the Polish State alley, 7, Kielce, Poland

**ABSTRACT**

The paper is devoted to the resource-saving technologies of cleaning the textiles in the aquatic environment. As a resource-saving technology the use of biosurfactant compositions replacing traditional detergents was chosen. These technologies are characterized by high quality cleaning the textile garments, reduced time of operations, reduction of the costs of chemicals and energy, improvement of environmental safety of the process and and also allow to extend the shelf life of products.

Resource-saving cleaning technologies (washing, aqua cleaning) have been improved and recommendations for their application have been developed, considering changes in the operational properties of new generation textiles, which will extend the service life of new generation textiles, save operational properties, enable their eco-recycling (reuse) and reduce the impact on the environment and human health through the use of biosurfactant compositions. Innovative compositions of biosurfactants with a synergistic effect in micelle formation were elaborated. Steric factor associated with the rational packaging of biosurfactants molecules in mixed micelles, as well as the possibility of forming micelles of optimal composition can influence synergistic effect. The use of elaborated compositions of biosurfactants in washing processes offers several environmental and health advantages.

The complex research of influencing parameters of chemical-technological processes and properties of washing compositions on the basis of correlations the products of new generation were developed that provides improvement of quality of removal of contaminations from textiles and process safety. It is proved that the application of the developed resource-saving technologies saves 10 liters of water per cleaning cycle, 0.0348 kWh of electricity, and 0.142 hours of working time.

**KEYWORDS**

Resource-saving technologies; Cleaning; Wet cleaning; Laundry; Textiles; Bio-surfactants.

## INTRODUCTION

Textile products are an integral part of people's routine life. During the use of textile products, the human body has direct contact with textile materials during the whole life. Therefore, today the issue of safety of textile materials and clothing is particularly important in manufacturing and exploitation. Modern textile materials and products, in terms of their impact on human health, are a source of potential exposure to a range of factors: the nature of raw materials, the characteristics of their production processes, and finishing agents [1, 2]. In recent years, there have been significant changes in the range of products, and we can witness a tendency towards the manufacturing of new generation textile materials with additional properties, which in most cases are considered by consumers as the main arguments in favour of purchasing goods [3, 4]. At the same time, a large amount of textile waste is generated every year due to the wear-out, deterioration of consumer properties of textile products during their usage and frequent laundering. In addition, there are substantial difficulties in choosing a cleaning technology for new generation textiles, as existing technologies are not effective enough for such products.

Currently, the textile industry is rapidly developing, the range of textile products is changing, new products for their cleaning are emerging, the cost of energy and material resources is growing, environmental and consumer requirements and the quality of cleaning services are getting higher. Therefore, the existing technologies for cleaning textiles in the aqueous environment need to be updated and improved in accordance to the modern requirements and consumers' demands [3-6].

Textile cleaning processes consist of sequential operations: washing, extraction, drying and ironing. Washing is the main operation in the technological

* **Corresponding author:** Paraska O., e-mail: *olgaparaska@gmail.com*
*Received October 20, 2023; accepted December 14, 2023*

cycle that restores the physical and hygienic properties of products.

When choosing technological processes for cleaning textile products, it is necessary to take into account the specifics of their range and processing modes, which will ensure high service quality for consumers, save the operational properties of new generation products, and extend their service life. Currently, textile cleaning technologies provide a wide range of services to consumers: washing, cleaning clothes, removing stains, ironing, garment repair, preserving fur products, and treatment of garments to prolong the cleanliness of products and protect them from pathogenic bacteria. High-quality cleaning of textile materials and products is achieved through the use of the latest technologies combined with effective detergents [7-9].

Synthetic detergent is difficult to be degraded by bacteria in water, so detergent waste remains in the water; therefore, the accumulation of the amount of detergent in water occurs. The accumulation of detergent in water can be a source of pollution in the water stream. Concerns over the persistence of detergent chemicals in the environment and possible contamination of groundwater, other surface water sources also their subsequent health-related issues have raised speculation over biodegradability. The shift to an era of more environmentally friendly products has encouraged the industry to create environmentally friendly detergents. The solution to this problem can be overcome by using surfactants made from oleochemicals and other bio-based products.

That is why this paper deals with replacement of synthetic detergents by biosurfactants. Innovative compositions of biosurfactants with a synergistic effect in micelle formation were elaborated. Steric factor associated with the rational packaging of biosurfactants molecules in mixed micelles, as well as the possibility of forming micelles of optimal composition can influence on synergistic effect. The use of elaborated compositions of biosurfactants in washing processes offers several environmental and health advantages. Biosurfactants are generally considered to have lower toxicity than synthetic surfactants. This can be beneficial for both environmental and human health. Biosurfactants tend to have lower ecotoxicity, making them less harmful to aquatic organisms when discharged into water bodies. Biosurfactants exhibit versatile properties and can be effective in various washing processes, including laundry detergents and household cleaners. Innovative compositions of biosurfactants can be produced from renewable resources, such as plant oils, contributing to sustainability.

The main goals of this research are to improve resource-saving technologies for cleaning textile products of the new generation, which are based on the creation of innovative highly effective detergent compositions using biosurfactants. This will allow to improve the quality of product processing, environmental safety of the process, extend the service life of products, and reduce the cost of cleaning industry services.

The technological characteristics of the technologies for cleaning products in an aqueous environment are shown in Table 1.

Thus, textile cleaning processes are characterized by multifactoriality and complexity. An analysis of modern textile cleaning processes has shown that they have a number of disadvantages, including possible damage to products, the risk of chemical contamination of wastewater, expensive services, and significant electricity and water consumption [4, 6, 8, 10]. Therefore, the development of resource-saving technologies for cleaning textiles is an important task for the textile industry, the cleaning and service industry, and solving it will help improve the quality of the new generation of products cleaning, extend their service life, reduce the environmental impact and the cost of services. Resource-saving technology refers to innovations and practices that aim to minimize the use of resources such as energy, water, raw materials, and time, while maximizing efficiency and reducing waste. These technologies play a crucial role in sustainable development and environmental conservation. The implementation of resource-saving technologies is crucial for achieving sustainable development goals, mitigating environmental impact, and creating a more resilient and efficient global infrastructure.

## EXPERIMENTAL PART

### Materials used

Studies of the efficiency of chosen biosurfactant compositions for cleaning the textile garments in the aquatic environment were performed on specimens of cotton, polyester and mixed fabrics, which are presented on the market of Ukraine (Table 2).

The experimental samples were treated with the developed compositions containing biosurfactants [11, 12]. The composition and basic colloidal and chemical properties of the developed biosurfactant compositions are given in Table 3. CMC is critical micellar formation concentration, was determined by plotting the equilibrium surface tension against the surfactant concentration, σ - surface tension was measured by capillary rice method, θ is wetting edge angle evaluated by the static (sessile) drop contact angle (it is defined geometrically as the angle formed by a liquid at the three-phase boundary point where a liquid, gas, and solid intersect), H is the foam height, S is foam stability established by the Ross-Miles method according to ASTM D 1173. Barvamid 2K according to TU U24.1-32257423-118:2005 is an acetic acid salt of the product of the interaction of the

**Table 1.** Technological characteristics of product cleaning technologies in an aqueous environment.

| Washing | Aqua-cleaning |
|---|---|
| Recommended only for underwear and hospitality products | Recommended for garments, textile products for the household |
| Drum rotation speed when washing textiles | |
| Fixed 36 or 40 revolutions per minute | Adjustable from 5 to 40 revolutions per minute |
| Drum rotation speed when extracting textiles | |
| Fixed 400 or 500 revolutions per minute, rigid fixation of the drum | Adjustable from 400 to 1000 revolutions per minute, drum on springs and shock absorbers |
| Drum rotation/stop time when washing textiles | |
| Fixed rotation time 12 s or 20 s, stop time 3 s or 4 s | Adjustable rotation time from 0.1 s to 90 s, stop time from 0.1 s to 90 s |
| Water temperature when washing textiles | |
| Varies from cold to 90℃ | Varies from 27℃ to 40℃ |
| Water level | |
| Varies between high and low | Varies gradually (from ml to l), from high to low |
| The amount of textile washing | |
| From 1 to 3 | Typically 1, for highly contaminated products 2 |
| Duration of washing in one bath | |
| 5 min to 20 min (without heating) | 4 min to 10 min (with heating) |
| The number of rinses | |
| 3 or more rinses | 1 rinse |
| Drying temperature for textile products | |
| From 50℃ to 110℃ | From 40℃ to 60℃ |
| Detergents used in the process | |
| Washing powders, soaps, bleaches | Liquid detergents, softeners |

**Table 2.** Parametrs of the studied textiles materials.

| The name of the fabric | Width [cm] | Density | | Warp, Weft | | Weave | Areal density [g/m$^2$] |
|---|---|---|---|---|---|---|---|
| | | Weft [wefts/cm] | Warp [warps/cm] | Yarn linear density [tex] | Material composition | | |
| Fabric 1 100 % cotton | 150±5 | 22 | 41 | 30 | $(C_6H_{10}O_5)_n$ | plain-weave | 180 |
| Fabric 2 80% cotton, 20 % polyester | 150±2 | 22 | 41 | 30 | 80 % $(C_6H_{10}O_5)_n$, 20 % $(C_{10}H_8O_4)_n$ | plain-weave | 220 |
| Fabric 3 65 % cotton, 35 % polyester | 150±2 | 22 | 41 | 30 | 65 % $(C_6H_{10}O_5)_n$, 35 % $(C_{10}H_8O_4)_n$ | plain-weave | 220 |
| Fabric 4 100% polyester | 150±2 | 22 | 41 | 30 | $(C_{10}H_8O_4)_n$ | plain-weave | 220 |

**Table 3.** Composition and basic colloidal and chemical properties of the developed biosurfactant compositions.

| Biosurfactant | Composition, *W*, [%] | *CMC*, [M] | *σ*, [mN/m] | *θ*,[°] | *H*, [mm] | *S*, [%] |
|---|---|---|---|---|---|---|
| Composition 1 | 67 % DEA cocamide, 33 % biguanidine derivative | $2.5{\cdot}10^{-4}$ | 38.18 | 19.15 | 14 | 56 |
| Composition 2 | 80 % barvamid 2K. 20 % sulphonol NP-3 | $4{\cdot}10^{-4}$ | 32.15 | 15.98 | 13 | 92 |
| Composition 3 | 67 % barvamid 2K, 33 % stearox 920 | $1.0{\cdot}10^{-4}$ | 35.63 | 35.75 | 14 | 85 |

**Table 4.** Initial data for the five-factor experiment according to the Hartley plan.

| The name of the factor | The factor | Levels | | |
|---|---|---|---|---|
| | | -1 | 0 | +1 |
| Solution concentration of compositions biosurfactants, [g/l] | $X_1$ | 1 | 3 | 5 |
| The liquid module | $X_2$ | 8 | 10 | 12 |
| Temperature, [℃] | $X_3$ | 20 | 30 | 40 |
| Processing time, [min] | $X_4$ | 2 | 5 | 8 |
| Extraction [revolutions per minute] | $X_5$ | 400 | 700 | 1000 |

cubic residue of β-oxyethylethylenediamine and higher fatty acids of coconut oil and stearox 920 is a mixture of polyoxyethylene glycol esters of stearic acid.

## Research methods

In order to mathematically describe the dependences of the technological parameters of the process of cleaning textile products and to rationally conduct research, the method of planning experiments was applied Hartley plan. The determination of the most significant factors on the operational properties ow washing process (using biosurfactants) was carried out using the five-factor experiment according to the Hartley plan [13, 14]. The coded values of the factors that have the most impact on the finishing process and their levels are given in Table 4. For this experiment the biosurfactant marked Composition 1, Composition 2, Composition 3 was used.

The homogeneity of the dispersions was checked by the Cochrane criterion: the dispersions for each experiment are homogeneous. The adequacy of the obtained mathematical models was checked by Fisher's criterion.

Analysis of the results of the experiment made it possible to obtain the coefficients of a polynomial that establishes the correlation between all factors of the technological process of cleaning textiles and the detergent (biosurfactant) effect. The analysis of the obtained coefficients allows us to exclude from the final expression the coefficients with values less than the critical ones. Accordingly, the regression equations of detergent action for the studied fabric samples in coded values were obtained. The washing effect regression equation for the investigated tissue samples in coded values $Y(X_1, X_2)$ was obtained:

Fabric 1: 100% cotton:

$$Y=79.952-0.163X_1-0.059X_2+0.052X_3-0.374X_1^2-0.121X_2^2-0.144X_1X_2 \quad (1)$$

Fabric 2: 80 % cotton, 20 % polyester:

$$Y=79.952-0.163X_1-0.059X_2+0.052X_3-0.374X_1^2-0.121X_2^2-0.144X_1X_2 \quad (2)$$

Fabric 3: 65 % cotton, 35 % polyester:

$$Y=74.009-0.183X_1-0.044X_2+0.067X_3-0.347X_1^2-0.115X_2^2-0.205X_1X_2 \quad (3)$$

Fabric 4: 100% polyester:

$$Y=76{,}112-0{,}185X_1-0{,}016X_2+0{,}046X_3-0{,}361X_1^2-0{,}178X_2^2-0{,}107X_1X_2 \quad (4)$$

Analysis of these equations allows us to come to several conclusions. This polynomial is a paraboloid. Considering the signs of the coefficients before $X_1$ and $X_2$, this paraboloid is directed down the Z-axis, and with the growth of $X_3$, the maximum value is continuously increasing. Moreover, as $X_3$ increases, the value of the maximum detergent action Y (washing effect) will also increase. According to the results of the optimization, it was found that the factors that affect washing have different effects on the cleaning process of cotton, polyester and mixed fabrics. When washing cotton fabrics, all three investigated factors were found to be significant. On the other hand, when washing PES fabrics, only two factors were found to be significant: the concentration of the composition in the solution and the modulus of the bath. In general, cotton materials are washed better in an aqueous environment from hydrophobic contamination than PES ones. The study on the redeposition of contaminants showed that the concentration of biosurfactants in the solution is a significant factor.

The washing parameters: washing ability (*WA*, [%]) and redeposition (*RD*, [%]) ability was determined by the photometric method SNI ISO 105-C06:2010 by fabric whiteness [15]. The white color fabric samples were cut into 5x10 cm rectangle and each of them was polluted by complex pollution. The fabric samples were removed by the resource-saving technology using different biosurfactant compositions, see Table 3.

The washing ability (*WA*, [%]) was calculated according to the equation:

$$\boldsymbol{WA} = \frac{(K/S)_d-(K/S)_c}{(K/S)_d-(K/S)_0} \times \mathbf{100}\ \% \quad (5)$$

where $K/S = \frac{(1-R)^2}{2R}$; *R* – the intensity of reflection of monochromatic light from samples; *K* – the coefficient of light reflection from the fabric sample; *S* – the light scattering coefficient; $(K/S)_0$ – the coefficient of light reflection from the original fabric sample; $(K/S)_d$ – the coefficient of light reflection from the contaminated fabric sample; $(K/S)_c$ – the coefficient of light reflection from the fabric sample after cleaning in an aqueous environment.

The redeposition capacity of biosurfactant compositions (*RD*, [%]) was calculated according to the formula:

$$\boldsymbol{RD} = \frac{R_0-R_{REFL}}{R_0} \times \mathbf{100}\% \quad (6)$$

where $R_0$ – the coefficient of light reflection from the original fabric sample; $R_{REFL}$ – the coefficient of light reflection from the fabric sample after cleaning in an aqueous environment.

The change in mechanical properties of fabrics after cleaning in the aquatic environment was determined according to standard methods DSTU ISO 13938-1:2007, DSTU ISO 13938-2:2007 [16, 17].

The assessment of the change in the mechanical properties of cellulosic materials was carried out according to the indicators of bursting strength $P_p$, [N] and bursting distension $l_p$, [mm].

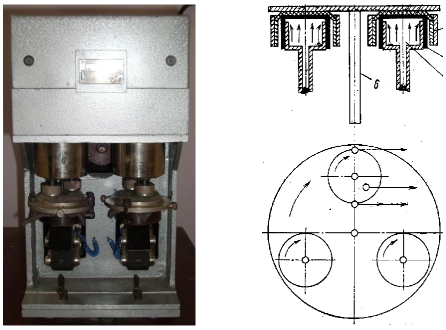

**Figure 1.** The external and schematic view of the IT-ZM-1 device.

To define the abrasion resistance of textile material samples, we used the durability characteristic - the number of abrasion cycles before the formation of holes. To define the resistance of textile materials to abrasion in laboratory conditions, the IT-ZM-1 device was used (Fig. 1).

Elementary specimens shaped like circles with a diameter of 27 mm were inserted into the runner holders with the front side up. A prepared 95 mm wide strip of overcoat fabric was inserted into the hoop, on which a ring was placed and secured with screws. A metal ring was placed on the fabric and the sample was fixed on the hoop using a 25 mm diameter abrasive wheel clip. After filling the fabric and abrasive in the hoop, the device was switched on. After the device was stopped, the number of rotation cycles at which the fabric surface was destroyed was recorded.

All measurements were repeated 10 times (n=10). Mean values together with 95% confidence intervals are shown to enable comparison of sample properties after multiple washing in an aqueous environment.

In order to study the energy characteristics of modern washing equipment, an experimental bench was used to determine the necessary parameters of the technological process of cleaning textile products in an aqueous environment. A block diagram of the study of operational indicators of the implementation of resource-saving technologies for cleaning textile products in an aqueous environment is shown in Fig. 2.

## RESULTS AND DISCUSSION

Technological processes for textile cleaning consist of sequential operations: washing, extraction, drying and ironing. The results of optimizing the process of textile cleaning according to detergent (biosurfactant) action, antiresorption capacity, capillarity and stiffness for samples of cotton, polyester and their combinations made it possible to obtain optimal values of the technological parameters of the process of textile cleaning of various assortments: composition concentration from 2.5 to 3 g/l; bath module 10; processing temperature from 20 to 30 ℃; processing time 8 min; extraction 400 revolutions per minute. Three types of biosurfactants (table 3) were applied and their effect on cleaning (washing and aqua-cleaning) of textiles in the aquatic environment was studied.

Tables 5-7 show different steps for washing and aqua-cleaning of textiles using biosurfactants.

According to Tables 5 - 7, the time required for operations is reduced from 18 to 38 minutes, as well as the processing temperature is reduced from 10 ℃ to 30 ℃ by one cleaning cycle, compared to the typical technology (Table 1) of cleaning products.

In order to evaluate the effectiveness of textile products cleaning using biosurfactants, the washing performance parameters (*WA*, *RD*, [%], according to: Eq. 1, 2) of the developed compositions (Table 3) were compared with similar indicators of detergents (Unix Klin A, Tuono Blu, Lanadol Aktiv, Amway Home SA8), which are widely used in product processing enterprises and in household conditions using technological parameters of washing specified in Table 5. The results of the research are given in Table 8.

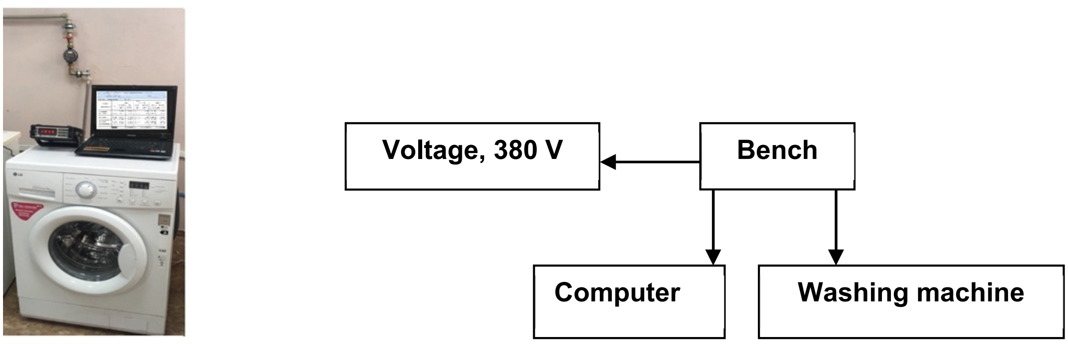


(a) (b)

**Figure 2.** Image and flowchart for defining equipment operational parameters: (a) general view; (b) bench diagram.

**Table 5.** Technological steps for washing combined fabrics.

| The name of operation | t, [℃] | Liquid module | Compositions of biosurfactants | Processing time, [min] |
|---|---|---|---|---|
| First washing | 30 | 10 | + | 8 |
| Second washing | 30 | 10 | + | 8 |
| First rinse | 30 | 12 | | 3 |
| Second rinse | 30 | 12 | | 3 |
| Final processing (treatment) | 30 | 10 | + | 6 |
| Total duration<br>without final processing<br>with final processing | | | | <br>22<br>28 |

**Table 6.** Technological steps for aqua-cleaning of mixed fabrics.

| The name of operation | Temperature, [°C] | Process/pause, [s] | Rotation speed, revolutions per minute | Processing time, [min] |
|---|---|---|---|---|
| Washing with the biosurfactant | 30 | 5/10 | 20 | 3 |
| Drain | - | 5/10 | 30 | 0.5 |
| Rinse | 30 | 5/10 | 30 | 3 |
| Drain | - | 13/4 | 40 | 0,5 |
| Extraction | - | - | 400 | 2 |
| Total duration | | | | 9 |

**Table 7.** Resource-saving technology for aqua-cleaning of mixed highly contaminated fabrics.

| The name of operation | Temperature, [°C] | Process/pause, [s] | Rotation speed, revolutions per minute | Processing time, [min] |
|---|---|---|---|---|
| Washing with the biosurfactant | 30 | 5/10 | 30 | 3 |
| Drain | - | 5/10 | 30 | 0.5 |
| Washing with the biosurfactant | 30 | 5/10 | 30 | 3 |
| Drain | - | 13/4 | 40 | 0.5 |
| Rinse | 30 | 5/10 | 30 | 3 |
| Drain | - | 13/4 | 40 | 0.5 |
| Extraction | - | - | 400 | 3 |
| Total duration | | | | 13.5 |

**Table 8.** Washing parameters of the developed compositions biosurfactants (washing ability (*WA*, [%]) and redeposition (*RD*, [%]) ability.

| Compositions | Fabric 1 (100 % cotton) | | Fabric 2 (80% cotton, 20 % polyester) | | Fabric 3 (65 % cotton, 35 % polyester) | | Fabric 4 (100% polyester) | |
|---|---|---|---|---|---|---|---|---|
| | *WA*, [%] | *RD*, [%] | *WA*, [%] | *RD*, [%] | *WA*, [%] | *RD*, [%] | *WA*, [%] | *RD*, [%] |
| Compositions biosurfactants 1 | 83.6 | 13.3 | 81.6 | 15.5 | 80.1 | 14.2 | 77.8 | 17.7 |
| Compositions biosurfactants 2 | 76.3 | 14.1 | 73.9 | 14.5 | 77.4 | 13.9 | 75.7 | 15.6 |
| Compositions biosurfactants 3 | 80.5 | 14.7 | 79.2 | 15.4 | 79.8 | 15.3 | 80.9 | 16.1 |
| Unix Klin A | 80.0 | 17.4 | 76.2 | 19.1 | 76.9 | 20.2 | 73.8 | 21.7 |
| Tuono Blu | 72.8 | 23.5 | 73.3 | 22.1 | 73.2 | 24.4 | 72.3 | 23.1 |
| Lanadol Aktiv | 80.1 | 22.2 | 75.8 | 20.9 | 78.4 | 21.0 | 74.4 | 21.1 |
| Amway Home SA8 | 79.9 | 25.0 | 76.3 | 19.3 | 77.2 | 21.1 | 73.5 | 22.1 |

Studies have shown that the highest washing ability was realized by Biosurfactant 1 on Fabric 1 (cotton), Fabric 2 (80% cotton, 20 % polyester) and Fabric 3 (65 % cotton). The highest washing ability for the 100 % PES fabric was provided by Biosurfactant 3. All traditional detergents have lowest washing ability compared to highest washing ability performed by Biosurfactant.

Products with a high content of cotton (Fabric 1, Fabric 2) are best cleaned, while dirt from polyester fabric is less effectively removed, which is explained by the affinity of cellulose fibers to the aqueous environment and the hydrophobicity of polyester products. Using Biosurfactants the redeposition capacity is significantly lower compared to usage of traditional detergents regardless of the material composition of the sample.

The use of the developed biosurfactant compositions can reduce the cleaning cycle by one rinse. However, in the presence of remaining particles of the detergent-soiling complex, with insufficient rinsing, greying of products is possible. Therefore, according to Eq. 2, the redeposition capacity (*RD*, [%]) of the developed compositions was additionally defined by reducing the cleaning cycle of fabrics by one rinse [8, 15]. The results of the study are presented in Table 9.

The study of the antiresorption ability of the developed biosurfactant compositions (Table 8) showed that the quality of textile cleaning of various types of fabrics does not deteriorate with a reduced number of rinses.

It should also be considered that reducing the washing cycle by one rinse reduces the duration of the process, electricity and water consumption, and wages for staff.

Previous studies have shown that the developed biosurfactant compositions should be used for cleaning and finishing of textile products for special and household purposes, which contributes to the proper care of products, removes static electric charges, increases the efficiency of removing contaminants from the surface of fabrics, reduces re-contamination of products, extends their service life, and imparts antimicrobial properties to products [11, 12].

Thus, the implementation of the developed technologies reduces the consumption of reagents, shortens the time of operations, the processing cycle of products, and improves the environmental safety of the process.

The effectiveness of the implementation of the developed technologies for the maintenance of operational properties was evaluated by the semi-cycle characteristics of wear resistance. The results of determining the semi-cycle bursting characteristics (bursting strength, $P_p$, $N$, bursting distension, $l_p$, [%]) of textile material samples after multiple washing in an aqueous environment are given in Table 10.

According to the results of the study, the bursting strength of the tested fabric samples after 30 cycles of cleaning is 600 N on the warp and 225 N on the weft for Fabric 1, 850 N on the warp and 600 N on the weft for Fabric 2, 1200 N on the warp and 1100 N on the weft for fabric 3, 1800 N on the warp and 1700 N on the weft for fabric 4. After 30 cycles of cleaning in an aqueous environment according to a typical technology (Table 1), partial destruction and destruction of cotton fabric occurs.

The abrasion resistance (number of cycles) on the surface of the studied samples of fabrics made of cotton, polyester and their combinations after multiple cleaning in an aqueous environment is given in Table 11.

According to Table 9, a similar tendency is observed for the wear resistance of the test samples after multiple cleaning in an aqueous environment. For the cotton fabric sample, partial destruction of the material occurs after 30 processing cycles using a typical technology. Combined and synthetic fabrics made of polyester fibres have greater wear resistance. Thus, the implementation of the developed technologies achieves high quality cleaning of products, increases the number of cleaning cycles compared to the typical technology, and extends the service life of products [6, 8, 10].

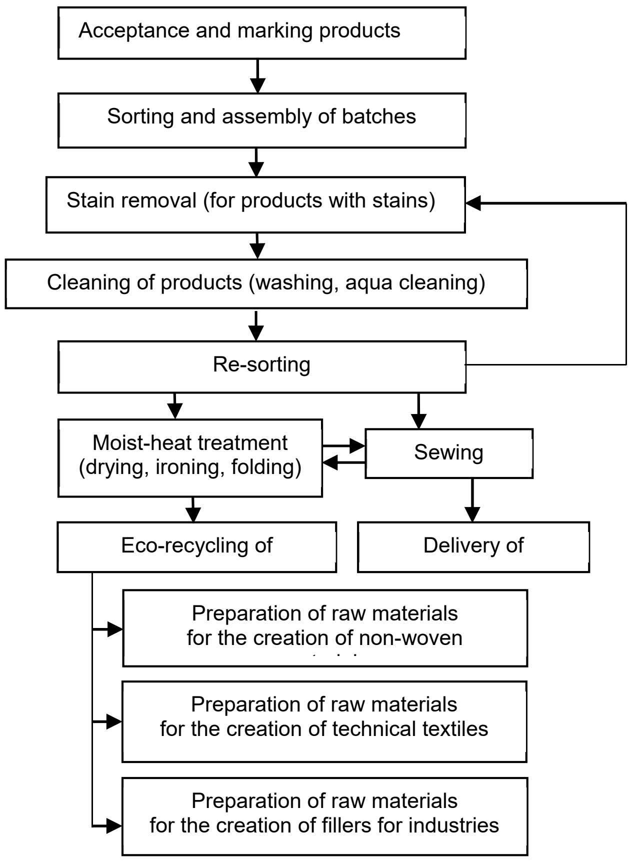


**Figure 3.** The technological scheme for cleaning textile products in an aqueous environment considering the eco-recycling operation.

In addition, due to the antimicrobial effect of composition 1 (67 % DEA cocamide, 33 % biguanidine derivative), disinfection and eco-recycling of worn products, which are raw materials for the creation of nonwovens, fillers, and technical textiles, is possible [11, 18, 19]. The technological scheme for cleaning textile products in an aqueous environment, considering the reuse of worn textile products, is shown in Fig. 3.

The implementation of eco-recycling of worn-out textiles in the technological process of cleaning products will help reduce the generation of textile waste, processing time in the preparation of raw materials for the reuse of textiles, and create safe reusable textile raw materials.

The cost of processing products at cleaning and service companies depends on the cost of energy, utilities, cleaning products, equipment maintenance costs, staff salaries, and the time required to process products [1, 5, 19, 20].

The summarized results of the efficiency of the implementation of the developed resource-saving technologies for cleaning textile products in the aqueous environment in comparison with the typical technology are given in Table 12.

Thus, with a reduction in the number of rinses per washing, water savings are 10 litres, working time savings are 0.142 hours, and electricity savings are 0.0348 kWh.

**Table 9.** Redeposition capacity (*RD*, [%]) of washing using biosurfactant compositions.

| The number of rinses | Fabric 1 (100 % cotton) | Fabric 2 (80 % cotton, 20 % polyester) | Fabric 3 (65 % cotton, 35 % polyester) | Fabric 4 (100 % polyester) |
|---|---|---|---|---|
| Composition 1 (67 % DEA cocamide, 33 % biguanidine derivative) | | | | |
| 3 rinses | 13.3 | 15.81 | 14.83 | 17.2 |
| 2 rinses | 13.2 | 15.28 | 13.79 | 17.2 |
| Composition 2 (80 % barvamid 2K, 20 % sulphonol NP-3) | | | | |
| 3 rinses | 15.01 | 15.25 | 14.95 | 15.62 |
| 2 rinses | 14.85 | 15.25 | 14.80 | 15.55 |
| Composition 3 (67 % barvamid 2K, 33 % strearox 920) | | | | |
| 3 rinses | 14.75 | 15.45 | 15.85 | 16.5 |
| 2 rinses | 14.55 | 15.00 | 15.55 | 16.25 |

**Table 10.** Half-cycle bursting characteristics of the studied textile materials.

| The sample of material | Untreated fabric | | Developed technology | | Typical technology | |
|---|---|---|---|---|---|---|
| | | | 30 cleaning cycles | | | |
| | warp | weft | warp | weft | warp | weft |
| **Bursting strength, $P_p$, [N]** | | | | | | |
| Fabric 1 (100 % cotton) | 655±14.52 | 245±5.75 | 600±12.7 | 225±5.55 | Partial fabric destruction | |
| Fabric 2 (80 % cotton, 20 % polyester) | 870±19.29 | 630±13.6 | 850±18.8 | 600±11.71 | 800±17.7 | 590±13.07 |
| Fabric 3 (65 % cotton, 35 % polyester) | 1235±27.3 | 1140±25.3 | 1200±20.3 | 1100±24.4 | 950±21.1 | 1050±23.28 |
| Fabric 4 (100 % polyester) | 1800±39.9 | 1700±37.7 | 1800±39.9 | 1700±37.7 | 1800±39.9 | 1700±37.7 |
| **Bursting distension, $l_p$, [%]** | | | | | | |
| Fabric 1 (100 % cotton) | 14±0.35 | 28,5±0.71 | 18±0.45 | 11±0.28 | Partial fabric destruction | |
| Fabric 2 (80 % cotton, 20 % polyester) | 25±0.63 | 41±1.03 | 25±0.63 | 39±0.98 | 20±0.50 | 32±0.80 |
| Fabric 3 (65 % cotton, 35 % polyester) | 33±0.83 | 46.5±1.16 | 32±0.80 | 43±1.08 | 30±0.75 | 40±1.00 |
| Fabric 4 (100 % polyester) | 45±1.12 | 47.5±1.19 | 50±1.25 | 48±1.20 | 48±1.20 | 47±1.18 |

**Table 11.** Abrasion resistance of the studied samples, cycles.

| The sample of material | Untreated fabric | Developed technology | Typical technology |
|---|---|---|---|
| | | 30 cleaning cycles | |
| Fabric 1 (100 % cotton) | 4550 | 4000 | Fabric destruction |
| Fabric 2 (80 % cotton, 20 % polyester) | 5200 | 5000 | 4500 |
| Fabric 3 (65 % cotton, 35 % polyester) | 8200 | 8000 | 7500 |
| Fabric 4 (100 % polyester) | 8600 | 8500 | 8000 |

**Table 12.** Summarised results of the efficiency of implementation of the developed resource-saving technologies for cleaning textile products.

| Costs | Typical washing technology | Resource-saving washing technology using biosurfactants | Cost savings |
|---|---|---|---|
| Water consumption | 48 l | 38 l | 10 l |
| Energy consumption | 0.2205 kWh | 0.1857 kWh | 0.0348 kWh |
| Time commitment | 1.085 hours | 0.943 hours | 0.142 hours |

## CONCLUSION

The article proposes optimal conditions for the implementation of resource-saving technologies using biosurfactants to improve the efficiency of the technological processes of washing, aqua-cleaning, and finishing of textile products. The developed resource-saving technologies for cleaning textile products are characterised by reduced time of operations, reduced cycle of cleaning products, reduced consumption of reagents, and improved environmental safety of the process.

It was proved that the usage of biosurfactant increases washing ability and at the same time decreases the redeposition capacity of all tested samples compared to usage of traditional detergents. The biosurfactant marked Compositon 1 offers the highest wasthing ability of cotton based textiles even in mixture with polyester. Biosurfactant marked Composition 3 provides the highe washing ablitity for 100 % PES fabrics.

It has been confirmed that due to the efficiency of the developed biosurfactant compositions Table 3 [11, 12], it is possible to reduce the cleaning cycle by one rinse without compromising the quality of cleaning of textile products of various assortments. Recommendations for the use of the developed biosurfactant compositions Table 3 [11, 12] in the technological processes of textile processing are given. It is substantiated that it is not recommended to exceed the working concentrations of the developed compositions more than in the range from 2 to 3 g/l for effective use in the cleaning process. The implementation of the developed technologies ensures a reduction in the time of operations from 18 to 38 minutes, as well as a decrease in the processing temperature from 10 °C to 30 °C, compared to the typical technology of cleaning products, by one processing cycle, respectively. The energy parameters of the equipment are determined, it is proved that by reducing the number of rinses per washing, water savings are 10 litres, working time savings are 0.142 hours, and electricity savings are 0.0348 kWh.

The implementation of eco-recycling of worn-out textiles in the technological process of cleaning products will help reduce the generation of textile waste, reduce processing time when preparing raw materials for the reuse of textiles, and create safe textile raw materials for nonwovens, technical textiles, geotextiles, and the needs of various industries.

## REFERENCES


1. Salerno-Kochan R., Kowalski M.: Safety Management of Textile Products in the European Union and Estimation of its Efficiency. Part 2. General problems of the fibre and textile industries, Fibres & Textiles in Eastern Europe, 2020, 28, 3(141), pp. 12-17. https://doi/org/10.5604/01.3001.0013.9012
2. Global fashion industry statistics – International apparel Available from: https://fashionunited.com/global-fashion-industry- statistics/, Accessed: 2023-08-30
3. Shcherban V., Paraska G., Orlovskyi B., et al.: Resource-saving technologies and equipment of the sewing and textile industry. T. 2: Ways to improve the efficiency of the sewing and textile industries of Ukraine based on the advanced technologies and management: Monograph, Kyiv, KNUTD, 2015, pp. 260. [in Ukrainian]
4. Mittal K., Bahners T.: Textile Finishing: Recent Developments and Future Trends, John Wiley&Sons, 2017, pp. 588.
5. Ilic S., Petrovic T., Djukic G.: Eco-innovation and Sustainable Development, Problems of sustainable development, 2022, 17(2), pp. 197-203. http://doi.org/10.35784/pe.2022.2.21
6. Laitala K., Klepp I., Kettlewell R., et al.: Laundry Care Regimes: Do the Practices of Keeping Clothes Clean Have Different Environmental Impacts Based on the Fibre Content? Sustainability, 2020, 12(18), pp.7537. https://doi.org/10.3390/su12187537
7. Louis Tan Tai Ho.: Formulating Detergents and Personal Care Products: A Complete Guide to Product Development, 2000, US: American Oil Chemists' Society, pp. 465.
8. Laundry Experience Event 2017. March 17-18th, 2017, Helmond, Netherlands. Available from: https://www.cinet-online.com/laundry-experience-event-2017/, Accessed: 2023-07-20
9. Paraska O., Kovtun H., Hes L., et al.: Study of the influence of antimicrobial agents on the operational and hygienic properties of cellulose materials, Vlakna a textil Journal, 2022, 29(2). pp. 73-78. http://dx.doi.org/10.15240/tul/008/2022-2-008
10. Troynikov O., Watson C., Jadhav A., et al.: Towards sustainable and safe apparel cleaning methods: A review, Journal of Environmental Management, 2016, 182(1), pp. 252-264. https://doi.org/10.1016/j.jenvman.2016.07.078
11. Patent for inventions 133667 Composition for laundring household textile products [in Ukrainian]
12. Patent for inventions 133668 Composition of environmentally safe substances for wet cleaning of textile products [in Ukrainian]
13. Belkacem Said-Houari.: Differential Equations: Methods and Applications, 2016, Springer Cham, pp. 212. https://doi.org/10.1007/978-3-319-25735-8
14. Ivasyshen S., Lavrenchuk V., Nastasiyev P., et al.: Differential equations: methods and applications, 2010, Chernivtsi: Chernivtsi National University, pp. 288. [in Ukrainian]

15. Paraska O., Sioma A., Karvan S.: Vision methods of examining the cleanliness of textile materials, Mechanics and control, 2012, 31(1), pp. 44-50. http://dx.doi.org/10.7494/mech.2012.31.1.44
16. DSTU 4143-2002/GOST 31101-2003. Textiles. Evaluation of the wrinkle recovery of fabrics.
17. DSTU GOST 3816:2009 (ISO 811-81). Textile fabrics. Methods for determination of hygroscoric and water-repellent properties.
18. Secondary Materials and Recycled Textiles (SMART) Association. Available from: https://www.smartasn.org/, Accessed: 2023-07-20
19. CINET. Available from: https://www.cinet- online.com/, Accessed: 2023-08-30
20. Paraska O., Ivanishena T.: Methodological bases of life cycle assessment of textile products cleaning technologies at the cleaning industry enterprises, Book of extended abstracts International scientific conference accounting, audit, analysis: Transformation of science and business in new economic reality, Vilnius, Lithuania, 25-26 November, 2021, Vilnius University Press, Vilnius, pp. 75-79. https://doi.org/10.15388/Transformation-of-science-and-business.2021

*Fibres and Textiles* **30**(5), 2023, 52-60 DOI: 10.15240/tul/008/2023-5-006

# RESEARCH OF VARIABLE PARAMETERS OF NEEDLE THREAD TAKE-UP MECHANISMS AND DEVELOPMENT OF RECOMMENDATIONS FOR ADJUSTING MULTI-THREAD CHAIN STITCH SEWING MACHINES

**MANOILENKO, OLEKSANDR*; HOROBETC, VASYL; DVORZHAK, VOLODYMYR; KOVALOV, YURII; KNIAZIEV, ILLIA AND SHKVYRA, VOLODYMYR**

Kyiv National University of Technology and Design, Mala Shiyanovska st.2, 01011Kyiv, Ukraine

## ABSTRACT

The purpose of this research is to develop specific recommendations for optimizing the adjustment of the thread take-up mechanisms of typical chain stitch sewing machines based on the analysis of the thread take-up process. These recommendations are intended to help manufacturers and machine operators achieve maximum productivity and increased product quality, while taking into account the specific technological parameters of the operations performed on these machines. The research is aimed at increasing the efficiency of the sewing process, reducing machine setup time, and improving the overall result of the technological process in the sewing industry. The research uses an analytical method of determining and investigating functions of the actual thread take-up as the instantaneous sum of sections of the take-up contour when adjustable parameters of the mechanisms are changed, taking into account accepted assumptions. In the research, an analytical method was used to determine functions of the actual thread take-up as the instantaneous sum of sections of the take-up contour, taking into account the change in regulated parameters of the mechanisms. At the same time, assumptions were made that has simplified analysis and modelling of this process with sufficient accuracy of calculation results. The scientific novelty of this research lies in discovery of new relationships and establishment of regularities that determine influence of adjustable parameters on the nature and scope of the thread take-up function in chain stitch machines. Further re-search in this area can be aimed to the development of more efficient methods of adjustment and optimization of needle thread take-up mechanisms, as well as to the implementation of new technologies in pro-duction to improve productivity and quality of sewing operations. The obtained results became basis for the development of nomograms for determining the optimal values of adjustable parameters for needle thread take-up mechanisms of typical flat chain stitch machines, taking into account technological parameters of specific operations. These nomograms allow operators and manufacturers of sewing machines significantly simplify adjustment of these mechanisms when using operational equipment or when switching to other technological operations. The obtained results can be applied directly in production during adjustment or repairing of specified ma-chines to increase their productivity by reducing adjustment time and for improving the quality of the technological process.

## KEYWORDS

Thread take-up mechanism of sewing machines; Sewing machines; Chain stitch; Thread take-up functions of sewing machines.

## INTRODUCTION

Chain stitch sewing machines have significantly lower values of maintainability indicators comparing with corresponding indicators of shuttle machines. This is explained by the peculiarity of their structure (preferred location of main shaft in the platform, complexity of trajectories and laws of movement of loopers comparing to shuttles, preferred using of differential transport mechanisms, presence of such working tools as expanders and spreaders, etc.). These factors lead to complexity of their design and increase cost of maintenance. However, despite this, their share in general nomenclature of sewing equipment in production is constantly increasing, which is explained both by well-known advantages of chain stitches compared to shuttle stitches, and by great diversity of the structure of their stitches [1]. One of the main reasons is that repairability of the chain stitch sewing machines, at least several times higher than repairability of the shuttle sewing machines, is that the significant difficulties in setting-

* **Corresponding author:** Manoilenko O.P., e-mail: *manojlenko.op@knutd.edu.ua*
*Received 3.11.2023; accepted 5.1.2023*

up thread take-up mechanisms, particularly needle ones.

Unlike shuttle machines, where needle thread take-up mechanisms [2] have only a few structural varieties with practically no adjustable parameters, the NTTM of the chain stitch machine has dozens of structural options, both purely mechanical and with electronic elements [2]. At the same time, usually, they have several adjustable parameters that affect the value and law of the effective take-up (*P(φ)*) of the thread [3-6]. However, in literature and instructions for the operation of specific machines, there is a complete lack of information about the quantitative effect of changing these parameters on nature of actual thread take-up function. Some sources mention possibility of more precise adjustment in case of using highly elastic threads [3] by changing the size of the thread receiver strokes.

In the works [7-10], the influence of thread tension during its unwinding from the bobbin on the quality of the stitch is examined. The authors in these works suggest equipping the existing thread feeding mechanisms with an additional system for monitoring thread tension during stitch formation.

The provided methodology for geometric modeling of chain stitches of type 406 [11] and type 504 [12] allows for the precise determination of thread consumption required to create a specific type of stitch, which eliminates the need for specific machine adjustments in accordance with the technological process of stitch formation.

Furthermore, in the study [13], the authors present the results of research on the impact of tension regulator settings on the quality of type 301 and 401 stitches, depending on material thickness and stitch length parameters. The authors provide mathematical relationships that enable achieving high-quality chain stitches by ensuring the appropriate tension on the thread regulator.

Additionally, there is no information about the separate effect of each parameter of the NTTM, on function of valid thread take-up, which complicates the process of their design and adjustment. Therefore, in practice, adjustment of NTTM is reduced to random selection of values of variable parameters, which significantly increases duration of this process.

## STATEMENT OF THE TASK

In works [14-17] obtained analytical definitions of function of necessary and valid take-up of needle threads of typical flat chain sewing machines, including sewing machines with a simple kinematic chain, which have only one thread receiver, that is fixed on the needle guide and regulation system of thread guides. At the same time at work [17] was conducted research of the effect of adjustable parameters on the value and law of ideal thread, and in [18-19] was performed comparative analysis of various structures of NTTM with a branched kinematic chain [2] in an example of sewing machines W562-05BB cl. of the company «Pegasus» [3] and CF 2300M-164 M class. of the company «Uamato» [4] and determining their advantages over take-up mechanisms formed by a simple kinematic chain. In works [15-16] was established that in order to achieve a high-quality stitch, it is necessary to ensure the correspondence between values of functions *P(φ)* and *P'(φ)* and this cannot be achieved only by stretching the threads. At the same time, in the paper [20] it is noted that the tension of the threads depends not only on the radius of curvature of the thread guides, but also on the type of threads, which also affects the actual thread take-up law *P(φ)*. This leads to the need of re-adjustment thread take-up mechanisms for all needles. The results of these works were taken as basis for conducting this study.

The main task is to identify influence of the values of the adjustable parameters on value and law of the valid thread take-up under various technological parameters, such as length of the stitch - t, thickness of the materials - m and type of thread, for the development of specific recommendations in form of nomograms for adjusting the NTTMs of typical chain stitch machines.

## RESEARCH RESULTS

NTTMs formed by branched kinematic chain [2], unlike those formed by simple one, contain larger number of adjustable parameters. Their main characteristic is that they have thread receiver with separate mechanism and system of thread guides (Fig. 1). At the same time, compliance with laws of valid thread take-up *P(φ)* to necessary one P´(φ) for each specific needle is achieved by different positions of thread guides $G_{11-13}$ (Fig. 1(a), Fig. 2 (a,b)). In most cases, adjustment is performed vertically (Fig. 2(a)), or according to two coordinates (Fig. 2 (b)), which, usually, is recommended by equipment manufacturer. More precise accordance of configuring is achieved by using other adjustment parameters (Fig. 2, 3). Among them, it is worth highlighting positions of U-shaped (Fig. 2(c,d)) and I-shaped thread guides (Fig. 2 (e)) in relation to thread receiver $T_2$, which is fixed on the needle guide. Parameters of the thread receiver $T_1$, in turn, include its length R and its horizontal position - $\alpha_0$ (Fig. 3).

Calculation of the parameters influence on law and value of needle thread take-up is for a group of sewing machines of leading manufacturers Pegasus and Yamato. To compare the laws of valid *P(φ)* thread take-up and necessary *P´(φ)* thread take-up law for the left needle is chosen, for the same purpose we choose the initial position of the thread guides $G_{11}$. As described in works [14-17] max value of the function *P´(φ)* has left needle, which is located lowest to the needle plate.

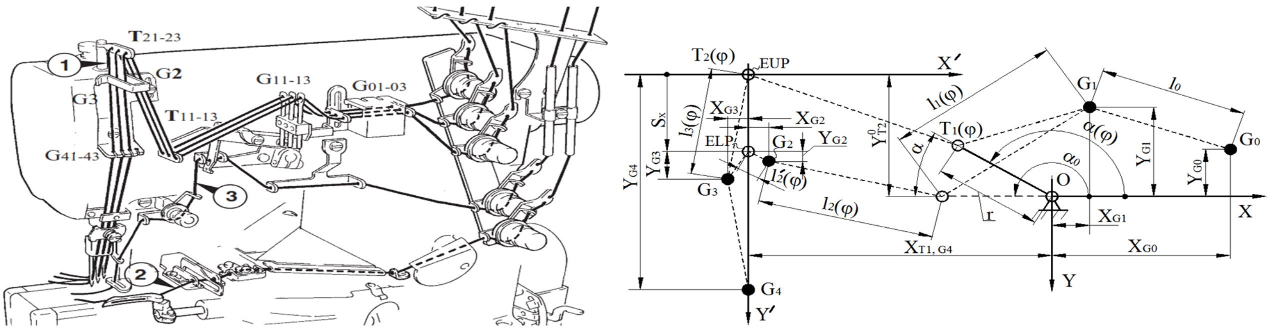


(a) (b)

**Figure 1.** Scheme of the thread take-up contours: (a) typical pattern of thread take-up for sewing machine of 600 class (1 – needle threads, 2 – loop thread, 3 – threads of the spreader); (b) calculation diagram of the NTTM's «take-up contour».

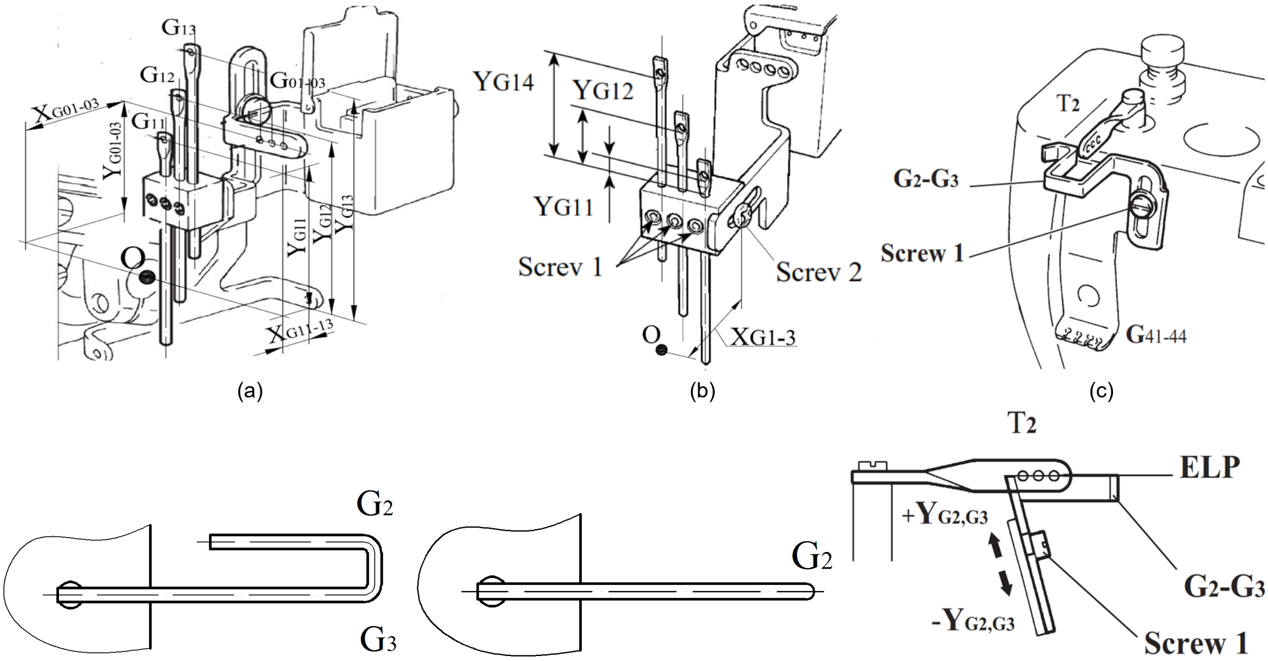


(a) (b) (c)

(d) (e) (f)

**Figure 2.** Parameters of thread guides *Gji*: (a) vertical adjustment, (b) both X and Y coordinates, (c,d) U-shaped thread guides of the W562-05BB «Pegasus» machine, (e) I-shaped thread guides of the CF 2300M-164M «Uamato» machine, (f) thread guides $G_{2\text{-}3}$ ($G_2$) adjustment parameters.

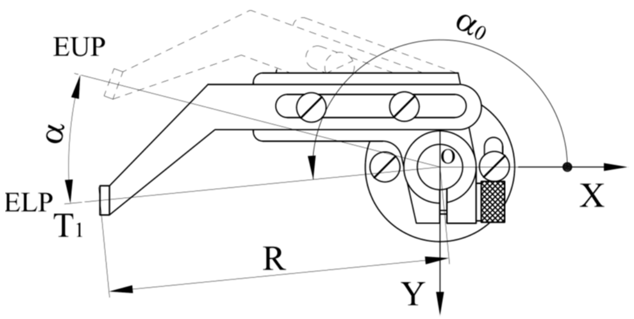


**Figure 3.** Adjustment parameters of thread receiver T1.

Calculation schemes of the contours of machine thread take-up contain i-th quantity of j-th types of thread receivers and thread guides, which are shown on Fig. 1(b) (where i-th types of j-th thread guides and thread receivers are marked accordingly by symbols Gji and Tji(φ)), and their construction is shown on Fig. 2, 3.

General diagram of thread filling ("take-up contour") of sewing machines W562-05BB "Pegasus", CF 2300M-164M «Uamato» are shown on Fig. 1, the difference is the parameter values and the type of thread guide applying [2]. Accordingly, following adjustable parameters can be defined. Thread guides $G_{11\text{-}13}$ of the W562-05BB "Pegasus" machine are adjustable only vertically $Y_{G11\text{-}13}$ (Fig. 2, a), and thread guide of the CF 2300M-164M «Uamato» machine has adjustment by two coordinates $X_{G11\text{-}13}$ and $Y_{G11\text{-}13}$ (Fig. 2, b). Sewing machine W562-05BB "Pegasus" uses U-shaped thread guides $G_2$-$G_3$ (Fig. 2 (c, d)), and CF 2300M-164M «Uamato» machine uses rod-shaped thread guides - $G_2$, (Fig. 2(e)). CF 2300M-164M «Uamato» which have adjustable vertical parameter relatively to extreme lowest position (ELP) of the thread receiver $T_2$, respectively - $Y_{G2-3}$ (Fig. 2, f), and thread guide $G_3$ (Fig. 1(b)) is fixed motionless and has corresponding coordinates of $Y_{G3}$ and $X_{G3}$. For the calculation location of the thread guides $G_{41-43}$, which close thread take-up contour and have their own coordinates (Fig. 1 (a)) are chosen to match projection of the needle guide axis and are located at the $Y_{G4}$ coordinate. Thread receiver $T_1$ of W562-05BB «Pegasus» and CF 2300M-164M «Uamato» sewing machines has two adjustable parameters: slope angle to the abscissa axis at its extreme lowest position (ELP) - $\alpha_0$ and length of thread receiver - $R$ (Fig. 3).

Values of adjustable parameters ranges selected from possible design parameters for a specific machine are given in Table 1. Selected reference points are similar to the adjustment guidelines of the considered machines. As the start of $G_2$-$G_3$ thread guide coordinates countdown is selected coordinate of the thread receiver $T_2(\varphi)$ (Fig. 1, b) at its lowest position. For thread guide $G_1$ of both sewing machines, the $Y_{G11}$ value is taken as zero, specified in the regulation manuals [3, 4]. As the origin of coordinates is taken point O - oscillation center of thread receiver $T_1$. $\alpha_0=2\pi$ is taken as zero at ELP of thread receiver $T_1$, in order to determine max effect of parameter $\alpha_0$ during its variation, max value of the parameter R is taken, and values of the rest of the parameters are taken in the middle of variations range of value of the rest of the parameters of adjustment range.

Since actual thread take-up function $P(\varphi)$ depends on rotation angle of the main shaft - $\varphi$ and three or four other variable parameters, in order to investigate the effect of each parameter on the value of $P(\varphi)$ function, sequential variations of these parameters were performed, while fixing values of others ($P(\varphi, a_0)$, $P(\varphi, R)$, $P(\varphi, Y_{G1})$, $P(\varphi, Y_{G2})$.

The calculation of the values of actual thread take-up function $P(\varphi)$ was performed according to the formulas given in works [14-19] depending on the type of thread take-up mechanism of sewing machines.

According to the calculation results, when varying one of the adjustable parameters spatial charts was build, for changes of the values of actual thread take-up function $P(\varphi, a_0)$, $P(\varphi, R)$, $P(\varphi, Y_{G1})$, $P(\varphi, Y_{G2})$ for each NTTM of W562-05M, class «Pegasus» and CF 2300M-164M class «Uamato» sewing machines. Along with this, diagrams to display values of these functions in parameters adjustment range with certain step were obtained (position 2 on Figures 4 and 5), and these values were compared with charts of the required needle take-up function $P'(\varphi)$ (position 2 on Figures 4 and 5) for the left needle of the relevant sewing machines.

The effect on $P(\varphi)$ of the final position of the thread receiver $T_1$, which is determined by parameter $\alpha_0$, is shown on Fig. 4, 5(a). It can be seen from it that in the range of variation of parameter $\alpha_0$, with negative values, take-up value changes insignificantly, and, vice versa, with positive values, take-up value increases significantly according to a nonlinear law.

As a result of varying values of the parameter $R$, given on Fig. 4, 5(b), it was discovered that when parameter $R$ is decreased, the value of thread take-up increases, and, vice versa, when $R$ is increased, it decreases. At the same time, changing of maximum of $P(\varphi)$ function is directly proportional to the changing of R parameter with an insignificant change in thread take-up law for both variants of NTTM of sewing machines.

## RESULTS

The result of varying values of parameter $Y_{G1}$ is depicted on Fig. 3, 5(c), it shows that changes of the maximum $P(\varphi)$ is directly proportional to changes of parameter $Y_{G1}$. At the same time, take-up law (in specified adjustment range) changes insignificantly.

At the same time, varying values of parameter $Y_{G2-3}$ (Fig. 4(d)) leads to significant effect for both value and law of thread take-up. So, for instance, with parameter value $Y_{G2-3}$=1mm, chart horizontal section (Fig. 4(d), curve 1) of actual thread take-up function is observed, and with negative values, a significant change in values is observed and chart of the function becomes "saddle-shaped".

**Table 1.** Ranges of adjustable parameters changing.

| Adjustable parameter | | W562-05M, class, «Pegasus» | CF 2300M-164M, class, «Uamato» |
|---|---|---|---|
| | | Adjustment range | |
| $R$ [mm] | | 55÷75 | 50÷70 |
| $Y_{G1}$ [mm] | | -20÷20 | -20÷20 |
| $Y_{G2-3}$ [mm] | | -10÷10 | -10÷10 |
| $\alpha_0$ [°] | | -20÷20 | -20÷20 |
| Relative coordinates of the uppermost position of thread receiver $T_2$ relative to the center point $O$ of the thread receiver $T_1$ [mm] | x | 62 | 148 |
| | y | 90 | 85 |

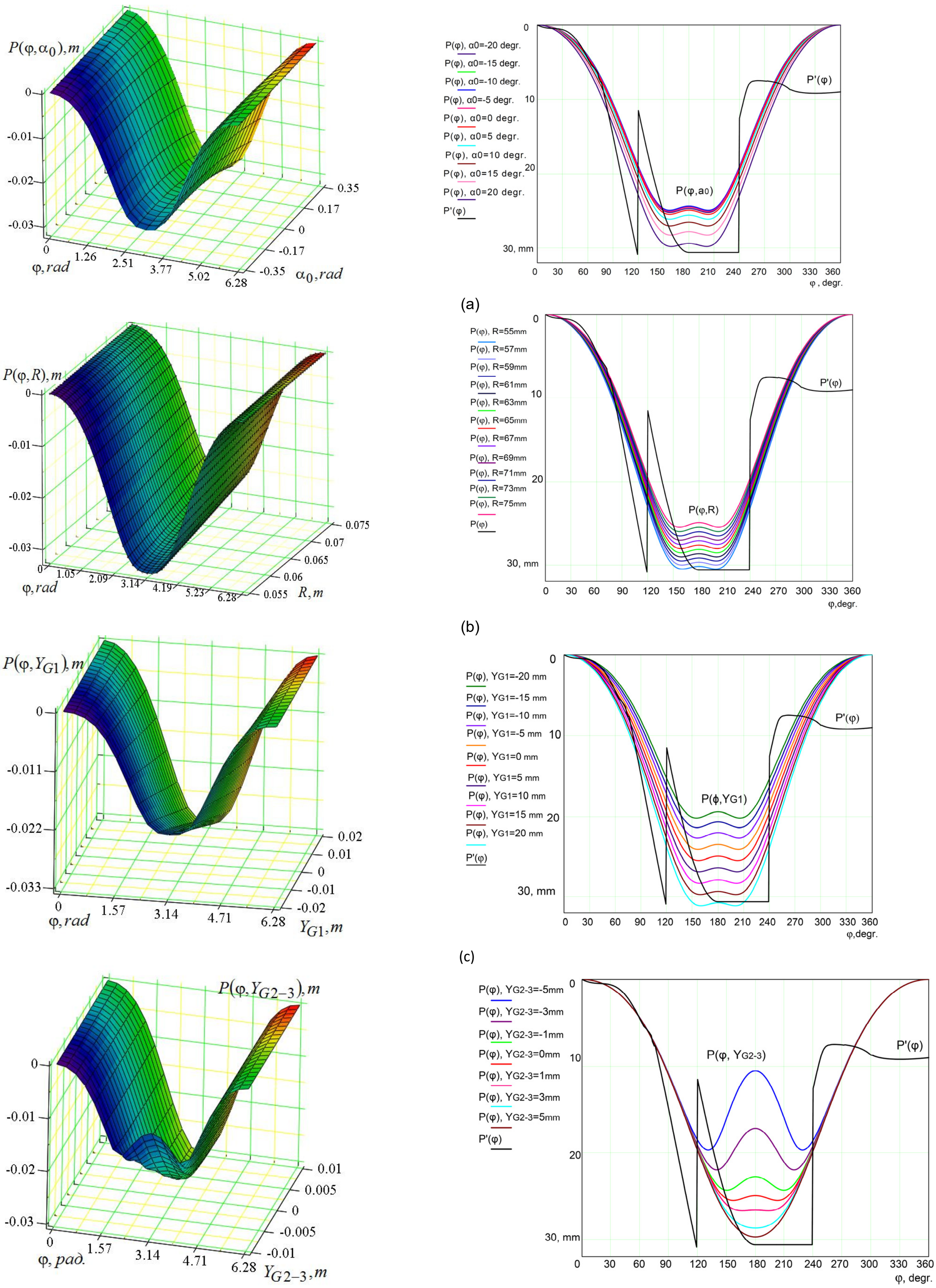


(d)

**Figure 4.** Spatial charts and diagrams of values of the actual *P(φ)* and necessary *P′(φ)* thread take-up when varying the adjustable parameters of the W562-05BB class «Pegasus» sewing machine: (a) $\alpha_0$, (b) *R*, (c) $Y_{G1}$, (d) $Y_{G3\text{-}2}$.

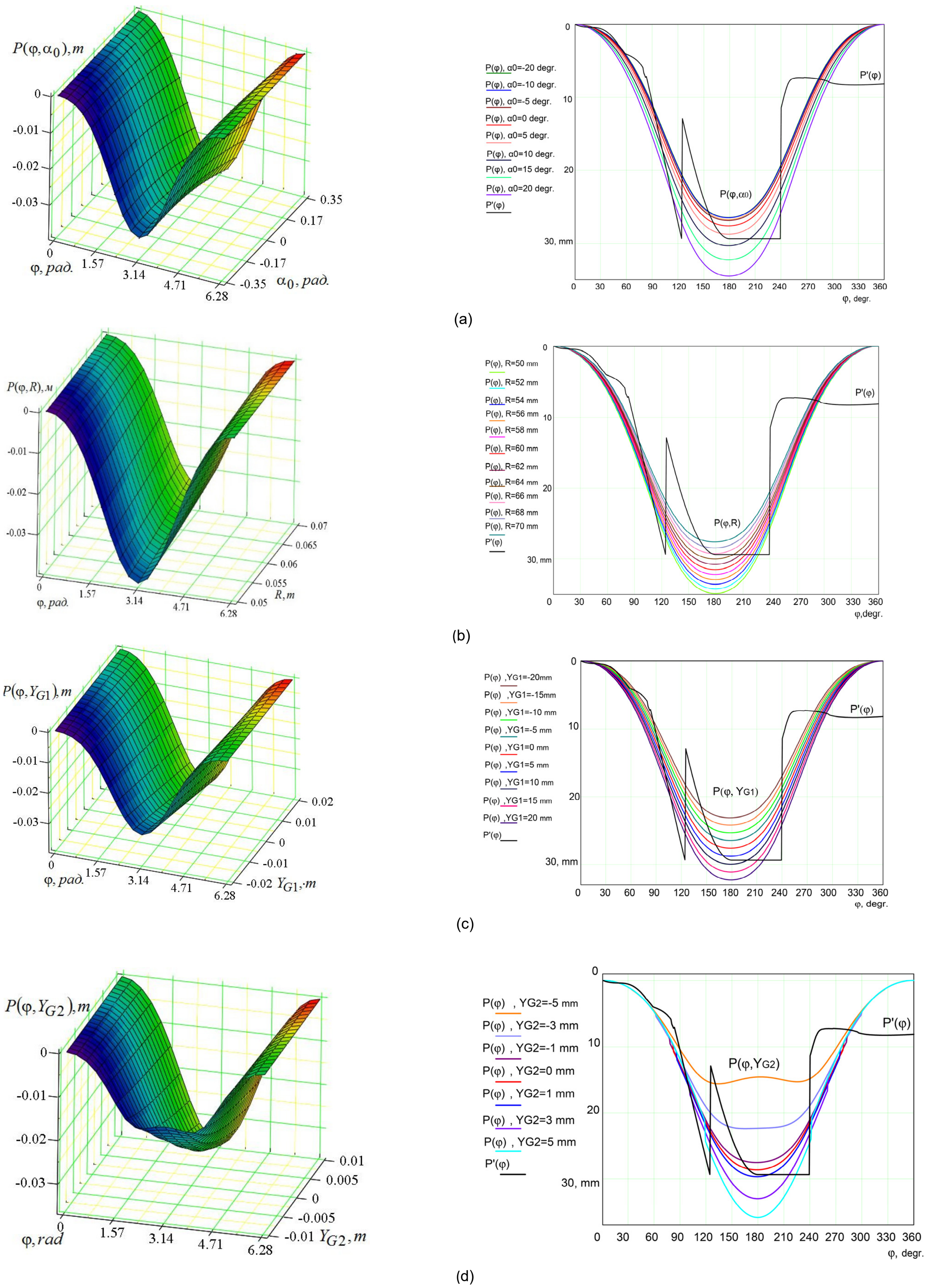


**Figure 5.** Spatial charts and diagrams of values of the actual P(φ) and necessary P'(φ) thread take-up when varying the adjustable parameters of the CF 2300M-164M class «Uamato» sewing machine: (a) $\alpha_0$, (b) R, (c) $Y_{G1}$, (d) – $Y_{G2}$.

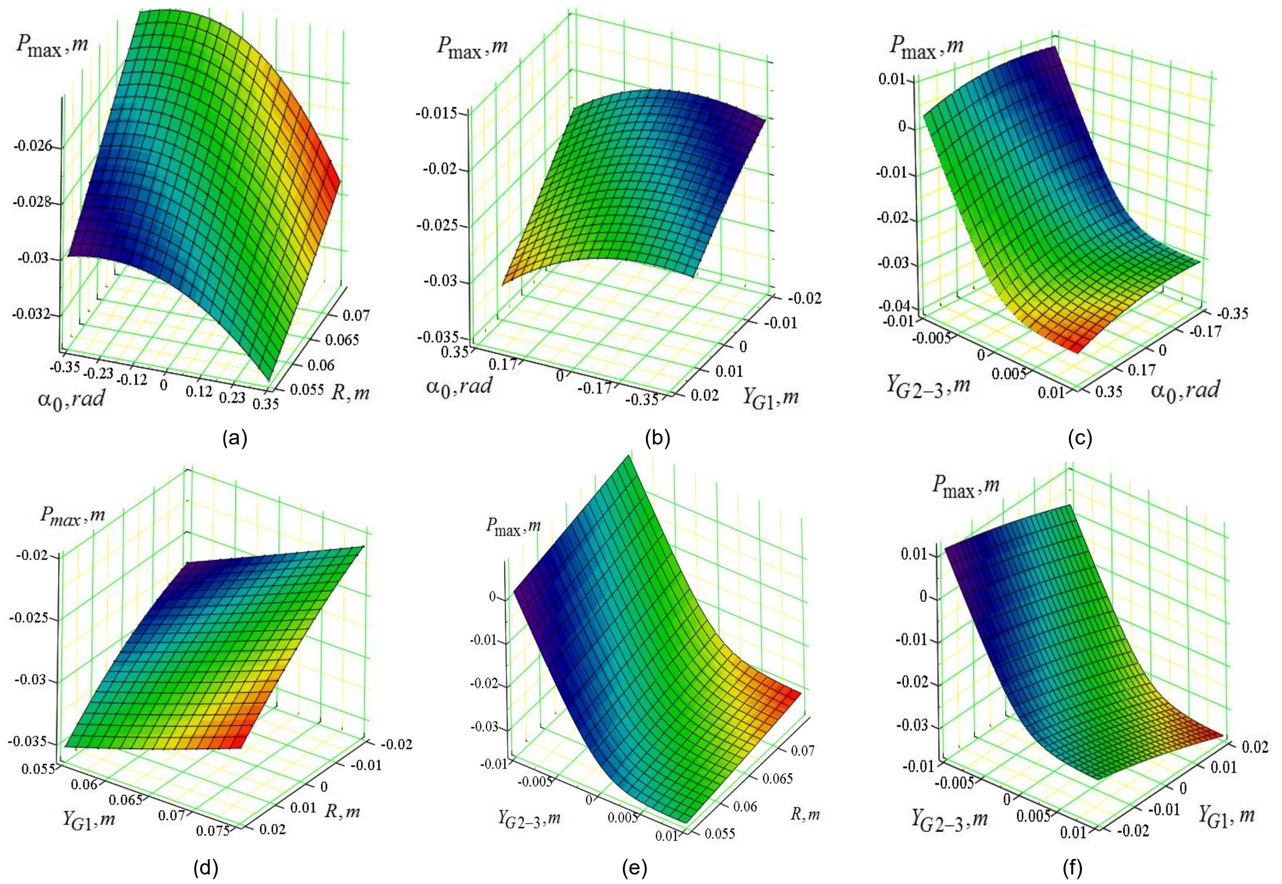


**Figure 6.** Charts of the maximum values of the actual thread take-up function *P(φ)* for W562-05BB class «Pegasus» sewing machine, when varying the parameter: (a) $\alpha_0$ and $R$; (b) $\alpha_0$ and $Y_{G1}$; (c) $\alpha_0$ and $Y_{G2\text{-}3}$; (d) $R$ and $Y_{G1}$; (e) $R$ and $Y_{G2\text{-}3}$; (f) $Y_{G2\text{-}3}$ and $Y_{G1}$.

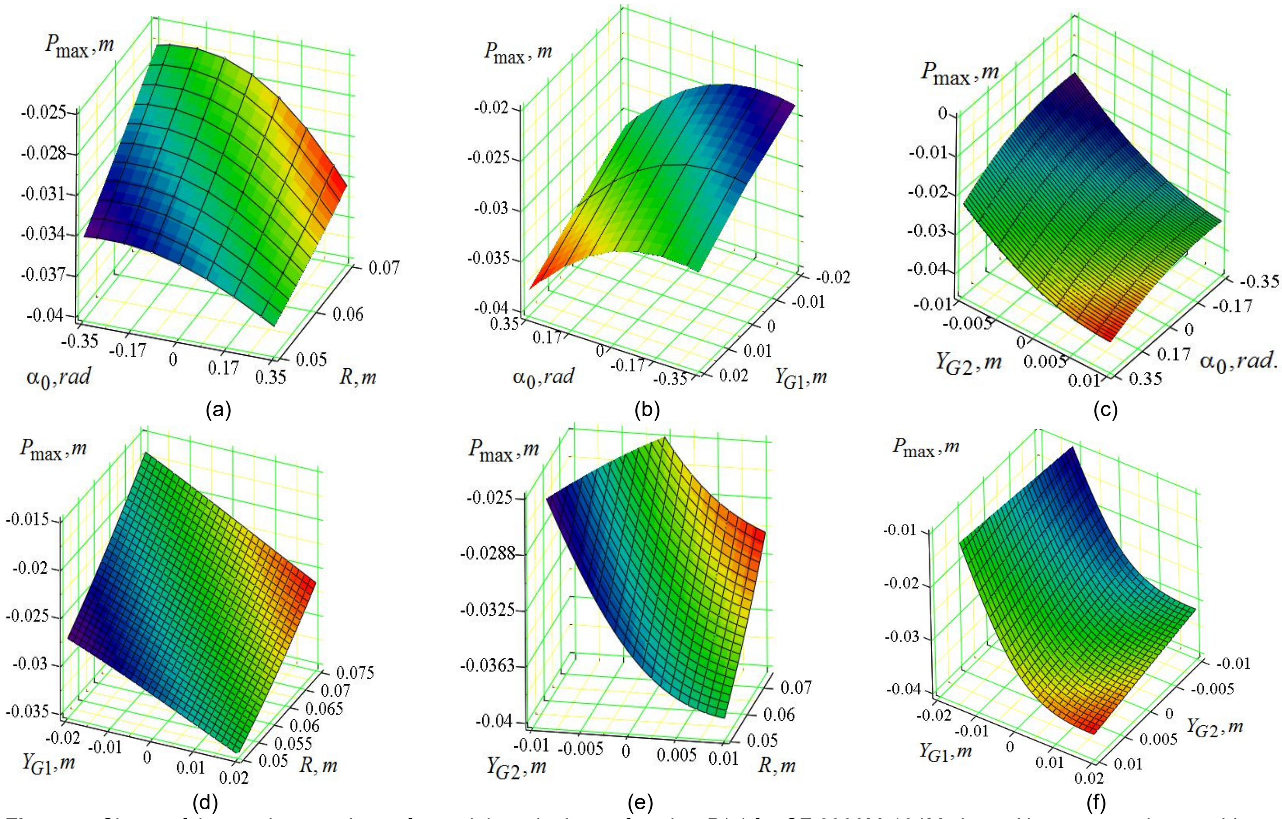


**Figure 7.** Charts of the maximum values of actual thread take-up function *P(φ)* for CF 2300M-164M class «Uamato» sewing machine, when varying the parameter: (a) $\alpha_0$ and $R$; (b) $\alpha_0$ and $Y_{G1}$; (c) $\alpha_0$ and $Y_{G2}$; (d) $R$ and $Y_{G1}$; (e) $R$ and $Y_{G2}$; (f) $Y_{G2}$ and $Y_{G1}$.

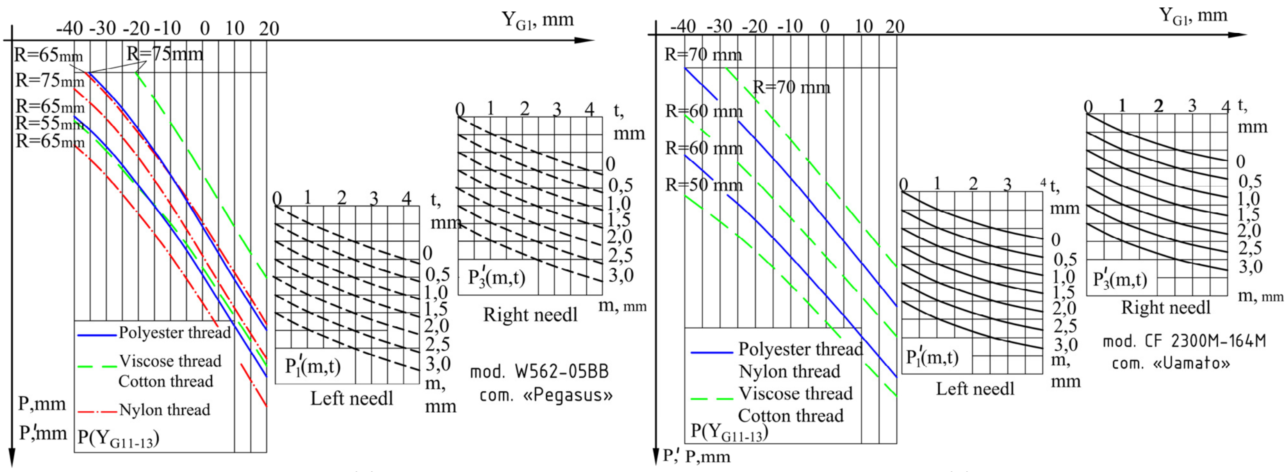


(a) (b)

**Figure 8.** Nomogram that determines value of NTTM parameters adjustment for sewing machines: (a) W562-05BB class «Pegasus» ($\alpha_0$=0 degr., $Y_{G2\text{-}3}$=0 mm), (b) CF 2300M-164M class «Uamato» ($\alpha_0$=0 degr., $Y_{G2}$=-4 mm).

The impact of parameter $Y_{G2}$ for CF 2300M-164M class «Uamato» (Fig. 5 (d)) is also similar to the impact of parameter $Y_{G2\text{-}3}$ for W562-05BB class "Pegasus" machine (Fig. 4 (d)). However, the impact of parameter $Y_{G2}$ (Fig. 5 (d)) is less important, since thread receiver with I-shaped thread guide forms only one new branch of thread take-up circuit in a certain period. An increase of horizontal linear part on *P(φ)* function chart is observed (Fig. 5 (g)) at the maximum values of $Y_{G2}$ parameter.

The certain parameter value was determined by its varying, at which the greatest matching between values of function *P(φ)* and values of required thread take-up function *P´(φ)* was observed.

For investigation purposes of the impact of two selected parameters (with fixed values of other parameters), the actual thread take-up function *P(φ)* was analyzed for its maximum value $P_{max}$ at $\varphi=\pi$. Pairwise influence of parameters on maximum value of the function *P(φ)* was performed for this purpose, which is illustrated by maximum response surface (Fig. 6, 7) accordingly W562-05BB class «Pegasus» and CF 2300M-164M class «Uamato» sewing machines models.

Parameters values were chosen as $\alpha_0=\pi$, $Y_{G2\text{-}3}$=0 mm and $Y_{G2}$=0, respectively, for W562-05BB class «Pegasus» and CF 2300M-164M class «Uamato» sewing machines, with such values, the thread take-up law is closer to the values of required thread take-up function (Fig. 4 (a,d) and Fig. 5 (a, d)).

Analysis of the combined impact of $\alpha_0$ and *R* parameters (Fig. 6(a), 7(a)) shows that the value of parameter $\alpha_0$ has greater impact on maximum of *P(φ)* function than value of parameter R, while certain regularity is observed for NTTMs of both sewing machines. Thus, when varying parameters $\alpha_0$ and $Y_{G1}$ (Fig. 6(b), 7(b)) and $\alpha_0$ and $Y_{G2\text{-}3}$ (Fig. 6(c)) and $\alpha_0$ and $Y_{G2}$ (Fig. 7(c)) more significant change in function maxima is observed. At the same time, pairwise changing of parameters $Y_{G2\text{-}3}$ and $Y_{G2}$ with other parameters (Fig. 6(c,e,f)) and (Fig. 7(c,e,f)) on function maxima retains the weight of its influence, thus the variation of its values leads to significant increase or decrease in values of function maxima. Pairwise variation of $Y_{G1}$ parameter values with $\alpha_0$ parameters (Fig. 6(b,d), 7(b,d)), *R* (Fig. 6(a,d,e) and Fig. 7(a,d,e)) is more significant than the individual impact of these parameters. Thus, the greatest effect on function maxima is observed when varying parameters $Y_{G2\text{-}3}$, $Y_{G2}$, $\alpha_0$, slightly smaller effect is observed when varying the parameter $Y_{G1}$, and weak effect has *R* parameter.

As a result, for each needle thread take-up mechanism of sewing machines, the optimal range of adjustment of its parameters was established.

Based on conducted analysis, nomograms (Figure 8) were developed, by using them it is possible to quickly and efficiently adjust needle thread take-up mechanisms of machines investigated in the work, depending on the technological parameters of technological process operations, particularly material thickness, stitch length and thread type.

Considering the fact that properties of «kapron» elementary and «kapron» complex threads are similar, parameters for these threads are selected accordingly to the «kapron» curve. Thus, when selecting adjustable NTTM parameters, the type of thread is taken into account by changing take-up amount of the thread for specific needle using adjustable parameters according to $G_{11\text{-}13}$.

The procedure of nomograms usage is following.

Determining *P'(m, t)* function maximum by given value of material thickness m depending on stitch length *t* (Figure 8). For this, firstly it is necessary to determine value of the parameter *R*, at which *P'(m, t)* function maximum value is reached for both uttermost needles, then to determine value of the parameter $Y_{G11\text{-}13}$ for each needle. This approach relates to the fact that thread receiver $T_1$ is shared between all needle threads and value of the parameter *R* will be the same for all of them. The obtained point, which corresponds to the maximum value of $P'(\varphi)$, is transferred parallel to abscissa axis on the curve of function $P(G_1)$ maximum of the corresponding thread. Based on the obtained value of function $P(G_1)$ maximum, the parameter $G_1$ is determined. To set the parameter $R$, it is necessary to transfer obtained point to $R(G_1)$ curve, and determine parameter $R$ from it. In the case when value of the parameter $R$ is outside nomogram's range, its value is accepted as maximum or minimum. The values of parameters $\alpha_0$, $Y_{G2\text{-}3}$, $Y_{G2}$ are set individually for each machine.

## CONCLUSIONS

1. As a result of the conducted research, it was established that the control parameters can be divided into those that are responsible for changing the law of thread take-up $Y_{G2}$, $Y_{G2\text{-}3}$ or the amount of thread take-up $Y_{G1}$, $R$ and $\alpha_0$. Varying of parameter $\alpha_0$ of the thread receiver $T_1$ leads to a change in both amount of thread take-up and law of the actual thread take-up function $P(\varphi)$.

2. It was found that nature of the thread take-up law is influenced by the type of thread guide, at the position of U-shaped $(Y_{G2\text{-}3})$ thread guide within the thread receiver $T_2$ at its extreme position, that allows to reach horizontal section with certain length of the $P(\varphi)$ function curve. At the same time, in order to achieve this value when using an I-shaped thread guide, the $Y_{G2}$ parameters must be significantly larger.

3. The developed nomograms allows to set adjustable parameters values of the thread take-up mechanisms, which provide optimal conditions for the process of stitch formation, depending on the given technological indicators.

4. The application of these recommendations in production will significantly reduce the time spent on machine reconfiguration for other technological operations.

5. The proposed method can be used at development of similar recommendations for chain stitch sewing machines of other classes and purposes.

## REFERENCES


1. Manoilenko O.: Topological analysis and synthesis of machine chain stitches, Vlakna a Textil, 2020, 27(4), pp. 58-69.
2. Manoilenko O. P., Horobetc V. A., Dvorzhak V. M.: Analytical review and development of a classification of needle thread feeding mechanisms of chain stitch sewing machines, Technologies and engineering, 2022, 4(9), pp. 35-47. https://doi.org/10.30857/2786-5371.2022.4.3
3. Company website «PEGASUS CO., LTD» Available from: https://www.pegasus.co.jp/en/machine/
4. Company website «Yamato Sewing Machine Mfg. Co., Ltd.» Available from: https://www.yamato-sewing.com/en/product/
5. Company website JUKI CORPORATION. Available from: https://www.juki.co.jp/en/products/
6. Company website «Rimoldi». Available from: http://www.rimoldiecf.com/en
7. Midha, V. K., Gupta, V., Mukhopadhyay, A. J.: Impact of positive thread feeding for high-speed industrial lock-stitch sewing machines: Part I. 2019, Development of device, Journal of The Institution of Engineers: Series E, 2019, 100(1), pp. 71-19. https://doi.org/10.1007/s40034-019-00136- 2
8. Midha, V. K., Gupta, V., Mukhopadhyay, A. J.: Impact of positive thread feeding for high-speed industrial lock-stitch sewing machines: Part II. 2019, Response with cotton and spun polyester needle threads, Journal of The Institution of Engineers: Series E, 2019, 100(2), pp. 147-153. https://doi.org/10.1007/s40034-019-00137-1.
9. Jaouadi, M., Msahli, S., Babay, A. et al.: Analysis of the modeling methodologies for predicting the sewing thread consumption. International Journal of Clothing Science and Technology, 2006, 18(1), pp. 7-18. https://doi.org/10.1108/09556220610637477
10. Randima, L. M. L., Sandaranga, D. M. B. C., Jayawardana, T. S. S., et al.: Design and fabrication of an automatic tension monitoring and regulation system for needle thread, Moratuwa Engineering Research Conference (MERCon), 2019, pp. 738-743. https://doi:10.1109/mercon.2019.8818866.
11. Rehman A., Rasheed A., Javed Z., et al.: Geometrical Model to Determine Sewing Thread Consumption for Stitch Class 406, FIBRES & TEXTILES in Eastern Europe, 2021, 29(6), pp. 72-76. https://doi.org/10.5604/01.3001.0015.2726
12. Rasheed A., Ahmad S., Ali N., et al.: Geometrical model to calculate the consumption of sewing thread for 504 over-edge stitch, Journal of the Textile Institute, 2018, 109(11), pp. 1418-1423.
13. Abeysooriya, R. P., Wickramasinghe, G. L. D. Regression model to predict thread consumption incor-porating thread-tension constraint: Study on lock-stitch 301 and chain-stitch 401. Fashion and Textiles, 2014, 1(1), pp. 14. https://doi.org/10.1186/s40691-014-0014-5
14. Horobetc V. A., Manoilenko O. P.: Analysis of the process of the necessary feeding of the upper thread in the formation of class 400 stitches. Bulletin of KhNU "Technical Sciences" volume 2, 6.2005, C. 36-41.
15. Horobetc V. A., Manoilenko O. P.: Diagrams of feeding the upper thread when forming class 400 stitches, taking into account its deformation. Message 1, KNUTD Bulletin, 2007, №2 (34), C. 21-24.
16. Horobetc V. A., Manoilenko O. P.: Diagrams of feeding the upper thread when forming class 400 stitches, taking into account its deformation. Message 2, KNUTD Bulletin, 2007, №3 (35), C. 16-22.
17. Horobetc V. A., Manoilenko O. P.: Study of take-up mechanisms for upper thread of two-thread and multi-thread chain stitch sewing machines, KNUTD Bulletin, 2005, №1 (21), C. 5-11.
18. Horobetc V. A., Manoilenko O. P.: Comparative analysis the take-up mechanisms of upper thread of sewing machines for performing class 400 stitches, KNUTD Bulletin, 2005, №6 (36), C. 30-34.
19. Horobetc V. A., Manoilenko O. P.: Optimization synthesis of the needle thread the take-up mechanism of chain stitch honing machines, KNUTD Bulletin, 2008, №1, C. 72-77.
20. Shcherban, V., Makarenko, J., Melnyk G., et al.: Effect of the yarn structure on the tension degree when interacting with high-curved guide, Vlakna a Textil, 2019, 26(4), pp. 59-68.

# AIMS AND SCOPES

“Vlakna a Textil” is a peer-reviewed scientific journal serving the fields of fibers, textile structures and fiber-based products including research, production, processing, and applications.

The birth of this journal is connected with three institutions, Research Institute for Man-Made Fibers, Svit (VÚCHV), Research Institute of Chemistry of Textiles (VÚTCH) in Žilina and Department of Fibers and Textiles at the Faculty of Chemical Technology, Slovak Technical University in Bratislava, having a joint intention to provide, utilize and deposit results obtained through the research, development and production activities dealing with the aforementioned scopes. „Vlákna a Textil“ journal has been launched as a consequence of a joing of existing magazines „Chemické vládkna“ (VÚCHV) and „Textil a chémia“ (VÚTCH). Their tradition should provide a good framework for the new journal with the main aim to create a closer link between the basic element of the product - fibre and its fabric - textile.

Since its founding in 1994, the journal introduces new concepts, innovative technologies and better understanding of textile materials (physics and chemistry of fiber forming polymers), processes (technological, chemical and finishing), garment technology and its evaluation (analysis, testing and quality control) including non-traditional applications, such as technical textiles, composites, smart textiles or garment, and nano applications among others. The journal publishes original research papers and reviews. Original papers should present a significant advance in the understanding or application of materials and/or textile structures made of them.

# VLÁKNA A TEXTIL

Volume 30, Issue 5, December 2023

## CONTENT